

**IONOMETALLURGY:
THE PROCESSING OF METALS USING IONIC LIQUIDS**

**Thesis submitted for the degree of
Doctor of Philosophy
at the University of Leicester**

by

Jennifer Marie Hartley MChem

Department of Chemistry

University of Leicester

April 2013



**University of
Leicester**

Parts of this work have already been published in the following papers:

A. P. Abbott, G. Frisch, J. Hartley and K. S. Ryder, *Green Chemistry*, 2011, **13**, 471-481. (see Chapter 1)

A. P. Abbott, G. Frisch, H. Garrett, J. Hartley, *Chem. Commun.*, 2011, **47**, 11876-8. (see Chapter 3)

A. P. Abbott, G. Frisch, S. J. Gurman, A. R. Hillman, J. Hartley, F. Holyoak and K. S. Ryder, *Chem. Commun.*, 2011, **47**, 10031-3. (see Chapter 3)

D. Jones, J. Hartley, G. Frisch, M. Purnell and L. Darras, *Palaeontologia Electronica.*, 2012, **15**, 15.2.4T. (see Chapter 6)

Abstract

Ionometallurgy: The Processing of Metals Using Ionic Liquids

Jennifer Marie Hartley

Metal processing is commonly carried out using hydrometallurgy or pyrometallurgy. These two techniques, whilst widespread, have inherent issues associated with selectivity and efficiency. The aim of this study is to investigate the use of ambient temperature ionic liquids (IL) to dissolve and recover metals from ionic media.

The first stage of the study involved the development of a new stable reference electrode for use in IL media. This was used to obtain activity coefficients for three different silver salts in three different imidazolium-based ILs containing matching anions. Activity coefficients were also obtained for silver chloride, anhydrous copper (II) chloride and trifluoromethanesulfonic acid in the deep eutectic solvent (DES) Ethaline and it was found that these solutions displayed ideal behaviour, even at high concentrations.

The electrochemistry of metal complexes in ionic liquids was studied using cyclic voltammetry in an ethylene glycol: choline chloride eutectic (Ethaline) and these potentials were plotted against the corresponding redox potentials in aqueous media to try to determine how speciation affected the reactivity of metals in solution.

The speciation of a range of metal chlorides in a range of DESs was investigated and it was found that the majority of the metal ions tended towards chloride speciation, with a few exceptions for the more oxophilic early transition metals. The addition of a substantial amount of water in the form of hydration shells did not affect the metal speciation significantly. In IL media, the speciation tended towards the anionic component of the liquid, depending on its strength as a ligand.

The fundamental redox behaviour and speciation data were used to develop a practical method to separate copper from gallium in waste semiconductor scrap. Lumps of the alloy were electrodissolved in Ethaline and this was followed by selective electrowinning of the copper as metal and precipitation of the gallium as a gelatinous white hydroxide. In addition, iodine could be used as a powerful oxidising agent in DES media to oxidise a small amount of gold and recover valuable paleontological microfossils.

Acknowledgements

I would like to thank my supervisors, Prof. Andy Abbott and Dr. Gero Frisch, for their invaluable assistance and the Leicester Ionic Liquids Group for sharing their combined experience and knowledge. Without them, this project would not have been possible. I would also like to thank the EPSRC and MCP Ltd for their funding. Throughout my degree, my parents and grandparents have supported and encouraged me, and I would like to thank them for helping me achieve my goals.

Finally, a big thank you goes to Jack, for always being there for me.

Table of contents

Abstract	iii
Acknowledgements	iv
Table of contents	v
List of abbreviations	ix

Chapter 1 Introduction	1
1.1 Metal processing from aqueous solution	2
1.2 Pyrometallurgical metal processing	4
1.3 Ionic liquids	5
1.3.1 Chloroaluminate ionic liquids/metal based eutectics	9
1.3.2 Discrete anion ionic liquids	10
1.3.3 Deep eutectic solvents	14
1.4 Metal processing from ionic liquids	16
1.4.1 Digestion of oxides and metals	17
1.4.2 Extraction	21
1.4.3 Electrowinning and cementation	27
1.5 Project objectives	31
1.6 References	32
Chapter 2 Experimental	42
2.1 Deep eutectic solvent (DES) formation and chemicals	43
2.2 Reference electrode	46
2.3 Ideal solutions and activity coefficients	48
2.3.1 In DES	49
2.3.2 In ILs	52
2.4 Redox potentials of d- and p-block metal salts in Ethaline	52
2.4.1 Cyclic voltammetry	53
2.4.2 Solutions for determination of redox potentials	55
2.4.3 Chloro-complexes in aqueous media	56
2.4.4 DES analogues	57
2.5 Speciation of metals	57

2.5.1	EXAFS	58
2.5.2	UV-Vis spectroscopy	64
2.6	Metal processing, separation, and recovery	66
2.6.1	Analytical techniques	66
2.6.2	Anodic dissolution	68
2.6.3	Electrochemical oxidation using iodine	72
2.7	References	75
Chapter 3 Ideal solutions and redox potentials		78
3.1	Reference electrode	79
3.1.1	Review of reference electrodes in ILs	80
3.1.2	Novel reference system for use in DES systems	84
3.2	Activity coefficients in ionic liquids	87
3.2.1	Activity coefficients in imidazolium liquids	89
3.2.2	Activity coefficients in DESs	92
3.3	Redox properties of metal salts in DESs	95
3.3.1	Redox properties in Ethaline vs. H ₂ O	96
3.3.2	Cyclic voltammetry of metal salts in Ethaline	98
3.4	Conclusions	107
3.5	References	108
Chapter 4 Speciation and EXAFS		113
4.1	Theory of EXAFS	114
4.1.1	Generation of X-rays	115
4.1.2	Absorption edges	116
4.1.3	Generation of EXAFS spectra	117
4.1.4	The different regions of EXAFS spectra	120
4.1.5	Methods and modes	122
4.2	The speciation of metal chloride salts in DES media	123
4.2.1	Speciation of metal chloride salts in glycol-based DESs	124
4.2.2	Speciation of metal chloride salts in Reline	132
4.2.3	Nickel: A special case	136
4.2.4	Speciation of iodine in DES media	141

4.3	Speciation in imidazolium liquids	142
4.3.1	Speciation of metal salts in [HMIM][Cl]	142
4.3.2	Other ILs with different anions	146
4.4	Conclusions	148
4.5	References	150
Chapter 5 The links between speciation and redox behaviour		152
5.1	Investigating the reversibility of redox processes	153
5.1.1	General redox behaviour	155
5.1.2	The unusual case of nickel	157
5.2	Relation of speciation to redox properties	160
5.2.1	Copper chloride	161
5.2.2	Cobalt chloride	166
5.2.3	Nickel chloride	167
5.2.4	Short summary	169
5.3	Voltammetry in LiCl:2H ₂ O	169
5.4	DES analogues	172
5.4.1	Copper chloride	173
5.4.2	Iron chloride	176
5.4.3	Short summary	177
5.5	Conclusions	178
5.6	References	180
Chapter 6 Metal processing and recovery		181
6.1	Current methods of semiconductor recycling	182
6.2	Processing of copper-gallium scrap by electrodisolution	184
6.2.1	Characterisation of the anode	185
6.2.2	Electrodisolution: Method 1 – Blue green slime	186
6.2.3	Electrodisolution: Method 2 – Filter paper set up	192
6.2.4	Electrodisolution from Reline	199
6.3	Processing of copper-indium-gallium scrap by electrodisolution	200
6.4	Application of redox potentials to the chemical oxidation of metals	202
6.4.1	Chemical oxidation of CG shavings	204

6.4.2	Recovery of gold-coated SEM samples	206
6.5	Conclusions	208
6.6	References	210
Chapter 7 Overall conclusions and future work		212
7.1	Conclusions	213
7.2	Future research	216
Chapter 8 Appendix		218

List of abbreviations

CG	Copper-gallium
ChCl	Choline chloride
CIG	Copper-indium-gallium
CV	Cyclic voltammetry
DES	Deep eutectic solvent
EDAX	Energy dispersive X-ray
EG	Ethylene glycol
EXAFS	Extended X-ray absorption fine structure
HBD	Hydrogen bond donor
ICP	Inductively coupled plasma
IL	Ionic liquid
OD	Oxygen donor
SEM	Scanning electron microscopy
TSIL	Task specific ionic liquid

Chapter 1 Introduction

Chapter 1	Introduction.....	1
1.1	Metal processing from aqueous solutions.....	2
1.2	Pyrometallurgical metal processing.....	4
1.3	Ionic liquids.....	5
1.3.1	Chloroaluminate ionic liquids/metal-based eutectics.....	9
1.3.2	Discrete anion ionic liquids.....	10
1.3.3	Deep Eutectic Solvents.....	14
1.4	Metal processing from ionic liquids.....	16
1.4.1	Digestion of oxides and metals.....	17
1.4.2	Extraction.....	21
1.4.3	Electrowinning and cementation.....	27
1.5	Project objectives.....	31
1.6	References.....	32

1.1 Metal processing from aqueous solutions

The processing and reprocessing of metals is probably one of the largest sources of low-grade waste and one of the largest users of energy of any industrial sector. Metal processing is often based on high temperature processes or hydrometallurgical methods. These processes can be complex due to the diverse range of starting materials *i.e.* metals, oxides, sulphides, carbonates, phosphates, silicates, selenides, tellurides and complex slags, sludges, slimes and alloys. As metal salts are insoluble in most non-aqueous molecular solvents, the solution based processes tend to be very acidic or basic. As shown in **Table 1.1**, there are numerous steps involved in the extraction and recycling of metals. Metals can be processed by electrolytic oxidation, chemical oxidation or chemical digestion, followed by recovery by electrowinning, precipitation, cementation or ion exchange. However, the specific recovery methodology used depends on the composition of the original matrix and the desired purity and value of the final product.

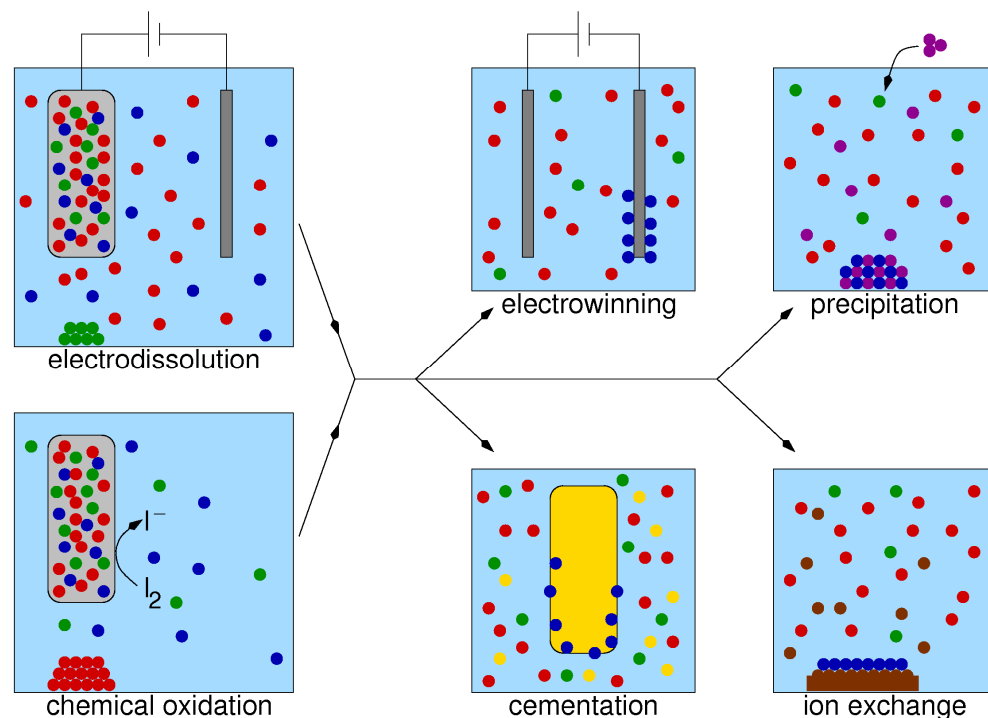


Table 1.1 Schematic of the steps and processes involved in metal recovery.

Hydrometallurgy has its origins at the end of the 19th century with the cyanide extraction of gold and the basic extraction of bauxite.¹ In processes which follow modern standards for environmental protection, all solutes must be removed before the solvent is discharged back into the watercourse. This will commonly lead to highly chemically and energetically intensive processes, as heavy metals must be removed from these aqueous solutions to extremely low concentrations. The solutions must also be neutralised before disposal and salt discharge can be an issue. In general, hydrometallurgy is used for more complex processes, with lower process volumes due to improved capital and labour considerations.²

There are four main methods of metal recovery: precipitation, electrowinning, cementation, and ion exchange. When metals are **precipitated** out from aqueous solution, it is usual to adjust the pH of the solution or to add chemical precipitants and flocculants, but the solubilities of the metals in solution will determine the process used. Metals will often precipitate as hydroxides, sulphides and carbonates.

Electrowinning metals from aqueous systems is an efficient and the most commonly used recovery process for metals with positive redox potentials such as copper, silver and gold, but is less efficient for other metals such as chromium, and is practically impossible for metals such as aluminium. The electrowinning process is often sensitive to parameters such as pH change, as the pH of a solution affects its potential window and the solubilities of any metal compounds dissolved in it. This is a well-studied area and pH-potential (Pourbaix) diagrams exist for most systems.³ Complexing agents, such as cyanide or ammonia, can be used to adjust metal speciation and therefore control the solubility and deposition properties of both the desired solute and any impurities present in solution.⁴ An over potential in water can cause hydrogen

gas evolution at the cathode and oxygen gas evolution at the anode, which can lead to embrittlement, a diminishing in the quality of the electrodeposit and resulting in poor current efficiency. Metals such as chromium and aluminium must be chemically or electrochemically reduced in high temperature processes, which often demand an aqueous pre-treatment of the ore. Most of these procedures have extremely high energy demands and can produce large volumes of waste.

Cementation is a process where metal ions are reduced to their elemental state at a solid metal interface. It is a common process for removing one metal from solution that is not important enough to be electrowon. **Ion exchange** is when ions are exchanged between two electrolytes or between an electrolyte solution and a solute or complex. The sacrificial metal is usually one of low value, typically zinc. These recovery processes can also be carried out in ionic liquid and deep eutectic solvent media, and will be discussed further in **Section 1.4**.

1.2 Pyrometallurgical metal processing

One alternative to hydrometallurgy is pyrometallurgy. This is a non-aqueous method based on high temperature processes. High temperature molten salts (with melting points of *c.a.* 500 to 1000°C) have been used to electrowin metals such as lithium, sodium, aluminium and titanium, which cannot be obtained from aqueous solutions.^{5, 6} High temperature molten salts are both ionic and aprotic, making them highly suitable for electrowinning metals. They have high conductivities compared to other non-aqueous solvents, wide potential windows, low viscosities and high solubilities for metal salts. Molten salts have similar solvating powers to aqueous solvents, whilst eliminating the detrimental hydrogen evolution associated with aqueous solutions and any competition from water as a ligand. The main issues involved with the

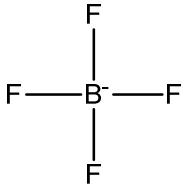
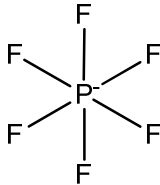
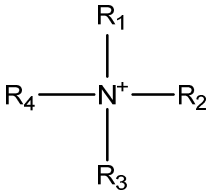
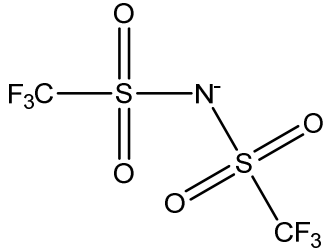
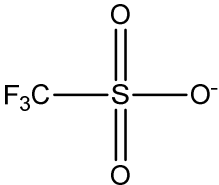
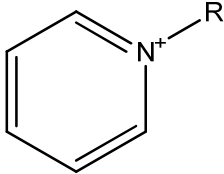
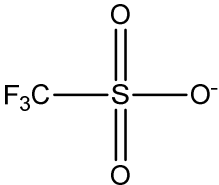
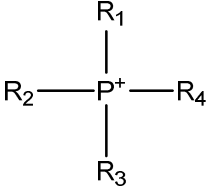
electrowinning of metals from molten salts are the high operating temperatures and associated practical aspects, such as substrate specificity, material compatibility and the high energy demand.

1.3 Ionic liquids

In solution, metal salts predominantly form charged species, and therefore have a greater solubility in polar or ionic solvents. Ionic liquids are commonly defined as systems which are composed entirely of ions and are liquid below 100°C.⁷ They can easily be differentiated from molten salts, as ionic liquids tend to contain organic cations instead of inorganic cations.⁸ Ionic liquid systems are of great interest as they have some similar properties to high temperature molten salts, but without the disadvantages that come with working at high temperatures. Despite there being a great number of cations and anions described in the literature, only a small selection of ionic liquids have been used for metal processing. These include imidazolium, pyridinium, phosphonium, and tetraalkylammonium salts as common cations, whilst tetrafluoroborate, $[\text{BF}_4^-]$, hexafluorophosphate, $[\text{PF}_6^-]$, chloride, Cl^- , and bis(trifluoromethanesulfonyl)amide, $[\text{Tf}_2\text{N}^-]$, are common anions (*Table 1.2*). By including potential ligands as the anionic component of the ionic liquid, a much greater control of the speciation is possible, and this will therefore allow control of the chemical properties of the metal in solution to a much greater extent than in aqueous media, as higher ligand activity can be achieved.

One of the first ILs to be synthesised was ethylammonium nitrate⁹ by Walden in 1914 and ILs have been since used in a range of processes from organic synthesis to electrodeposition, with applications as lubricants, plasticisers, solvents for catalysis, electrolyte in batteries, fuel cells, solar panels, and many other possibilities.¹⁰

Table 1.2 A selection of common cations and discrete anions used for making ionic liquids.

Cations	Anions
	
<p>Where $R_1 = \text{CH}_3$, $R_2 = \text{Et}$ EMIM $R_2 = \text{Bu}$ BMIM $R_2 = \text{Hex}$ HMIM</p>	
	
<p>Where $R_1 = R_2 = R_3 = \text{CH}_3$ $R_4 = \text{C}_2\text{H}_4\text{OH}$ Choline</p>	
	
	

The **melting point** of an ionic liquid defines the lower temperature limit of the liquid-phase gap in which they can be used as solvents and thermal decomposition often marks the upper limit of the range. Thermodynamic properties of these ionic liquids are dependent on the mutual fit of the anion and cation, with respect to their size,

geometries and charge distributions. As the anion or cation increases in size, the decrease in Coulombic attraction contributions to the lattice energy of the crystal and simultaneous increase in covalency of the ions will cause the melting point of the ionic liquid to be reduced. In addition, the symmetry of the cation or anion will also have a profound effect on the melting point of the solid crystal. Having highly symmetrical ions will cause higher melting points, due to more efficient ion-ion packing in the crystal cell. By reducing the symmetry of the ions, distortion of the ideal close-packing of ionic charges in the solid state lattice can be achieved, which in turn leads to a reduction in the lattice energy of the crystal and, hence, a depression of the melting point.⁸

One example of the effect of cation size on melting points is the imidazolium-based liquids, where the melting point decreases as the size and asymmetry of the cation increases, but increases with greater branching of the alkyl chain.¹¹ Melting points of many ionic liquids can be difficult to determine as the liquids tend to be susceptible to supercooling. Many ionic liquids form glasses and glass transition points are usually reported instead of melting points. The glass transition point is the point at which an amorphous solid becomes brittle on cooling, or soft on heating. Glass transitions for ionic liquids tend to be very low, *e.g.* -70 to -90°C for 1-alkyl-3-methylimidazolium salts,⁸ and in addition, the viscosity tends to be very high at low temperatures.¹²

In general, ionic liquids have much higher **viscosities** than water, comparable to the viscosities of oils,¹³ but the viscosity will decrease with an increase in temperature. The higher viscosities of these liquids may cause a reduction in the rates of reactions and decrease the diffusion coefficient of species in solution. Both anionic and cationic species will affect the viscosity of the liquid. For example, altering the length of the

alkyl chain on an imidazolium cation will change the viscosity due to van der Waals forces.¹⁴

The overall **density** of the ionic liquid will be affected by the molar mass of both cation and anion and most ionic liquids tend to be more dense than water. As the length of the alkyl chain increases, the density has been found to decrease.^{15, 16}

Ionic liquids have comparatively low **vapour pressure** to most common molecular solvents. Vapour pressure can often be dependent on the thermal stability of the liquid and most ionic liquids exhibit a high thermal stability, with decomposition temperatures generally being reported as greater than 400°C.¹³ Vapour pressures are minimal below these temperatures, therefore allowing the effective separation of reaction mixtures by distillation as there is no azeotropic effect between the solvent and the products.¹⁷ This has allowed ultra-high vacuum techniques to be applied to ionic liquids.¹⁸

Ionic liquids could potentially be used to make processes 'green' by reducing the volume of aqueous waste produced during metal processing. Ionic liquids are not inherently green due to the nascent toxicity of the constituent ions. The solubility of ionic liquids in water is an important factor, as it is sometimes necessary to extract reagents from an aqueous stream or to wash ionic liquids to extract products from solution and this offers the potential for ionic liquids to escape to the environment through a waste water supply. Another factor is the water content of hydrophilic ionic liquids, where the selectivity or rate of a reaction can be affected by the presence of water. For instance, the water content of an ionic liquid can significantly narrow their electrochemical windows, compared to the anhydrous liquid.¹⁹

Attempts have been made to design ionic liquids with low toxicity ions, such as functionalised imidazoles,²⁰ lactams,²¹ amino acids²² and choline.²³ Of these, only choline-based liquids have been extensively applied to metal processing.

1.3.1 Chloroaluminate ionic liquids/metal-based eutectics

One of the key breakthroughs in the study of ionic liquids was in 1951 when Hurley and Weir synthesised a 1 mol. eq. *N*-ethylpyridinium bromide: 2 AlCl₃ liquid which was a eutectic liquid at 20°C.²⁴ This was used for the electrodeposition of aluminium,²⁵ which then sparked off a large amount of research into metal deposition. Wilkes and co-workers developed an AlCl₃: 1-ethyl-3-methylimidazolium ionic liquid that was a room temperature ionic liquid (RTIL) between 33 and 67 mol% AlCl₃.²⁶ Chloroaluminate liquids in general are complex mixtures of alkyl halides and aluminium chloride, often having melting temperatures that are much lower than most other inorganic eutectic salts.²⁷ Arguably one of the best established forms of ionic liquid, chloroaluminate liquids have been used extensively in studies for the development of low melting point organic ionic liquids, mainly focussing on electrochemical and electrodeposition applications, transition metal coordination chemistry and as liquid Lewis acid catalysts for organic synthesis.⁸

Depending on the apparent mole fraction of aluminium chloride, the ionic liquid can be considered as acidic [$X(\text{AlCl}_3) > 0.5$] (where the main Al species is the halide ion acceptor $\text{R}^+\text{Al}_2\text{Cl}_7^-$), basic [$X(\text{AlCl}_3) < 0.5$] (where some of the halide ions are unbound in solution) or neutral [$X(\text{AlCl}_3) = 0.5$] (where both alkyl halide and aluminium chloride are bound together as the species $\text{R}^+\text{AlCl}_4^-$).^{10, 28} These so-called “first generation” ionic liquids have significantly lower viscosities than the corresponding pyridinium liquids and it is the imidazolium ion that continues to dominate the literature. The main

disadvantage of chloroaluminate liquids is that they are highly moisture sensitive and must be handled under a controlled inert gas atmosphere. Other, more stable, eutectics have been developed based on ZnCl_2 . However, this leads to an increase in viscosity.²⁹
³⁰ Further eutectics, based on SnCl_2 and FeCl_3 , have also been synthesised,³¹ along with systems based on metal hydrates, *e.g.* $\text{CrCl}_3 \cdot 6\text{H}_2\text{O}$.³²

When extracting metals it is clearly undesirable to have a high concentration of other metals already present in solution, as there is the potential for them to co-deposit with the desired metal, hence eutectic based ionic liquids have not been used extensively for metal extraction. A variant of these metal-containing eutectics is to replace the Lewis acid component with a Brønsted acid. Eutectics formed from quaternary ammonium salts and hydrogen bond donors, such as amides, alcohols or carboxylic acids,^{23, 33} have advantages for metal extraction, in that they are simple to prepare, moisture insensitive (although miscible with water) and have high solubilities for a range of metal oxides.³⁴ These so-called deep eutectic solvents (DES) have been tested out on a large scale for metal digestion and recovery³⁵ and will be discussed further in **Section 1.3**.

1.3.2 Discrete anion ionic liquids

Instead of having a complex mixture of anions in equilibrium, discrete anion ionic liquids are composed of simple anions and cations. The discovery is attributed to Wilkes and Zarotwoko, who, in the 1900s, produced the first air- and water-stable ionic liquids. They synthesised the 1-ethyl-3-methylimidazolium tetrafluoroborate $[\text{EMIM}][\text{BF}_4]$ and acetate $[\text{EMIM}][\text{OAc}]$ liquids for the first time.³⁶ Anions such as $[\text{BF}_4]^-$ and $[\text{PF}_6]^-$ were initially used because of their wide potential windows,^{37, 38} however they were found to slowly hydrolyse, producing HF.³⁹ Liquids with more

hydrophobic anions, such as trifluoromethanesulfonate $[\text{CF}_3\text{SO}_3^-]$ and bis-trifluoromethanesulfonylimide $[(\text{CF}_3\text{SO}_2)_2\text{N}^-]$ (or alternatively $[\text{Tf}_2\text{N}^-]$) have become more popular recently.¹⁴ The potential window of these liquids can be rather large, making them potentially useful for the electrowinning of the more reactive metals.⁴⁰ Hydrolysis of fluorinated anions must not be ignored in metal processing, as along with the more obvious environmental and safety issues and the problems of electrode and cell corrosion, fluoride acts as a strong ligand for many metals and can significantly change metal speciation during a recovery process.

These discrete anion ionic liquids are mostly made from the metathesis of a halide salt with, for example, a silver, group 1 metal or ammonium salt of the desired anion, followed by acid-base neutralisation reactions.⁴¹ The ammonium or phosphorus salts are produced from a quaternisation reaction between amines or phosphanes with a halogenated alkyl chain. The discrete anion ionic liquids can be formed from simply the first step, for example the quaternisation reaction between 1-ethyl-3-methylimidazole and methyl triflate to form $[\text{EMIM}][\text{CF}_3\text{SO}_3]$.¹⁴ In most cases the synthesis of these ionic liquids needs to occur in an air and moisture free environment and at low a temperature as possible. The purity of the starting materials must be kept as high as possible, as the non-volatility and viscous nature of the final product makes it further purification difficult.

Four different routes to a tetraalkylammonium ionic liquid are shown in *Table 1.3*. These are the addition of a Lewis acid to form a metallo-halide, such as the chloroaluminates described above, addition of a metal salt, a Bronstead acid or use of an ion exchange resin to form a discrete anion ionic liquid.

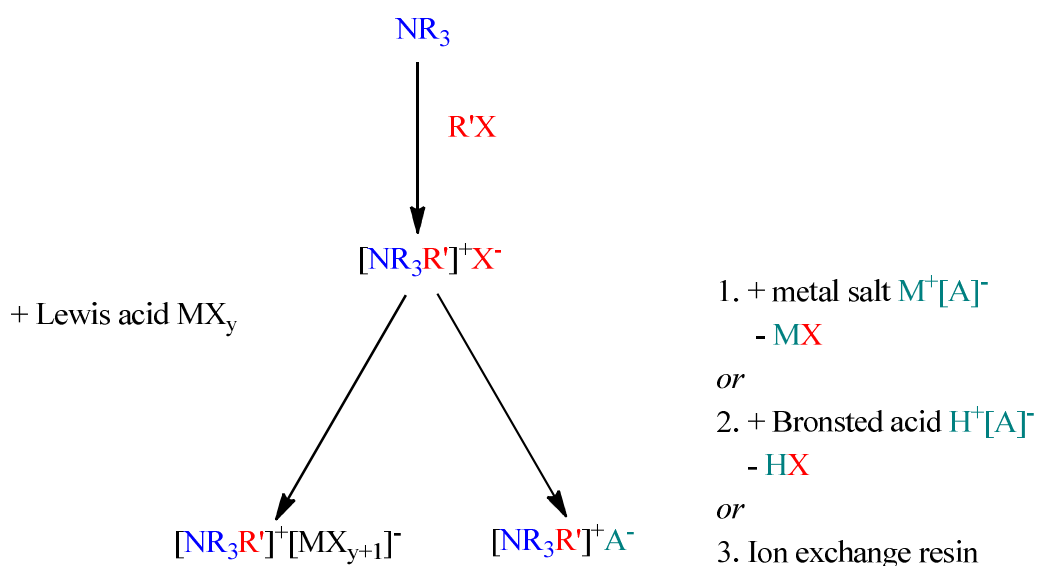


Table 1.3 Synthetic scheme showing the different methods of IL production,¹⁷ where “R” is an alkyl group and “X” is a halide group.

When selecting an ionic liquid to use, it is important to consider both the **melting point and viscosity**. These properties are largely controlled by the cation and it has been found that chains of two to four carbons as substituents on the imidazolium or pyridinium ring provide optimum fluidity.⁴² The anion has a more controlling effect on the chemistry of the system as it will interact more with the Lewis acidic metal solute. Complexation of the anion with the metal controls the speciation and hence all aspects of reactivity, solubility, etc.

Different anions and complexing agents present in the ionic liquids will change the **speciation** of metal ions present and therefore will also alter the reactivity. This effect can be seen on the copper ions in solution, as shown by the colour changes in **Table 1.4**. Subsequent effects on redox potentials are hard to quantify due to the issue of liquid junction potentials. However, in principle, the reactivity of the solute can be controlled through judicious choice of the anion, although anion effects on speciation are currently poorly understood.

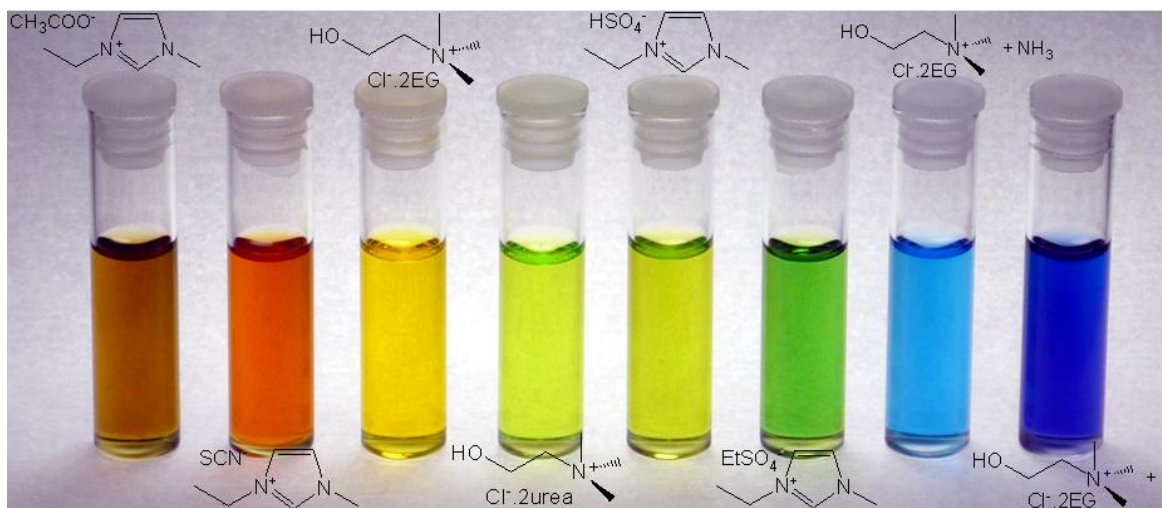


Table 1.4 Solutions of $\text{CuCl}_2 \cdot 2\text{H}_2\text{O}$ dissolved in eight different ionic liquid and DES environments.⁴³

To be useful for electrochemical processes, ionic liquids need to be good at dissolving metals and their salts. The high **solubility of metal salts** in ionic liquids generally results from the high concentration of anions. However, Branco *et al.* studied the solubility of LiCl , HgCl_2 and LaCl_3 for a series of imidazolium tetrafluoroborate and hexafluorophosphate ionic liquids and found that the solubility constants were relatively independent of the anion or cation.⁴⁴ Although this independence could be considered an unexpected outcome in an ionic liquid environment, it should be noted that the anions of these discrete anion liquids are often weakly coordinating and will have similar solvation properties to each other. By adding halides to the system, or making that cation task specific, the solubilities of metals and their salts in these discrete anion ionic liquids can be improved. If functional groups are added to the cation, the solubilities of metal salts in the ionic liquid will be altered, as has been shown by Visser *et al.* through the addition of thioether and thiourea groups to the side chain of

imidazolium cations. This has the effect of increasing the solubility of Hg^{2+} and Cd^{2+} in solution.⁴⁵

The **conductivity** of the medium is another important consideration for metal processing, as the metals are often electrochemically recovered. The conductivity of an electrolyte is dependent upon both the number of charge carriers and their mobility in solution, which in turn is dependent on ion size, ion association and viscosity of the electrolyte. Whilst ionic liquids have a very high concentration of charge carriers, their high viscosity causes them to have lower than expected conductivities, which are similar to organic solvents with the addition of inorganic electrolytes.⁴⁶ The conductivity and viscosity of ionic liquids have been modelled by Abbott *et al.* using hole theory.⁴⁷ In dilute aqueous solutions molar conductivities will decrease with an increasing electrolyte concentration due to the effects of the surrounding ionic atmosphere, whilst in concentrated aqueous solutions ion pairing will cause a decrease in the number of available charge carriers.⁴⁸ In ionic liquids conductivity can be considered to be limited by the availability of holes for ions to move into and has been found to vary inversely with viscosity.²³

1.3.3 Deep Eutectic Solvents

Deep eutectic solvents (DESs) are eutectic mixtures formed from quaternary ammonium salts, such as choline chloride, that have been complexed with simple hydrogen bond donors, such as ethylene glycol and urea.³³ The eutectic point is a point on a crystallisation curve which has the greatest freezing point depression. In DESs, the eutectic point is often significantly lower than the melting point of the two individual components. This depression in the melting point arises from a strong interaction between the two components forming a material with a reduced lattice enthalpy.⁴⁹

Lattice enthalpies tend to be small for large and weakly coordinating ions, as they cannot pack together easily and the charges on these ions are more delocalised. There is a substantial entropy difference between the solid and gaseous states due to conformational flexibility of the (often bulky and asymmetric) anion. When these two parameters are combined, small lattice energies are produced. This lattice energy, which can be defined for an ionic compound as “the change in internal energy that accompanies the formation of one mole of the solid from its constituent gas-phase ions at 0 K,”⁵⁰ can then be overcome by the free energy of solvation of the ions in the bulk solvent, resulting in a liquid phase.

For instance, the 1:2 choline chloride: urea DES (Reline) has a freezing point of 12°C, whereas the separate solids have melting points of 302°C and 133°C, respectively.²³ The formation of the eutectic is aided by charge delocalisation due to hydrogen bonding of the chloride to the hydrogen bond donor. The depression in freezing point is less for DESs than for chloroaluminates, however there is the opportunity for a wide range of hydrogen bond donors to be used, some of which are depicted in **Table 1.5**, producing an extensive range of liquids.

DESs are relatively highly conducting solvents (*ca.* 1 to 10 mS cm⁻¹ at 30°C), which indicates that the ionic species are dissociated within the liquid and can move independently.²³ They have properties which are comparable to most imidazolium liquids.⁴¹ The viscosity and conductivity of DESs are strongly affected by both the hydrogen bond donor and the quaternary ammonium salt, which suggests that these two properties could potentially be tailored to suit a specific process.

Table 1.5 Common hydrogen bond donors (HBDs) used in combination with choline chloride for DES formation.^{23, 33}

HBD structure	HBD name	Ratio of Cl ⁻ :HBD	DES
	Ethylene glycol	1:2	Ethaline
	Propylene glycol	1:2	Propaline
	Urea	1:2	Reline
	Oxalic acid	1:1	Oxaline
	Malonic acid	1:1	Maline

In addition, DESs have similar solvent properties to ionic liquids, but are easier to produce on a large scale, as the separate components are less reactive than those of traditional ionic liquids. However, the DESs reported so far are completely miscible with water and therefore cannot be used for aqueous biphasic extraction.

1.4 Metal processing from ionic liquids

Ionic liquids have been applied to most of the processes in *Table 1.1*, although the majority of past work has been carried out in the field of extraction. One of the reasons

for this is the practicality of using ionic liquids on a large scale: metal solubilities are unlikely to exceed 10%, meaning the need for at least a 10-fold excess of ionic liquid even for relatively soluble salts. Physical losses and mutual solubilities with water will limit the range of ionic liquids that are suitable for use. Physical losses from digestion tend to be large due to absorption onto the sample matrix. It is therefore likely that only high value metals will be extracted with ionic liquids, especially for the second generation discrete anion liquids. Their high cost and viscosity means that they are better suited to small volume applications, which can be beneficial as it means that metals can be concentrated from large volumes of aqueous solution into small volumes of ionic liquids. Replacing the traditional ionic liquids with deep eutectic solvents (DESs) may be advantageous because of their relatively low cost (compared to the imidazolium-based ionic liquids) and environmental compatibility.

1.4.1 Digestion of oxides and metals

In aqueous solutions, the oxidation of metals from their elemental state is usually carried out using strong oxidising agents such as sulphuric acid, nitric acid or *aqua regia*. The digestion of metal oxides also requires the use of strong acids or bases, such as sulphuric acid or ammonia, to compete with the ~55 M concentration of water. In ionic liquid and DES media, these strong oxidising agents are mostly unnecessary as there is no competition from water. One of the major issues associated with digestion is the solubility of the metals and metal oxides in the chosen ionic liquids. Very little work has been carried out into the factors that control solubility, mainly due to the lack of consistent data in a single ionic liquid with a given series of comparable solutes.

1.4.1.1 Chloroaluminate liquids

One of the first studies of the digestion of metal salts in ionic liquids was by Dai *et al.*, who studied the dissolution of UO_3 in imidazolium chloroaluminate melts.⁵¹ The solubility of UO_3 was found to be within the range of 1.5 to $2.5 \times 10^{-2} \text{ mol dm}^{-3}$ in Lewis basic melts and the main species was $[\text{UO}_2\text{Cl}_4]^{2-}$. Although chloroaluminate liquids might not be the most suitable choice for digestion because of their high water sensitivity and high initial metal ion concentration, they have provided the catalyst for all subsequent novel solvatometallurgical processes.

1.4.1.2 Discrete anion liquids

The first digestion study of a complex matrix in discrete anion ILs was done by Huang *et al.*, who used an imidazolium $[\text{PF}_6]^-$ salt to study the recovery of nano-scale zinc particles from phosphor ashes.⁵² Classical solubility models are more difficult to apply to these types of processes due to the current lack of data on the species formed. Speciation of metals in solution is a complex issue which is largely dependent on the Lewis acidity of the metal and the Lewis basicity of any possible ligands that are available in the ionic liquid. To determine the speciation of metals in ionic liquids a wide range of techniques have been previously employed, most of which have largely been centred on EXAFS, Raman, FAB-MS and UV-visible spectroscopy.^{43, 53}

By using bis(trifluoromethanesulfonyl)amide based ionic liquids for digestion and electrochemistry, an effort to investigate the complexation that arises with these relatively weak ligands has been initiated. Through a combination of EXAFS, Raman, X-ray crystallography and NMR, unexpected complexes were shown to form. For instance, the dissolution of AlCl_3 in 1-butyl-1-methylpyrrolidinium bis(trifluoromethanesulfonyl)amide is shown to form one of the complexes

$[\text{AlCl}_3(\text{Tf}_2\text{N})]^-$ or $[\text{AlCl}_2(\text{Tf}_2\text{N})]^{2-}$.⁵⁴ Nockemann *et al.* used betainium bis(trifluoromethanesulfonyl)amide ($[\text{Hbet}][\text{Tf}_2\text{N}]$) for the dissolution of europium and yttrium oxides, which resulted in the formation of the monomeric species $[\text{Eu}_2(\text{bet})_8(\text{H}_2\text{O})_4][\text{Tf}_2\text{N}]_6$, $[\text{Eu}_2(\text{bet})_8(\text{H}_2\text{O})_2][\text{Tf}_2\text{N}]_6 \cdot 2\text{H}_2\text{O}$ and $[\text{Y}_2(\text{bet})_6(\text{H}_2\text{O})_4][\text{Tf}_2\text{N}]_6$. The metal oxide is either protonated or substituted by the anionic component of the solvent.⁵⁵ A second investigation by the same group on the dissolution of uranium oxide in $[\text{BMIM}][\text{Tf}_2\text{N}]$ found that results suggested the existence of $[\text{UO}_2(\text{NO}_3)_3]^-$, *i.e.* for these more highly charged ions, oxide was still bound to the metal centre.⁵⁶

The solvation of metal ions in ionic liquids is still poorly understood, mainly because of the complexity of the interactions between the solute and ionic components. A review by Kobrak has attempted to express the links between liquid structure, dynamics and solvation.⁵⁷ Polarity parameters have been measured for ionic liquids^{58, 59} and have been shown to be good at predicting kinetics of reactions in ionic liquids where hydrogen bonding interactions dominate.⁶⁰ However, these parameters are not an accurate measurement of Lewis acidity and basicity and are therefore less informative for metal oxide solubility.

Whitehead *et al.* studied the recovery of gold and silver from ores using 1-butyl-3-methylimidazolium hydrogen sulphate $[\text{BMIM}][\text{HSO}_4]$ with iron (III) sulphate as the oxidant and thiourea as a complexing agent. A relatively high yield for both gold (>85%) and silver (>60%) was obtained at room temperature, although the rate of recovery was fairly slow. The process was reasonably selective over the other metals present in the ore (Cu, Zn, Pb and Fe) and the results were comparable with the analogous sulphuric acid system. An additional benefit was that the ionic liquid could be recycled by stripping any remaining dissolved species with activated carbon and then reused. Further studies investigated the effect of water content on the system, along with

variation of the sulphide complexing agent and the anionic component of the ionic liquid.^{61, 62}

1.4.1.3 Deep eutectic solvents

Extensive studies into the solubilities of a range of metals and their salts in a variety of DESs have been made by Abbott *et al.*^{27, 28} These novel solvents have the ability to dissolve a wide range of metal oxides and the solubility of 17 metal oxides in the elemental series Ti to Zn has been reported in three different DES based on choline chloride.⁶³ A selection of this data is shown in **Table 1.6**, with comparison made to the solubility of metal oxides in hydrochloric acid (HCl). Although HCl still provides the most solubility for the majority of the metals, it can be seen quite clearly that for some metals DESs have comparable solubility strength. Due to the high anionic concentrations in DES, these liquids will often form complexes with the metal ions in solution.⁴³ By judicious choice of the hydrogen bond donor, selectivity for the extraction of specific metals from a complex matrix can then be obtained.³³

DESs have been shown to have similar solvent properties to discrete anion liquids⁶⁴ but have the additional advantage of being easier to produce on a large scale, which has obvious implications for metal recovery processes. Ligands such as urea, thiourea and oxalate are already well-known complexing agents for a range of metals and can also be included as part of the ionic liquid. These liquids can then be used to electrochemically separate metals from a complex mixture.⁶⁵

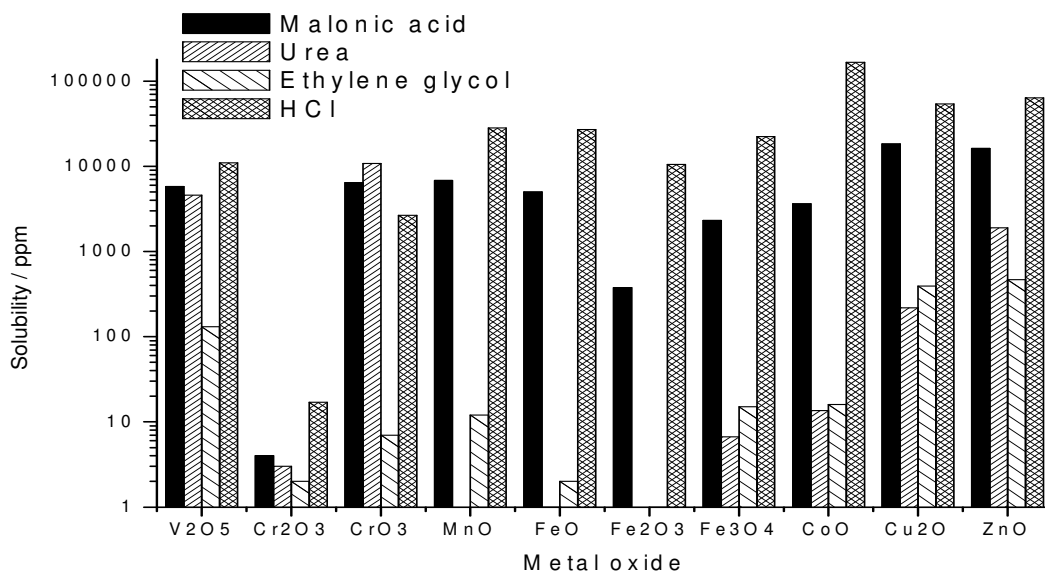


Table 1.6 Graph showing the solubility of a range of d-block metal oxides dissolved in three different DESs, compared to HCl.⁶⁷

In **Chapter 6**, we describe the effects of using iodine as a stable, reversible electrocatalyst for the dissolution of a range of metals in DES.⁶⁸ The redox potential of I_2/I^- was shown to be more positive than most common metals and could be even used for the oxidation of gold.⁶⁹ It could also be used for the electrocatalytic dissolution of copper/zinc mixtures and the copper could be recovered quantitatively by electrodeposition.

1.4.2 Extraction

Non-aqueous solvents have a long history in metal processing for the extraction of metals from an aqueous solution by using an organic solvent containing a complexing agent that is immiscible with the aqueous phase⁷⁰ and this area is one of the first to which ionic liquids have been applied and remains the most widely studied. Ionic

liquids are not just simple replacements for organic solvents, as some ionic liquids become mutually soluble with water when neutral extractants are included, decreasing extraction efficiency.⁷¹ Most of the previous studies have used classical non-aqueous ligands dissolved in a range of liquids to partition metals.

So far, the majority of studies into the extraction of metals from ionic liquids have used imidazolium cations and Rogers *et al.* were the first to use ionic liquids with discrete anions for biphasic extractions.⁷² Ionic liquids have also been used for the extraction of organic solutes⁷³ and biomolecules.⁷⁴ The use of ionic liquids for metal ion extraction can be split generally into three main methodologies; classical, neutral ligands being used to complex metal ions, the selective extraction of metals through anion interaction and task-specific ionic liquids. One of the first studies into the extraction of metals from aqueous solutions was by Dai *et al.* through the use of crown ethers and calixarenes.⁷⁵ It was found that by using ionic liquids instead of organic solvents, large distribution coefficients could be achieved.

The mechanism of metal extraction is important as it governs the viability of a process. Efficient extraction of metals can only be achieved if the ionic liquid part of the system does not leach out during extraction process. Charged complexes are more soluble in ionic liquids and the transfer of ionic species must be accompanied either by an ion of the opposite charge from the aqueous phase or of an ion of the same charge from the ionic liquid going into the aqueous phase. Compared to most non-aqueous solvents, the mechanism in ionic liquids is different, primarily due to the difference in the speciation of the metal as it transfers between the two phases.

One example where this difference in metal speciation can be seen is for the extraction of strontium from an aqueous nitric acid solution using an 18-crown ligand. If a non-aqueous solvent is used, two axial nitrate ligands are seen to bind to the metal

centre, giving a neutral strontium complex. If instead the ionic liquid [C₅MIM][Tf₂N] is used as the extraction phase, a cationic strontium complex with axial water ligands is formed.^{76, 77} Although they are less well studied, acidic and neutral ligands can provide interesting parallels to molecular non-aqueous solvents, in that mostly neutral complexes are transferred. This can assist in the easier prediction of extraction behaviour.

Nockemann *et al.* used hydrophobic ionic liquids with the hexafluoroacetylacetonate (hfac) anion to extract neodymium, cobalt and copper salts from aqueous solution. The aqueous phase of the metal salt reacts with the ionic liquid phase to form anhydrous anionic hfac complexes. Once the ionic liquid is saturated with metal ions, the metal complexes precipitate out of solution.⁷⁸ Interestingly, by supporting ionic liquids on silica particles, rare earth metal ions can be extracted from solution. With the undiluted hydrophobic ionic liquid trihexyl(tetradecyl)phosphoniumchloride, transition elements such, as iron, cobalt, copper, manganese and zinc, have been separated from rare earth elements, such as neodymium and samarium, *via* extraction from aqueous HCl solution with high extraction coefficients.⁷⁹

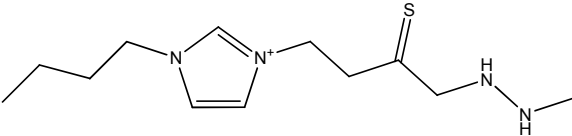
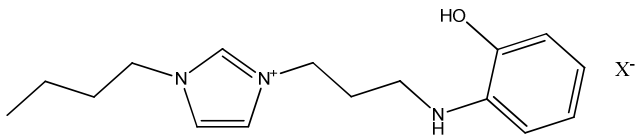
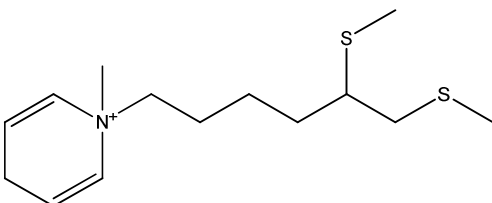
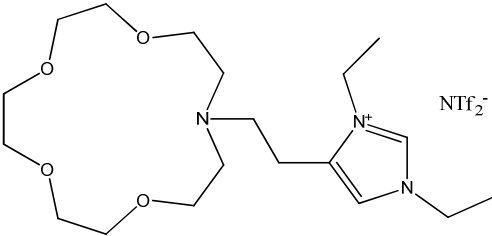
High extraction coefficients were also obtained by Liu *et al.* through the use of binary mixtures of imidazolium and phosphonium ionic liquids.⁸⁰ These materials show similar properties to ion exchange resins, such as a high interfacial surface area, and are easier to modify because there is a simple physical relationship between the ionic liquid and its support.

1.4.2.1 Task-specific ionic liquids

Task-specific ionic liquids (TSILs) are ionic liquids which have been designed and synthesised with functional groups to perform a specific task.⁸¹ This allows the ionic liquid to simultaneously be both a solvent and a complexing agent, simply by chemically modifying one of the constituents or using a complexing agent as the anionic component of the liquid. A range of metals have already been extracted with TSILs, and these are shown in **Table 1.7**. Visser *et al.*⁸² have developed TSILs that incorporate fragments of monoaza-crown ethers on imidazolium cations and can be used for the biphasic extraction of Cs^+ and Sr^{2+} . If urea or thiourea functionalities were added instead and combined with $[\text{PF}_6^-]$ anions, the extraction efficiencies of these liquids for Hg^{2+} and Cd^{2+} were reported as being several orders of magnitude larger than organic solvents.⁴⁵ Further studies showed that when a mixture of the TSIL and 1-alkyl-3-methylimidazolium hexafluorophosphate was used, the extraction efficiency was dependent on the proportion of TSIL present.

Nockemann *et al.* tested the dissolution of a range of metal oxides, including PbO , ZnO , CuO , Ag_2O and NiO , along with various lanthanides, in the protonated betaine bistriflamide ionic liquid $[\text{Hbet}][\text{Tf}_2\text{N}]$.⁸³ The metal salts could then be stripped from the ionic liquid by treatment with an acidic aqueous solution. Above 55°C both phases were miscible but separated out below this temperature. A more in-depth study of cations functionalised with carboxylate groups showed that they were also effective at dissolving a similarly wide range of metal oxides, although the relevant solubilities were not quantified.⁸⁴

Table 1.7 Task specific ionic liquids used for metal extraction

TSIL	Metal	Ref
$(\text{CH}_3)_3\text{N}^+\text{CH}_2\text{COO}^-$	Sc ₂ O ₃ , Y ₂ O ₃ , La ₂ O ₃ , Pr ₆ O ₁₁ , Nd ₂ O ₃ , Sm ₂ O ₃ , Eu ₂ O ₃ , Gd ₂ O ₃ , Tb ₄ O ₇ , Dy ₂ O ₃ , Ho ₂ O ₃ , Er ₂ O ₃ , Tm ₂ O ₃ , Yb ₂ O ₃ , Lu ₂ O ₃ , UO ₃ , PbO, ZnO, CdO, HgO, CuO, Ag ₂ O, NiO, PdO	83, 84
	Hg ²⁺ , Cd ²⁺	85
 Where X = N(CF ₃ SO ₂) ₂ ⁻ X = PF ₆ ⁻	Am ³⁺	86
	Zn ²⁺ , Cd ²⁺ , Hg ²⁺ , Tl ⁺ , Pb ²⁺ , Sn ⁴⁺ , Ba ²⁺	87
	Cs ⁺ , Sr ²⁺	88

The distribution coefficients of 14 metal ions into a range of hydrophobic pyridinium, pyrrolidinium and piperidinium liquids, with BF_4^- , OTf^- and nonafluorobutyl sulfonate anions, was studied by Papaiconemou *et al.*⁸⁷ Good extraction was observed for mercury ions however other metals could not be significantly extracted. To obtain a high extractive selectivity, functional groups could be added to the cations, such as disulfide or nitrile. The addition of aminodiacetic acid moieties to imidazolium cations as di-*t*-butyl esters by Harjani *et al.* were found to be effective chelators for Cu^{2+} , Ni^{2+} and Co^{2+} from aqueous solution.⁸⁹ A range of generic synthetic methods has already been devised to produce modified cation structures but there is still significant scope to tailor new metal-specific cations. In addition, the high cost of IL synthesis can be offset by supporting the IL in an inorganic or polymeric substrate.

One alternative to this approach is to include a well-known anionic complexing agent as the anion of the ionic liquid. Jensen *et al.* studied the extraction of lanthanides with 2-thenoyltrifluoroacetone (Htta) in a biphasic RTIL-water system.⁹⁰ It was found that anionic complexes, such as $\text{Nd}(\text{tta})_4^-$ and $\text{Eu}(\text{tta})_4^-$, were formed if $[\text{BMIM}][\text{Tf}_2\text{N}]$ was used as the solvent. If compared with the species that form in non-polar molecular solvents, it was seen that the hydrated and neutral complexes $\text{M}(\text{tta})_3(\text{H}_2\text{O})_n$ (where $n = 2$ or 3) would form instead. Therefore, formation of the anionic lanthanide complexes requires the transfer of anions from the ionic liquid into the aqueous phase. Similarly, Mehdi *et al.* used alkyl imidazolium-based ionic liquids containing hexafluoroacetylacetonate (hfac) anions to extract Nd^{3+} , Co^{2+} and Cu^{2+} .⁷⁸ To confirm the speciation of said metals, X-ray crystallography was used and $[\text{BMIM}][\text{Nd}(\text{hfac})_4]$ and $[\text{BMIM}][\text{Co}(\text{hfac})_3]$ were isolated.

Metal ions such as Fe^{3+} , Cu^{2+} , Ni^{2+} and Mn^{2+} were extracted from aqueous solutions by Egorov *et al.* through the use of trioctylmethylammonium salicylate.⁹¹ The salicylate-based ionic liquid could also be used to modify and electrode surface and it was shown that stripping voltammetry could be used to determine the concentration of metal ions in the aqueous solutions. This methodology could potentially be used for direct, selective electrowinning of metals from aqueous solution.

1.4.3 Electrowinning and cementation

Electrowinning is one of the most common methods of recovering metals from solution and an important factor in this process is the electrochemical window. This is the potential range in which the electrolyte is neither reduced nor oxidised at the electrode surface. Some ionic liquids have very large potential windows, for example up to 4.15 V for [BMIM][PF₆] at a Pt electrode,⁹² and up to 5.5 V for [BMP][Tf₂N] at a glassy carbon electrode.⁹³ These potential windows are important as hydrogen can be evolved outside of these limits in aqueous systems, which can be hazardous and lead to brittle electrodeposits (hydrogen embrittlement). Ionic liquids may even be chemically altered and destroyed if potential limits are not considered. These wide potential windows can make it possible to electrodeposit elements, such as aluminium, magnesium, germanium and silicon that are not accessible from other media.⁹⁴⁻⁹⁷ Addition of water to these systems causes a decrease in the potential window, as the water molecules will aggregate at the electrode surface and encourage hydrogen evolution.⁹⁸ The effect of water on imidazolium-based systems has been studied by Schroeder *et al.*⁹² and Matsumoto⁹⁹ and it was found that the cathodic limits were reduced by ~2 V.

Metals can, in principle, be selectively electrowon from complex solution mixtures if the redox potentials are sufficiently different. Recent work has shown that some metal salts behave like ideal solutions in some ionic liquids.⁶⁸ This means that redox potentials can therefore be predicted as a function of concentration, without having to worry about the activity coefficient.

In aqueous solutions, redox potentials can be selectively shifted by careful choice of appropriate ligands. The same should theoretically be achievable by using the same ligands in ionic liquids; however the relative strengths of any potential metal-anion complexes are currently unknown. The first studies into a comparable electrochemical series in two DESs are described in **Chapter 3** of this thesis.⁶⁸

When applying electrowinning to a process, there are several technical issues that must first be addressed, one of which is side reactions at the counter electrode. In water, it is generally oxygen that is evolved at the anode but for an ionic liquid, decomposition is distinctly undesirable as it can alter the properties of the solution, potentially rendering it useless. The alternatives to this are a soluble anode, also undesirable due to solution composition changes, or a sacrificial species which produces a gas upon decomposition. Another alternative is to use an electrocatalyst to oxidise metallic species and collect them at the cathode.

Chloroaluminate liquids were among the first ionic liquids to be used for the direct electrodeposition of metals, due to their ability to dissolve an extensive range of other metals. By varying the Lewis acidity of the liquid from acidic, through neutral, to basic, different metals can be processed and recovered.

Neutral chloroaluminate melts have been used by Gray *et al.*¹⁰⁰ and Piersma *et al.*¹⁰¹ for the electrodeposition of sodium and lithium, respectively, in a high proton environment. Neither of these metals could be deposited from basic or acidic

environments. It was found that the proton rich, NaCl or LiCl buffered, neutral liquid had an expanded electrochemical window in the cathodic direction, such that the alkali metal region could be accessed. Gallium has been electrodeposited from both chloroaluminate¹⁰² and chlorogallate¹⁰³ Lewis acidic ionic liquids. In these Lewis acidic melts, Ga³⁺ has been seen to initially reduce to Ga⁺ and from there to gallium metal. No alloying with of the gallium with the aluminium was observed in the Ga⁺ to Ga⁰ region.

Indium could be electrodeposited onto glassy carbon, tungsten and nickel from basic chloroaluminate melts in a one-step three-electron reduction process of the [InCl₅]²⁻ complex, directly to indium metal.¹⁰⁴ Carpenter *et al.* also reported the In⁺ species being deposited.¹⁰⁵ When using acidic chloroaluminate melts, it was found that indium cannot be electroplated independently, but if an ionic liquid based on InCl₃ and organic salts is used, an alloy of indium and antimony can instead be obtained.¹⁰⁵

By using air and water stable ionic liquids, a wide range of different metals have been electrodeposited, including less reactive metals, highly reactive metals and refractory metals. Giridhar *et al.* have shown that metals can be extracted from aqueous solution into an ionic liquid phase and subsequently electrodeposited.¹⁰⁶ Palladium was extracted from an aqueous nitric acid solution using tri-*n*-octylmethylammonium-chloride and -nitrate and it was shown that Pd could then be directly electrodeposited onto an electrode in the ionic liquid phase. However, as significant amounts of water and acid were carried over into the ionic liquid, the metal extraction efficiency was decreased due to an elevated acid concentration in the ionic liquid phase.

Copper has been electrodeposited from DES solution by Abbott *et al.*⁹⁸ It was observed that from the neat DES a powdery black deposit was obtained, but on the addition of a suitable complexing agent, shiny deposits were produced instead. Complexing agents assist the formation of smooth and shiny metal deposits by making

it harder to reduce the metal in solution. Nucleation is hindered, leading to less nuclei being formed, and therefore the crystals present are allowed to grow to a greater size before coming into contact with another crystal. Zinc and tin could also be electrodeposited from Ethaline and Reline. The deposited sample had a different morphology depending on the liquid used: two separate phases formed in Ethaline and a homogeneous alloy phase formed in Reline.¹⁰⁷ It has been proposed that the change in deposition morphologies is caused by a change in speciation of the metal salts in the two different DESs. In Reline, the only zinc species observed was ZnCl_3^- , however in Ethaline, three different zinc species were observed: $[\text{ZnCl}_3]^-$, $[\text{Zn}_2\text{Cl}_5]^-$ and $[\text{Zn}_3\text{Cl}_7]^-$. This would suggest that urea is stronger ligand for $[\text{ZnCl}_3]^-$ and that speciation and morphology can be controlled by the choice of hydrogen bond donor.

Cementation is a commonly used alternative to electrowinning. A more reactive metal (often in powder form) is added to the solution containing metal ions. The metal in the solution chemically oxidises this added metal and is deposited on its surface. While commonly used in aqueous solutions it cannot be used in acidic matrix due to the hydrogen evolution side reaction. This method has been applied to the extraction of lead from electric arc furnace dust using ionic liquids.³⁵ The advantage of this technology over the corresponding aqueous method is that the deposit obtained is porous, ensuring complete dissolution of the sacrificial additive and efficient extraction of metal from solution. This process has also been applied to the immersion coating of silver onto copper.¹⁰⁸

1.5 Project objectives

The main objectives of this project are to:

- Create a new and stable reference electrode for use in DES media
- Create a redox series for metal chloride salts in DES media
- Determine the speciation of metal salts dissolved in DESs
- Dissolve, separate and recover the individual metals from scrap alloys

In order to separate and recycle the individual metals from scrap alloys by electrodisolution, it is necessary to understand their redox potentials in the chosen electrolyte. In this case, the electrolyte will be a DES, for which there is currently no redox series. When creating a redox series, a **stable reference electrode** is essential, along with an understanding of the effects of solute concentration on the redox potential of the cell. In aqueous solutions an Ag/AgCl electrode is often used, however this is not suitable for use in ionic liquid media due to liquid junction potentials. In ionic liquids, a silver wire directly in contact with the solution can be used as a quasi-reference electrode. We have discovered that this form of reference electrode does not provide a constant potential, since the silver wire can react with components of the system under investigation. Therefore a new reference electrode for use in ionic liquid media will be created.

There is currently no **redox series** of metal salts in ionic liquids, so it is necessary to create a redox series in the relevant solvents, using this new reference electrode. It will also allow us to identify the effects of solute concentration on the redox potentials. In addition, the electrochemical series in ionic liquids may be different from that in aqueous systems, potentially allowing access to different procedures for the recovery of metals.

To fully understand and utilise the redox properties of the metal salts in solution, one must first understand their **speciation**. Previously, Abbott *et al.* have investigated the speciation of a range of metal oxides in Reline and Maline with fast atom bombardment mass spectrometry (FAB-MS).⁶³ However, as the species are recorded in the gas phase it is not certain that the speciation will be accurate for the bulk solution, as they may have disintegrated during ionisation and vaporisation. An alternative *in-situ* method for determination of metal speciation is extended X-ray absorption fine structure (EXAFS), where the speciation of the metal salts can be studied in the solution, with minimal sample destruction.

Once these four issues have been addressed, it is then possible to begin the **separation of individual metals** from scrap alloys. The copper-indium-gallium (CIG) samples and the copper-gallium (CG) samples for this project were obtained from MCP Ltd, in Wellingborough. The main aim of this project is to separate the constituent metals from the CIG and CG alloys, especially the gallium and indium as they are the high value metals: in 2009 gallium was \$480/kg and indium was \$500/kg.¹⁰⁹

1.6 References

1. F. Habashi, *Hydrometallurgy*, 2005, **79**, 15-22.
2. C. K. Gupta and T. K. Mukherjee, *Hydrometallurgy in extraction processes*, CRC Press, Boca Raton, Fla., 1990.
3. M. Pourbaix, *Atlas of electrochemical equilibria in aqueous solutions*, National Association of Corrosion Engineers, Houston, Tex., 1974.
4. C. Vayenas, *Modern Aspects of Electrochemistry*, Springer, 2007.
5. W. H. Kruesi and D. J. Fray, *Metallurgical Transactions B-Process Metallurgy*, 1993, **24**, 605-615.

6. D. J. Fray and G. Z. Chen, *Materials Science Technology*, 2004, **20**, 295-300.
7. K. R. Seddon, *Nature Materials*, 2003, **2**, 363-365.
8. P. Wasserscheid and T. Welton, *Ionic liquids in synthesis*, Wiley-VCH, Weinheim, 2008.
9. P. Walden, *Bull. Acad. Imper. Sci. (St. Petersburg)*, 1914, 1800.
10. N. V. Plechkova and K. R. Seddon, *Chemical Society Reviews*, 2008, **37**, 123-150.
11. J. G. Huddleston, A. E. Visser, W. M. Reichert, H. D. Willauer, G. A. Broker and R. D. Rogers, *Green Chemistry*, 2001, **3**, 156-164.
12. J. Wilkes, *Journal of Molecular Catalysis A: Chemical*, 2004, **214**, 11-17.
13. C. Chiappe and D. Pieraccini, *Journal of Physical Organic Chemistry*, 2005, **18**, 275-297.
14. P. Böhne, A. P. Dias, N. Papageorgiou, K. Kalyanasundaram and M. Grätzel, *Inorganic Chemistry*, 1996, **35**, 1168-1178.
15. A. A. Fannin, D. A. Floreani, L. A. King, J. S. Landers, B. J. Piersma, D. J. Stech, R. L. Vaughn, J. S. Wilkes and J. L. Williams, *Journal of Physical Chemistry*, 1984, **88**, 2614-2621.
16. K. N. Marsh, J. A. Boxall and R. Lichtenthaler, *Fluid Phase Equilibria*, 2004, **219**, 93-98.
17. P. Wasserscheid and W. Keim, *Angewandte Chemie-International Edition*, 2000, **39**, 3773-3789.
18. E. F. Smith, F. J. Rutten, I. J. Villar-Garcia, D. Briggs and P. Licence, *Langmuir*, 2006, **22**, 9386-9392.
19. A. M. O'Mahony, D. S. Silvester, L. Aldous, C. Hardacre and R. G. Compton, *Journal of Chemical & Engineering Data*, 2008, **53**, 2884-2891.

20. N. Gathergood, P. J. Scammells and M. T. Garcia, *Green Chemistry*, 2006, **8**, 156-160.
21. Z. Y. Du, Z. P. Li, S. Guo, J. Zhang, L. Y. Zhu and Y. Q. Deng, *Journal of Physical Chemistry B*, 2005, **109**, 19542-19546.
22. K. Fukumoto, M. Yoshizawa and H. Ohno, *Journal of the American Chemical Society*, 2005, **127**, 2398-2399.
23. A. P. Abbott, G. Capper, D. L. Davies, R. K. Rasheed and V. Tambyrajah, *Chemical Communications*, 2003, 70-71.
24. F. H. Hurley and Thomas P. Wier Jr., *Journal of the Electrochemical Society*, 1951, **98**, 203-206.
25. F. H. Hurley and Thomas P. Wier Jr., *Journal of the Electrochemical Society*, 1951, **98**, 207-212.
26. J. S. Wilkes, J. A. Levisky, R. A. Wilson and C. L. Hussey, *Inorganic Chemistry*, 1982, **21**, 1263-1264.
27. P. Wasserscheid and T. Welton, *Ionic liquids in synthesis*, Wiley-VCH, Weinheim, 2003.
28. C. L. Hussey, *Pure and Applied Chemistry*, 1988, **60**, 1763-1772.
29. A. P. Abbott, G. Capper, D. L. Davies, H. L. Munro, R. K. Rasheed and V. Tambyrajah, *Chemical Communications*, 2001, 2010-2011.
30. N. Koura, T. Endo and Y. Idemoto, *Journal of Non-Crystalline Solids*, 1996, **207**, 650-655.
31. M. S. Sitze, E. R. Schreiter, E. V. Patterson and R. G. Freeman, *Inorganic Chemistry*, 2001, **40**, 2298-2304.
32. A. P. Abbott, G. Capper, D. L. Davies and R. K. Rasheed, *Chemistry-A European Journal*, 2004, **10**, 3769-3774.

33. A. P. Abbott, D. Boothby, G. Capper, D. L. Davies and R. K. Rasheed, *Journal of the American Chemical Society*, 2004, **126**, 9142-9147.
34. A. P. Abbott, G. Capper, D. L. Davies, R. K. Rasheed and P. Shikotra, *Inorganic Chemistry*, 2005, **44**, 6497-6499.
35. A. P. Abbott, J. Collins, I. Dalrymple, R. C. Harris, R. Mistry, F. L. Qiu, J. Scheirer and W. R. Wise, *Australian Journal of Chemistry*, 2009, **62**, 341-347.
36. J. S. Wilkes and M. J. Zaworotko, *Journal of the Chemical Society-Chemical Communications*, 1992, 965-967.
37. J. Fuller, R. T. Carlin and R. A. Osteryoung, *Journal of the Electrochemical Society*, 1997, **144**, 3881-3886.
38. B. M. Quinn, Z. F. Ding, R. Moulton and A. J. Bard, *Langmuir*, 2002, **18**, 1734-1742.
39. R. P. Swatloski, J. D. Holbrey and R. D. Rogers, *Green Chemistry*, 2003, **5**, 361-363.
40. F. Endres, D. MacFarlane and A. Abbott, *Electrodeposition from Ionic Liquids*, Wiley-VCH, 2008.
41. T. Welton, *Chemical Reviews*, 1999, **99**, 2071-2083.
42. H. Tokuda, K. Hayamizu, K. Ishii, M. A. Susan and M. Watanabe, *The Journal of Physical Chemistry. B*, 2005, **109**, 6103-6110.
43. A. P. Abbott, G. Frisch and K. S. Ryder, *Annual Reports on the Progress of Chemistry, Section A: Inorganic Chemistry*, 2008, **104**, 21-45.
44. L. C. Branco, J. N. Rosa, J. J. M. Ramos and C. A. M. Afonso, *Chemistry-A European Journal*, 2002, **8**, 3671-3677.

45. A. E. Visser, R. P. Swatloski, W. M. Reichert, R. Mayton, S. Sheff, A. Wierzbicki, J. H. Davis and R. D. Rogers, *Environmental Science & Technology*, 2002, **36**, 2523-2529.
46. M. C. Buzzeo, R. G. Evans and R. G. Compton, *Chemphyschem*, 2004, **5**, 1106-1120.
47. A. P. Abbott, *Chemphyschem*, 2005, **6**, 2502-2505.
48. J. O. M. Bockris and A. K. N. Reddy, *Modern Electrochemistry*, Plenum Press, 1998.
49. I. Krossing, J. M. Slattery, C. Daguene, P. J. Dyson, A. Oleinikova and H. Weingartner, *Journal of the American Chemical Society*, 2006, **128**, 13427-13434.
50. C. E. Housecroft and A. G. Sharpe, *Inorganic Chemistry*, Pearson Prentice Hall, 2008.
51. S. Dai, Y. S. Shin, L. M. Toth and C. E. Barnes, *Inorganic Chemistry*, 1997, **36**, 4900-4902.
52. H. L. Huang, H. P. Wang, E. M. Eyring and J. E. Chang, *Environmental Chemistry*, 2009, **6**, 268-272.
53. C. Hardacre, in *Annual Review of Materials Research*, 2005, vol. 35, pp. 29-49.
54. N. M. Rocher, E. I. Izgorodina, T. Ruther, M. Forsyth, D. R. MacFarlane, T. Rodopoulos, M. D. Horne and A. M. Bond, *Chemistry-A European Journal*, 2009, **15**, 3435-3447.
55. P. Nockemann, B. Thijs, K. Lunstroot, T. N. Parac-Vogt, C. Gorller-Walrand, K. Binnemans, K. Van Hecke, L. Van Meervelt, S. Nikitenko, J. Daniels, C. Hennig and R. Van Deun, *Chemistry-A European Journal*, 2009, **15**, 1449-1461.
56. K. Servaes, C. Hennig, I. Billard, C. Gaillard, K. Binnemans, C. Gorller-Walrand and R. Van Deun, *European Journal of Inorganic Chemistry*, 2007, 5120-5126.

57. M. N. Kobrak, *Advances in Chemical Physics*, 2008, **139**, 85-137.
58. J. M. Lee, S. Ruckes and J. M. Prausnitz, *The Journal of Physical Chemistry. B*, 2008, **112**, 1473-1476.
59. A. Oehlke, K. Hofmann and S. Spange, *New Journal of Chemistry*, 2006, **30**, 533-536.
60. I. Correia and T. Welton, *Dalton Transactions*, 2009, 4115-4121.
61. J. A. Whitehead, G. A. Lawrance and A. McCluskey, *Green Chemistry*, 2004, **6**, 313-315.
62. J. A. Whitehead, J. Zhang, N. Pereira, A. McCluskey and G. A. Lawrance, *Hydrometallurgy*, 2007, **88**, 109-120.
63. A. P. Abbott, G. Capper, D. L. Davies, K. J. McKenzie and S. U. Obi, *Journal of Chemical and Engineering Data*, 2006, **51**, 1280-1282.
64. A. P. Abbott, R. C. Harris and K. S. Ryder, *The Journal of Physical Chemistry. B*, 2007, **111**, 4910-4913.
65. A. P. Abbott, G. Capper, D. L. Davies and P. Shikotra, *Mineral Processing and Extractive Metallurgy*, 2006, **115**, 15-18.
66. *Manuscript in preparation.*
67. A. P. Abbott, G. Frisch, J. Hartley and K. S. Ryder, *Green Chemistry*, 2011, **13**, 471-481.
68. A. P. Abbott, G. Frisch, S. J. Gurman, A. R. Hillman, J. Hartley, F. Holyoak and K. S. Ryder, *Chemical Communications (Camb)*, 2011, **47**, 10031-10033.
69. D. Jones, J. Hartley, G. Frisch, M. Purnell and L. Darras, in *Palaeontologia Electronica*, 2012, vol. 15.
70. J. Rydberg, *Solvent extraction principles and practice*, Marcel Dekker ; London : Taylor & Francis, New York, 2004.

71. P. G. Rickert, D. C. Stepinski, D. J. Rausch, R. M. Bergeron, S. Jakab and M. L. Dietz, *Talanta*, 2007, **72**, 315-320.
72. J. G. Huddleston, H. D. Willauer, R. P. Swatloski, A. E. Visser and R. D. Rogers, *Chemical Communications*, 1998, 1765-1766.
73. M. Matsumoto, K. Mochiduki, K. Fukunishi and K. Kondo, *Separation and Purification Technology*, 2004, **40**, 97-101.
74. S. V. Smirnova, Torocheshnikova, II, A. A. Formanovsky and I. V. Pletnev, *Analytical Bioanalytical Chemistry*, 2004, **378**, 1369-1375.
75. S. Dai, Y. H. Ju and C. E. Barnes, *Journal of the Chemical Society, Dalton Transactions*, 1999, 1201-1202.
76. M. L. Dietz and J. A. Dzielawa, *Chemical Communications*, 2001, 2124-2125.
77. M. P. Jensen, J. A. Dzielawa, P. Rickert and M. L. Dietz, *Journal of the American Chemical Society*, 2002, **124**, 10664-10665.
78. H. Mehdi, K. Binnemans, K. Van Hecke, L. Van Meervelt and P. Nockemann, *Chemical Communications (Camb)*, 2010, **46**, 234-236.
79. T. Vander Hoogerstraete, S. Wellens, K. Verachtert and K. Binnemans, *Green Chemistry*, 2013.
80. Y. Liu, L. Zhu, X. Sun, J. Chen and F. Luo, *Industrial and Engineering Chemistry Research*, 2009, **48**, 7308-7313.
81. J. J. H. Davis, *Chemistry Letters*, 2004, **33**, 1072-1077.
82. A. E. Visser, R. P. Swatloski, W. M. Reichert, R. Mayton, S. Sheff, A. Wierzbicki, J. H. Davis and R. D. Rogers, *Chemical Communications*, 2001, 135-136.

83. P. Nockemann, B. Thijs, S. Pittois, J. Thoen, C. Glorieux, K. Van Hecke, L. Van Meervelt, B. Kirchner and K. Binnemans, *The Journal of Physical Chemistry B*, 2006, **110**, 20978-20992.
84. P. Nockemann, B. Thijs, T. N. Parac-Vogt, K. Van Hecke, L. Van Meervelt, B. Tinant, I. Hartenbach, T. Schleid, V. T. Ngan, M. T. Nguyen and K. Binnemans, *Inorganic Chemistry*, 2008, **47**, 9987-9999.
85. R. Renner, *Environmental Science Technology*, 2001, **35**, 410A-413A.
86. A. Ouadi, B. Gadenne, P. Hessemann, J. J. Moreau, I. Billard, C. Gaillard, S. Mekki and G. Moutiers, *Chemistry*, 2006, **12**, 3074-3081.
87. N. Papaiconomou, J. M. Lee, J. Salminen, M. von Stosch and J. M. Prausnitz, *Industrial and Engineering Chemistry Research*, 2008, **47**, 5080-5086.
88. H. M. Luo, S. Dai, P. V. Bonnesen and A. C. Buchanan, *Journal of Alloys and Compounds*, 2006, **418**, 195-199.
89. J. R. Harjani, T. Friscic, L. R. MacGillivray and R. D. Singer, *Dalton Transactions*, 2008, 4595-4601.
90. M. P. Jensen, J. Neuefeind, J. V. Beitz, S. Skanthakumar and L. Soderholm, *Journal of the American Chemical Society*, 2003, **125**, 15466-15473.
91. V. M. Egorov, D. I. Djigailo, D. S. Momotenko, D. V. Chernyshov, Torocheshnikova, II, S. V. Smirnova and I. V. Pletnev, *Talanta*, 2010, **80**, 1177-1182.
92. U. Schroder, J. D. Wadhawan, R. G. Compton, F. Marken, P. A. Z. Suarez, C. S. Consorti, R. F. de Souza and J. Dupont, *New Journal of Chemistry*, 2000, **24**, 1009-1015.
93. D. R. MacFarlane, P. Meakin, J. Sun, N. Amini and M. Forsyth, *Journal of Physical Chemistry B*, 1999, **103**, 4164-4170.

94. J. Robinson and R. A. Osteryoung, *Journal of the Electrochemical Society*, 1980, **127**, 122-128.
95. Y. NuLi, J. Yang, J. L. Wang, J. Q. Xu and P. Wang, *Electrochemical Solid State Letters*, 2005, **8**, C166-C169.
96. W. Freyland, C. A. Zell, S. Z. El Abedin and F. Endres, *Electrochimica Acta*, 2003, **48**, 3053-3061.
97. N. Borisenko, S. Z. El Abedin and F. Endres, *Journal of Physical Chemistry B*, 2006, **110**, 6250-6256.
98. A. P. Abbott and K. J. McKenzie, *Physical Chemistry Chemical Physics*, 2006, **8**, 4265-4279.
99. H. Ohno, *Electrochemical Aspects of Ionic Liquids*, John Wiley & Sons, 2005.
100. G. E. Gray, P. A. Kohl and J. Winnick, *Journal of the Electrochemical Society*, 1995, **142**, 3636-3642.
101. B. J. Piersma, D. M. Ryan, E. R. Schumacher and T. L. Riechel, *Journal of the Electrochemical Society*, 1996, **143**, 908-913.
102. P. Y. Chen, Y. F. Lin and I. W. Sun, *Journal of the Electrochemical Society*, 1999, **146**, 3290-3294.
103. M. W. Verbrugge and M. K. Carpenter, *AIChE Journal*, 1990, **36**, 1097-1106.
104. J. S. Y. Liu and I. W. Sun, *Journal of the Electrochemical Society*, 1997, **144**, 140-145.
105. M. K. Carpenter and M. W. Verbrugge, *Journal of Materials Research*, 2011, **9**, 2584-2591.
106. P. Giridhar, K. A. Venkatesan, T. G. Srinivasan and P. R. Vasudeva Rao, *Hydrometallurgy*, 2006, **81**, 30-39.

107. A. P. Abbott, G. Capper, K. J. McKenzie and K. S. Ryder, *Journal of Electroanalytical Chemistry*, 2007, **599**, 288-294.
108. A. P. Abbott, S. Nandhra, S. Postlethwaite, E. L. Smith and K. S. Ryder, *Physical Chemistry Chemical Physics*, 2007, **9**, 3735-3743.
109. United States. Bureau of Mines. and Geological Survey (U.S.), *Mineral Commodity Summaries, 2010*, Bureau of Mines : Supt. of Docs., U.S. G.P.O., 2010.

Chapter 2 Experimental

Chapter 2	Experimental	42
2.1	Deep eutectic solvent (DES) formation and chemicals	43
2.2	Reference electrode	46
2.3	Ideal solutions and activity coefficients	48
2.3.1	In DES	49
2.3.2	In ILs	52
2.4	Redox potentials of d- and p-block metal salts in Ethaline	52
2.4.1	Cyclic voltammetry	53
2.4.2	Solutions for the determination of redox potentials	55
2.4.3	Chloro-complexes in aqueous media	56
2.4.4	DES analogues	57
2.5	Speciation of metals	57
2.5.1	EXAFS	58
2.5.2	UV-Vis spectroscopy	64
2.6	Metal processing, separation, and recovery	66
2.6.1	Analytical techniques	66
2.6.2	Anodic dissolution	68
2.6.3	Electrochemical oxidation using iodine	72
2.7	References	75

2.1 Deep eutectic solvent (DES) formation and chemicals

Ethaline was prepared from a 1:2 molar ratio mixture of choline chloride and ethylene glycol. This was heated and stirred in a beaker covered with parafilm, on a stirrer-hotplate at around 60°C until a homogenous colourless liquid had formed.

Reline and Propaline were prepared in the same manner, substituting urea or 1,2-propanediol for the ethylene glycol, respectively. A Propaline variant was also made using 1,3-propanediol instead of the 1,2-propanediol.

Oxaline was prepared from a 1:1 mixture of choline chloride and oxalic acid dihydrate. The temperature during liquid formation was reduced for this liquid to 40°C, as the oxalic acid tends to decompose if heated too much.

Table 2.1 Chemicals for DES production

Chemical	Purity	Source
Choline chloride	≥98%	Sigma-Aldrich
Ethylene glycol	≥99%	Sigma-Aldrich
Urea	98%	Aldrich
1,2-Propanediol	99%	Sigma-Aldrich
1,3-Propanediol	98%	Aldrich
Oxalic acid dihydrate	98%	Fisher

All reagents were used as-received and the resulting DESs were stored in an airtight container in an oven at 40°C when not in use, to prevent the choline chloride from precipitating out. The dry imidazolium ionic liquids, as shown in *Table 2.2*, were used as-received.

Table 2.2 *Imidazolium ionic liquids used*

Chemical	Purity	Source
1-butyl-3-methylimidazolium tetrafluoroborate	≥98%	Aldrich
1-ethyl-3-methylimidazolium thiocyanate	98%	Merck
1-ethyl-3-methylimidazolium acetate		BASF
1-butyl-3-methylimidazolium chloride	≥98%	Aldrich
1-ethyl-3-methylimidazolium trifluoromethanesulfonate	98%	Merck
1-hexyl-3-methylimidazolium chloride	98%	Merck
1-ethyl-3-methylimidazolium bis(trifluoromethylsulfonyl)imide	98%	Merck
1-ethyl-3-methylimidazolium tris(pentafluoroethyl)trifluorophosphate	98%	Merck

In addition to the more conventional DESs, three DES analogues were prepared by mixing a 1:2 ratio of chloride salt to hydrogen bond donor, followed by heating and stirring in the same manner as previously. These analogues were: choline chloride and water, lithium chloride and water and finally, lithium chloride and ethylene glycol.

Table 2.3 Metal salts used in solution preparation.

Chemical	Purity	Source
Chromium (III) chloride hexahydrate	>96%	Aldrich
Cobalt (II) chloride	99.7%	Alfa Aesar
Cobalt (II) chloride hexahydrate	99.9%	Alfa Aesar
Copper (II) acetate monohydrate	>98%	BDH
Copper (II) chloride	99%	Acros Organics
Copper (II) chloride dihydrate	99%	Aldrich
Copper (II) sulphate pentahydrate	>98.5%	S&C
Copper (II) thiocyanate	99%	Aldrich
Gallium (III) chloride	99.99%	Aldrich
Gold (I) chloride	99.9%	Aldrich
Indium (III) chloride	99.99%	Aldrich
Iron (II) chloride	99.5%	Alfa Aesar
Iron (II) chloride tetrahydrate	≥99.0%	Sigma-Aldrich
Iron (III) chloride	>97%	Fisher
Iron (III) chloride hexahydrate	≥98%	Sigma
Manganese (II) chloride	98%	Aldrich
Manganese (II) chloride tetrahydrate	≥99.9%	Sigma-Aldrich
Nickel (II) chloride hexahydrate	97%	BDH
Nickel (II) acetate tetrahydrate	≥99%	Aldrich
Palladium (II) chloride	99%	Aldrich
Platinum (II) chloride	98%	Aldrich
Silver acetate	98%	BDH
Silver chloride	99%	Sigma-Aldrich

Chemical	Purity	Source
Silver nitrate	≥99.0%	Aldrich
Silver oxide	99%	Aldrich
Silver tetrafluoroborate	98%	Aldrich
Tin (II) chloride	98%	Sigma-Aldrich
Tin (II) chloride dihydrate	98%	Aldrich
Zinc chloride	≥98%	Fluka

2.2 Reference electrode

In aqueous solutions an aqueous Ag/AgCl electrode is commonly used as a reference electrode. This electrode is comprised of a silver wire, a low saturated silver chloride concentration ($\sim 1.3 \times 10^{-5} \text{ mol dm}^{-3}$) and a known concentration of potassium chloride, either saturated ($\sim 3.5 \text{ M}$) or 1 M . This particular reference electrode cannot be used for deep eutectic solvent solutions as there will be a liquid junction potential caused by a difference in the viscosity of the aqueous reference solution and the DES. The difference in viscosity will cause a difference in the ion mobility and will add an unknown amount to the reference potential. If this electrode was made using Ethaline instead of water, it would still not be feasible as silver chloride is substantially more soluble in Ethaline. To solve this, a high Ag^+ concentration is needed to keep the relative variation in concentration low.

A reference electrode (*Figure 2.1*) for the determination of redox potentials and activity coefficients in **Chapter 3** was constructed from a 0.1 M solution of silver chloride (Sigma-Aldrich, ReagentPlus[®], 99%) in Ethaline, a cleaned (wet and dry sandpaper) silver wire and a glass electrode body with a porous Vycor glass frit, which

had been attached using heat-shrink tubing. When not in use, the electrode was stored in a vial of Ethaline and kept in an oven at 40°C to prevent the choline chloride from crystallising out of solution due to fluctuations in ambient temperature.

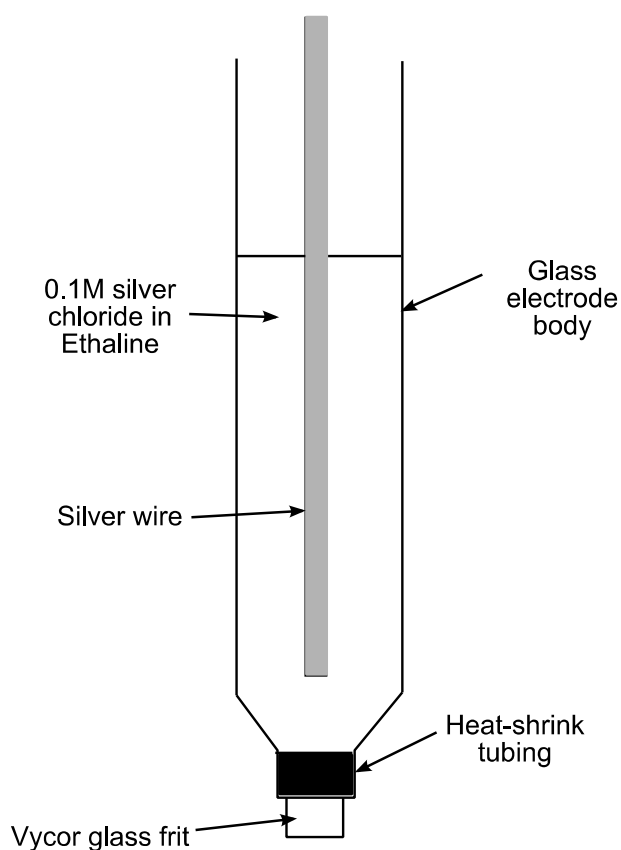


Figure 2.1 Schematic diagram of the Ag/Ag⁺ in Ethaline reference electrode.

Solutions of 100 mM anhydrous tin (II) chloride (SnCl₂), iodine (I₂) (Fisher, ≥99.5%), potassium ferrocyanide (BDH, 99.0%) and anhydrous copper (II) chloride (CuCl₂) (Acros Organics, 99%) were made up in Ethaline and used to test qualitatively whether this electrode was a suitable reference electrode, *i.e.* reversible couples do not shift potentials between subsequent scans, using cyclic voltammetry. The working electrode was a 1 mm diameter platinum disc and the counter electrode was a platinum flag. The platinum disc electrode was polished with 0.05 μm alumina powder, then rinsed with deionised water and dried with acetone prior to use. Cyclic voltammograms

(CVs) were measured at 10 mV/s, using an Autolab potentiostat, with GPES analytical software. These CVs were then normalised to the peak current of the oxidation wave for the reversible redox couple and compared with the equivalent voltammograms measured using a silver wire quasi-reference electrode in the same solutions.

2.3 Ideal solutions and activity coefficients

In aqueous solution, the concentration of the solute affects the redox potential, as the solute molecules can interact with each other. This causes a plot of the natural log of concentration versus potential to deviate from a straight line at higher concentrations (*Figure 2.2*).

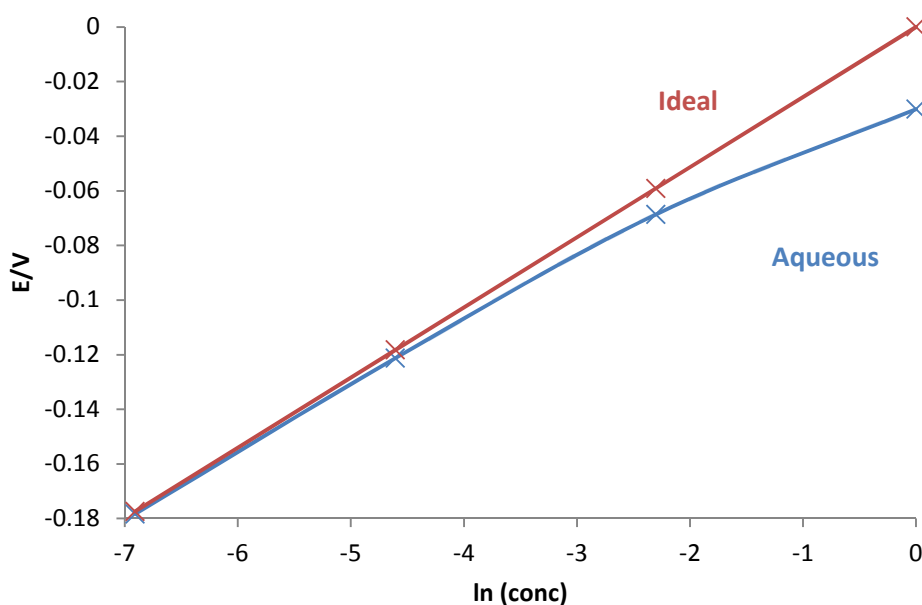


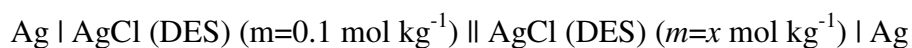
Figure 2.2 Theoretical values for CuCl_2 in aqueous system and in an ideal solution.

In ionic liquids, it can be considered that the solute molecules are electrostatically shielded from each other by the anions and cations that form the liquid. This would mean that there would be no deviations from the theoretical gradient predicted by the Nernst equation during an experiment in ionic liquids, suggesting that these ionic

liquids are ideal solutions. An ideal solution is a solution where the enthalpy of mixing is equal to zero, or a solution in which the activity coefficients are equal to one. In aqueous solvents the activity coefficient can only be considered as being one at infinite dilution.

2.3.1 In DES

The cells studied in **Chapter 3, Section 3.2.2** for the determination of redox potentials and activity coefficients in deep eutectic solvents were:



Successive dilutions (100, 50, 20, 10, 5, 2, and 1 mM) of a 0.2 M silver chloride in Ethaline solution were made up and the potential difference was measured at 0, 1, 2, 5, and 10 minute intervals at room temperature (24°C), using a Solartron Schlumberger 7060 Systems voltmeter. A two-electrode system was employed, using the previously constructed reference electrode (**Section 2.2**) vs. a silver wire. This series was measured four times. After each reading, the counter electrode was rinsed with deionised water, followed by acetone. The outside of the reference electrode was rinsed with neat Ethaline and the excess patted off. From the four repeated series of this experiment, the final potential differences after 10 minutes were averaged and plotted against $\ln(m)$, where m is molality.

To determine if this ideality is observed for metal salt solutions other than AgCl, anhydrous CuCl_2 (Acros Organics, 99%) was made into a 1 M solution in Ethaline and successive dilutions of this solution were made (500, 200, 100, 50, 20, 10, 5, 2, and 1

mM). The above process was repeated for this series, except measurements were made at 21°C and the counter electrode was a platinum flag. As the concentration of Cu⁺ in the anhydrous CuCl₂ solution was not known, a comparative series of dilutions were made with either a constant 1:10 ratio of Cu⁺ to Cu²⁺ ions or at a constant 10 mM Cu⁺ concentration with varying Cu²⁺.

The first of these two methods used a solution of CuCl₂ (100 mM) with CuCl (10 mM) (Sigma-Aldrich, ≥99%) diluted down to 50, 20, 10, 5, 2 and 1 mM, with respect to CuCl₂, using neat Ethaline. It was expected that these solutions would give a line of zero gradient, however this experiment produced a line of gradient = 0.0061 V. This is most likely due to the Cu⁺ ions in solution oxidising to Cu²⁺ over time, possibly due to reactions with atmospheric oxygen. Although the Cu^{2+/+} ratio theoretically stays the same, the actual concentration of Cu⁺ is reduced so much that the effects of any oxidation is more obvious than if there were a constant Cu⁺ concentration.

The second method used a stock solution of CuCl (10 mM) in Ethaline to both form the 1 M CuCl₂ solution and dilute it down into 500, 200, 100, 50, 20, 10, 5, and 2 mM solutions. Nitrogen was bubbled through the Ethaline for the stock solution for ~30 minutes to remove most of the oxygen from it in an attempt to prevent oxidation of the Cu⁺ ions. Four experimental runs of this series were made at 20°C. It should be noted that at this temperature, the 1 M solution was saturated and needed to be kept warm prior to measurements to reduce precipitation of the copper chloride.

To get a suitable zero-reference point for the redox potentials of these metal salts in DES it is useful to have the DES equivalent of a standard hydrogen electrode (SHE). This electrode must have a platinised platinum electrode in a 1 M acid solution with hydrogen at 1 atmosphere pressure. In order to do this, solutions of trifluoromethanesulfonic acid (F₃CSO₂H) (Sigma-Aldrich, ≥99%) in Ethaline were

made up to 1, 0.1, 0.01 and 0.001 M concentrations. Triflic acid was chosen because of its ability to fully dissociate and to hopefully provide a proton activity of exactly 1 (*i.e.* unity) in the DES. Nitrogen was initially bubbled through the solution to remove all air from the system before hydrogen readings were taken. Using the previously created reference electrode (**Section 2.2**) and a platinised platinum electrode, hydrogen was bubbled through the solution and measurements were taken after 30 minutes, at which point the voltmeter readings had become stable. The experiment was run with the cell held in a water bath at a temperature of 38°C, as at lower temperatures the solution began to form crystals. Five experimental runs of this solution were made. The set-up for this cell is depicted in **Figure 2.3**.

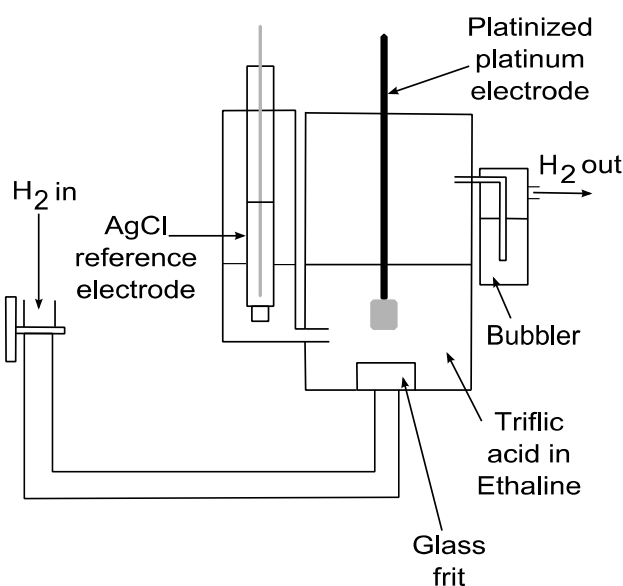


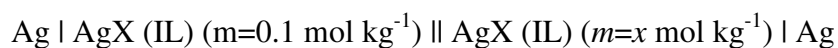
Figure 2.3 Schematic of the cell used for the determination of hydrogen redox potentials.

To create the platinised platinum electrode, a 0.072 M solution was made up of potassium tetrachloroplatinate (K_2PtCl_4) (0.0597 g, 1.438×10^{-4} mol) (Aldrich, 99.99%) in deionised water (2 ml). A platinum flag electrode was platinised in this solution for 10 minutes, with a current of 30 mA cm^{-2} and a second platinum flag was used as a

counter electrode. The electrode was cleaned prior to platinisation with concentrated HNO₃. After creation, the electrode was rinsed and stored in deionised water.

2.3.2 In ILs

To determine whether the reference electrode set-up described in **Section 2.2** is valid for solutions containing anions other than chloride, redox potentials were measured for solutions of silver salts in imidazolium ionic liquids, in **Chapter 3, Section 3.2.1**, using the same method as in **Section 2.3.1** above, for the cell



where X is acetate, chloride, tetrafluoroborate (BF₄⁻) or thiocyanate (SCN) and IL is the corresponding imidazolium liquid. Once again, solution concentrations were made to 100 mM to 1 mM of the silver salt.

It was observed for the BF₄⁻ solution that after about an hour the solution became cloudy and red, which quickly turned brown. As silver salts are often photosensitive, the experiment was repeated in a darkened environment. This modification to the experiment slowed down the formation of red particles significantly and measurements could then be obtained.

Pure [BMIM][Cl] is a solid at ambient temperatures, therefore it was necessary to both make these solutions and take the redox potential measurements at 60-80°C, instead of the much lower temperatures used for the other liquids.

2.4 Redox potentials of d- and p-block metal salts in Ethaline

Redox potentials in aqueous media are well defined versus a standard electrode, which allows easy determination of the correct potential for electrochemical applications. The same cannot also be said for DESs and therefore it is necessary to

construct a redox series for metal salts in the DES Ethaline before attempting any other electrochemical processes, such as metal separation and recovery. To be able to construct this redox series, one must first understand the redox properties of the desired metals in solution. This section will focus on the experiments and techniques used to determine the redox potentials of various metal chloride salts in Ethaline.

2.4.1 Cyclic voltammetry

Cyclic voltammetry is a technique whereby electrolysis mechanisms and redox couples can be determined by sweeping a potential between two values at a fixed rate to measure a change in current. Peaks in current will be visible wherever species are oxidised or reduced in solution. Redox potentials are commonly determined from the average of either the peak positions or from the half wave potential.¹ Here we use a different method because several of the redox processes of interest, such as metal stripping and deposition, are not completely reversible.

A general method is therefore needed to determine the redox potentials. By calculating an average of the onset potentials of the oxidation and reduction waves, errors from the variation in peak potential or half wave position are minimised. If the example of copper (II) chloride is used, *Figure 2.4*, the average of points A & B provides the redox potential for the $\text{Cu}^{+/0}$ couple and the average of points C & D provide the potential for the $\text{Cu}^{2+/+}$ couple. Values determined with this method were found to differ by less than 10 mV from the anodic and cathodic peak potentials.

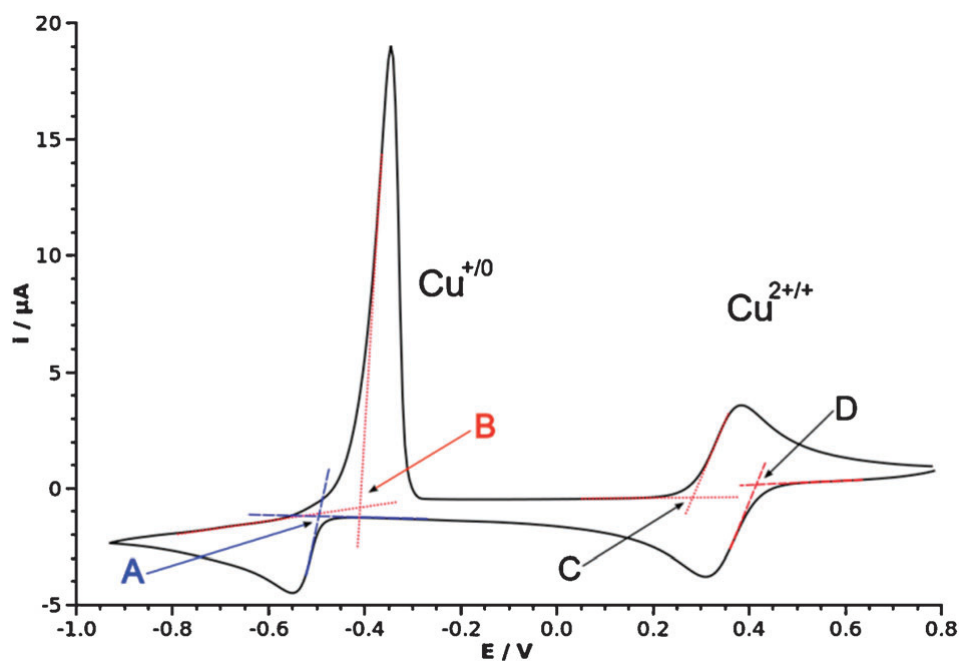


Figure 2.4 Schematic diagram showing how redox potentials can be determined from cyclic voltammetry of the relevant metal salt.² The CV of copper chloride in Ethaline is used here as an example.

A reversible redox couple such as the $\text{Cu}^{2+/.}$ couple (C & D) is generated from the reduction and oxidation of two soluble species. Reversible couples can be identified by peaks which are the same shape and magnitude in both directions. When the potential is swept in a cathodic direction, the magnitude of current will increase as a greater proportion of the species in solution are reduced. Once a certain proportion of these species have been reduced, indicated by the current minimum on the CV, the concentration of oxidised species in solution close to the working electrode will decrease and any further reduction of the metal species will become diffusion controlled. Therefore the current will also decrease in magnitude.

For a metal deposition and stripping redox couple such as Cu^{+0} (A & B) reduction of the soluble species will proceed in the same manner as for a reversible couple. However on the oxidative sweep, all oxidisable species are adhered to the surface of the

working electrode. Once all of these species are completely stripped, the current does not have the opportunity to become diffusion controlled, hence the sharp cut-off in current.

When comparing the redox potentials of the various metal couples in Ethaline to the equivalent aqueous solution, an internal standard is necessary. This is a known reversible redox couple that the silver wire pseudo-reference electrode used here can be referenced to. The $[\text{Fe}(\text{CN})_6]^{3-/4-}$ couple was used due to its high stability in high chloride environments, both DES and aqueous. The activity of the chloride ion can effectively be considered as constant due to the high chloride content (*ca.* 4.8 M) compared to the solute (*ca.* 0.1 M).

2.4.2 Solutions for the determination of redox potentials

Cyclic voltammetry was carried out for metal chloride solutions in Ethaline using a three electrode system, with a 1 mm Pt disc working electrode, a silver wire or the Ag/AgCl/Ethaline electrode developed above in **Section 2.2** as a reference electrode and a Pt flag counter electrode. Scans were measured at room temperature, with a scan rate of 10 mV s⁻¹. The potential range for each system was selected based on the position of the redox peaks with respect to the electrochemical window of the solvent. The plot of these DES potentials compared to aqueous potentials can be seen in **Chapter 3, Section 3.3**.

The solutions used were 100 mM chromium (III) chloride, manganese (II) chloride, iron (II) chloride, iron (III) chloride, cobalt (II) chloride, nickel (II) chloride, palladium (II) chloride, platinum (II) chloride, copper (II) chloride, silver chloride, gallium (III) chloride, indium (III) chloride or tin (II) chloride in Ethaline. To obtain a clear set of redox peaks from zinc chloride in Ethaline, it was necessary to make this

solution up to 300 mM. Due to solubility issues, gold (I) chloride and bismuth (III) chloride solutions in Ethaline were made to 20 mM. The purity and sources of these chemicals are described above, in **Table 2.3**.

Certain metal species, such as Ni, Fe and Co, did not show clear deposition and stripping responses in their CVs when using a Pt disc working electrode. To determine if this was a surface effect (such as passivation) or a speciation effect, the previous experiments were repeated for these three metals, but substituting a native metal working electrode for the Pt disc, *e.g.* Fe electrode for Fe deposition. All other parameters were kept the same to ensure that these did not have an effect on the results.

2.4.3 Chloro-complexes in aqueous media

It is possible that the metals which displayed unusual redox behaviour on a Pt working electrode may have a non-chloride speciation in DES media. To ensure that a known speciation is obtained, a source of chloride can be added to aqueous solutions of metal salts. It is highly likely that the chloride will still be competing with oxygen from the water (~55 M). Any chloride source must be suitably concentrated, hence a highly soluble source must be used, *e.g.* lithium chloride, which has a solubility in water of up to 83 g per 100 ml.³

Solutions of anhydrous CoCl₂, FeCl₂, FeCl₃, NiCl₂, AgCl and CuCl (100 mM) were made up in aqueous 8 mol kg⁻¹ and 16 mol kg⁻¹ LiCl (Aldrich, 99%) to see if there was a visible change from the water speciation to that of Ethaline, evidenced by a colour change. The corresponding solutions in deionised water and Ethaline were also prepared for comparison purposes. Cyclic voltammetry of these solutions was carried out using native metal working electrodes for Co, Fe and Ni solutions and a Pt working electrode for Ag and Cu solutions. CVs were recorded using the method described above in

Section 2.2. These were initially scanned in a cathodic direction, ensuring that these scans were started at a zero current potential. Redox potentials were taken from the average of the onset of the oxidation and reduction potentials. These results were then compared to CVs of the corresponding solutions in Ethaline and deionised water.

2.4.4 DES analogues

For certain metals, such as copper, the solutions of LiCl in water were not sufficient to change the speciation completely. Other salts, such as silver chloride, were not completely soluble, as would have been expected from an Ethaline solution.

To determine whether the chloride donor is assisting with the change in speciation from aqua to chloride or whether it is due to the HBD, three DES analogues were prepared as described in **Section 2.1**, from 1:2 ratios of chloride salt to hydrogen bond donor, using either LiCl or ChCl as the salt and either H₂O or EG as the HBD. Solutions of 100 mM CuCl₂, AgCl, and FeCl₃ were made up in these analogues to see what effect the variation in chloride salt or HBD would have on the speciation or redox properties of these metals in solution.

2.5 Speciation of metals

In order to use ionic liquids or deep eutectic solvents for electrochemical processes, one must first understand both the redox properties of the desired metals in solution, along with their speciation. This section will focus on the experiments and techniques used to determine speciation *in situ*.

Whilst research has previously been carried out into the speciation of metal salts in DES media *via* the use of mass spectroscopy^{4, 5} the results obtained from this method cannot be definitively used for the liquid phase due to the possible fragmentation of the

solute. A different, perhaps more suitable, method to determine speciation in solution is extended X-ray absorption fine structure (EXAFS)⁶ and the results presented in **Chapter 4**. The data obtained this way can also be compared with UV-vis spectroscopy, as will be shown in **Chapter 5**.

2.5.1 EXAFS

EXAFS (extended X-ray absorption fine structure) is a technique that involves firing monochromatic X-rays at a sample to excite an atom, at which point it will emit a photoelectron wave. From the oscillations in absorptivity after the absorption edge caused by interference between the emitted and backscattered wave, properties such as atomic number, distance and coordination number of the atoms surrounding the central excited atom can be determined. As a broad tuneable source of X-rays is necessary, a synchrotron must be used to produce them. The synchrotrons used were BESSY II (KMC-2 beamline), ESRF (BM26A beamline) and Diamond Light Source (B18 beamline).

Technical details

Measurements were carried out at the absorption edges specific to the metals being studied, using a double crystal Si(111) monochromator for the ‘softer’ lower energy edges and a double crystal Si(311) monochromator for ‘harder’ higher energy edges or for mixed samples. A 9-element Ge solid state detector (BM26A operating on seven elements) in total fluorescence yield mode was used for the liquid samples, which can be seen in the experimental set-up below in *Figure 2.5*. The detector is the central tube with a yellow ring on the end. Transmission detection was also possible for these

samples but yielded significantly lower quality data due to the relatively low metal salt concentration with respect to the absorption of the solvent.

Transmission mode could however be used for metal foils and solid metal salt reference samples, using ionisation chamber detectors. This detector can also be seen in **Figure 2.5** as the tube to the far left of the image. To ensure that the X-rays were not completely absorbed by the sample, the solid salts were diluted with boron nitride (BN) powder.



Figure 2.5 *Experimental set-up at B18, including sample stage, sample holder and both detectors. The fluorescence detector is centre and back, with yellow ring around end. The transmission detector is at the far left.*

The liquid samples were injected into a Perspex cell with a sample chamber of 15 x 8 mm, at 1.5 mm thick, as shown in **Figure 2.6**, covered on both sides with 40 μm thick Kapton tape, after which the two holes at the top were sealed off with a narrower piece of Kapton tape to prevent spillage and reduce atmospheric moisture absorption.

The sample cells were then mounted at the beamline on a movable stage that could be raised and lowered or rotated as necessary (also seen in *Figure 2.5*).

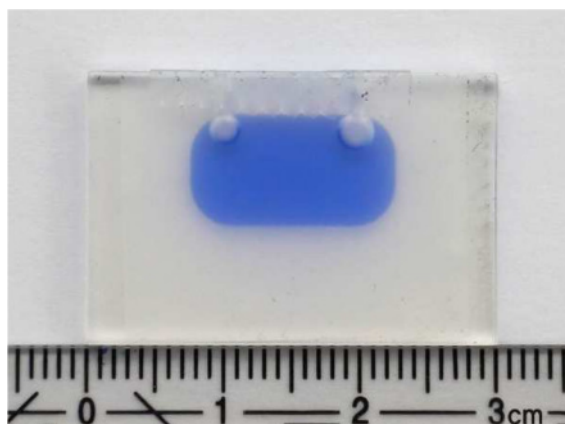


Figure 2.6 Perspex cell used to hold liquid samples for EXAFS analysis.

The X-ray beam size varied, depending on the beamline used, from 200 x 250 μm at Diamond and 2-4 x 0.3 mm at ESRF. A bigger spot size was better for studying the liquid samples, as it helped to prevent X-ray damage to the sample. If damage did occur, as was observed for elements with the harder edges (Pd, Pt, Au), the sample was moved between each scan by *approx.* 1 mm to ensure minimal sample damage and reduce any noise caused by burnt samples. This damage could be identified by darkened areas appearing in the sample, along with bubble formation at the point of beam incidence, as can be seen in *Figure 2.7*.



Figure 2.7 Example of X-ray damage to a liquid DES sample. Note the two dark patches in the centre of the liquid sample where the X-ray beam was focussed.

The sample was aligned at approximately 45° with respect to the incident X-ray beam. The fluorescence detector was positioned perpendicular to the beam to minimise any elastic scattering signals. Two to three spectra were recorded in step scan mode or eight spectra were recorded in quick EXAFS mode. These were averaged, calibrated and background subtracted using the Athena⁷ program. Any instrumental errors in the data, detected by spikes in the data occurring in the same place throughout all scans on a single sample, were removed by manually deleting bad data points in the individual spectra before they were merged.

Methods of fitting EXAFS spectra

After processing the raw spectra in ATHENA, the EXCURV⁸ program was used to fit the data by calculating interatomic distances and their root mean square variation (σ^2). Electron scattering parameters were calculated and used to determine the type and number of coordinating atoms, using the Hedin-Lundqvist potential.⁶ Uncertainties in the fitted parameters, R(min), are quoted to two standard deviations.

The amplitude correction factor (AFAC) is different for each metal and was determined from fitting known numbers of atoms, shells and distances from a crystal structure to an experimentally determined reference spectrum of either a metal foil or a solid metal salt sample. AFAC values determined by this method are shown in **Table 2.4**, along with the type of reference sample.

Table 2.4 Amplitude correction factor (AFAC) values for the metal edges studied.

Metal	AFAC	Reference Sample
Chromium	0.79(8)	Foil ⁹
Manganese	0.81(8)	Foil ¹⁰
Iron	0.76(2)	Foil ¹¹
Cobalt	0.83(7)	Foil ¹²
Nickel	0.77(6)	Foil ^{13, 14}
Palladium	0.87(6)	Foil ^{13, 15}
Platinum	0.82(7)	Foil ¹³
Copper	0.71(5)	Foil ¹⁴
Silver	0.89(5)	AgCl ⁹
Gold	0.86(7)	Foil ¹³
Zinc	0.77(4)	ZnCl ₂ ¹⁶
Gallium	0.90(6)	GaAs ¹⁷
Indium	0.97(5)	In ₂ O ₃ ¹⁸
Tin	0.91(5)	SnCl ₂ ·2H ₂ O ¹⁹
Arsenic	0.59(4)	As ₂ O ₃ ²⁰
Iodine	0.9(1)	KI ²¹

To obtain the correct speciation for each of the solutions, several fitting parameters needed to be determined: atom type and number, their distance from the excited atom, the number of shells around the excited atom, Debye-Waller factor, and Fermi Energy.

The Debye-Waller factor is a measure of thermal vibration and static disorder in the system which can give an indication of the size and number of any nearby atoms. A

larger Debye-Waller factor will shrink and broaden the Fourier transform of the EXAFS spectrum, showing more atomic wobbling. The signal will start large and rapidly decay. Conversely, a small Debye-Waller factor will increase and narrow the EXAFS signal, indicating less atomic wobbling.

Each different type of atom will cause a certain phase shift. The Fermi energy shows where the defined zero energy state for the system is and corrects for this phase shift. There is also an energy offset E^0 (or E_{\min}) associated with the EXAFS spectra, corresponding to the energy between the mean potential in the sample and the lowest unoccupied molecular orbital (LUMO). This is effectively the position of the edge with respect to the nominal value.

In the EXCURV program, it was necessary to input values for these parameters. In the DES solutions, the main coordinating species was likely to be either chlorine or oxygen, whilst in the imidazolium liquids a greater variation was possible. Suitable coordination numbers and bond lengths, from literature solid crystal structures, were applied to the data fit. The spectrum was then refined until a good fit was obtained.

To ensure that the data fit was correct, all reasonable species were examined. The incorrect data fits could easily be identified by abnormally long or short M-X bond lengths compared to the solid crystal structure, excessively large coordination numbers, or a Debye-Waller factor that was significantly different for the atom being fitted.

Sample preparation for EXAFS analysis

A range of metal salts in different ionic liquids and DESs were made up in concentrations ranging from 20 to 300 mM. The DESs were made, as described in **Section 2.1**, and the metal salts to be analysed can be seen in **Table 2.3**. The solutions were stirred and heated at 60°C, until all of the solids had dissolved or that it had

become apparent that the solution was saturated, as determined by no more solid dissolving after 24 hours. Moisture sensitive salts, such as GaCl₃, were weighed out in a glove bag under dry nitrogen gas.

The 100 mM samples of copper acetate, copper chloride, copper sulphate, chromium chloride, nickel acetate and nickel chloride in the dry imidazolium-based ILs 1-ethyl-3-methylimidazolium trifluoromethanesulfonate [EMIM][OTf], 1-hexyl-3-methylimidazolium chloride [HMIM][Cl], 1-ethyl-3-methylimidazolium bis(trifluoromethylsulfonyl)imide [EMIM][NTf₂], 1-ethyl-3-methylimidazolium tris(pentafluoroethyl)trifluorophosphate [EMIM][FAP], 1-butyl-3-methylimidazolium tetrafluoroborate [BMIM][BF₄], and 1-ethyl-3-methylimidazolium thiocyanate [EMIM][SCN] (purities and sources of the ILs are in **Table 2.2**) were made up in a glove box to reduce the amount of moisture absorbed by the solution. The metal salts were kept under vacuum overnight to ensure that the only water present in the final solution was in the form of the salts' hydration shells.

2.5.2 UV-Vis spectroscopy

UV-vis spectroscopy can be used as a complementary technique to EXAFS to determine the speciation of a metal salt in solution, along with the concentrations of these salts if two different species are seen to be present. Unusual redox properties were observed for certain metal salts in **Chapter 3, Section 3.3** and it was hoped that by using a high chloride solution, a known species could be obtained. By comparing the UV-vis spectroscopy of these solutions with Ethaline, the amount of speciation mixing could be observed.

UV-Vis spectroscopy is based on the absorption of light by the sample, such that electronic transitions will be caused. Each electronic transition has a set energy

requirement and will only absorb specific wavelengths of light. In this region, charge transfer bands (CT bands) and *d-d* transitions will be observed for metal complexes. The molar absorptivity of these absorptions can be calculated from the Beer-Lambert law:

$$A = \epsilon cl \quad \text{Equation 2.1}$$

where *A* is absorbance, ϵ is molar absorptivity ($\text{dm}^3 \text{mol}^{-1} \text{cm}^{-1}$), *c* is concentration (mol dm^{-3}) and *l* is path length (cm).

There are two selection rules which must be taken into account for how strong these transitions will be. Firstly, there is the Laporte selection rule ($\Delta l = +/-1$), which states that if a molecule has an inversion centre of symmetry (*i.e.* octahedral compounds), electronic transitions within a given set of p- or d-orbitals are forbidden. The second is the spin selection rule ($\Delta S = 0$), where the electronic transitions are spin forbidden if the overall electron spin changes.²²

CT bands are expected to be very strong ($\epsilon_{\text{max}} = 10^3 - 10^5$) as they are completely allowed. Any *d-d* transitions would be expected to be much weaker than the CT bands, as they tend to be forbidden by at least one of the two selection rules ($\epsilon_{\text{max}} = 1 - 10^3$ if partially allowed or $\epsilon_{\text{max}} = 10^{-3} - 1$ if fully forbidden). The reason that fully forbidden transitions can still be observed is that these rules can be relaxed in a number of ways, such as spin-orbit coupling (shows weak spin forbidden bands), vibronic coupling (an octahedral complex can have allowed vibrations where the molecule is temporarily asymmetric), or mixing of the d-orbitals with pi-acceptor and donor ligands.

UV-vis spectroscopy of the different solutions (aqueous LiCl, deionised water, Ethaline ChCl:2H₂O, LiCl:2H₂O and LiCl:2EG) was carried out using a Shimadzu UV-1601 UV-visible spectrophotometer, with UVprobe 1.10 controlling software. The cells were synthetic quartz glass with a path length of 10 mm and the baseline was obtained

with the empty cells in place. Measurements were taken between 1100 and 220 nm at 0.1 nm intervals. The metal salt solutions were initially made up to 100 mM but were diluted as necessary, down to a minimum of 0.1 mM, to ensure a clear signal of the absorption peaks. Spectra were measured from 1100 nm to 220 nm, at ambient temperature. The LiCl:2EG mixture was particularly viscous and the LiCl did not completely dissolve, preventing UV-vis analysis of these particular solutions.

2.6 Metal processing, separation, and recovery

Metal processing is often dominated by high temperature processes or the need for additives which are either highly soluble, such as strong acids and bases, or ones which are highly reactive, such as cyanide, in order to compete with the $\sim 55 \text{ mol dm}^{-3}$ concentration of water ligands and change the speciation. The hydrometallurgical recycling of copper-gallium scrap is a prime example of this need for strong acids and bases.^{23, 24}

By switching away from water to a deep eutectic solvent (DES) environment, the need for these speciation-altering additives is reduced, along with the need for high temperatures, as the solute speciation is now controlled by the anionic component of the DES (as has been seen from EXFAS analysis). Therefore, in this section, a combination of chemical oxidation and electrodisolution will be used to bring the metals into solution. These can then be recovered *via* electrowinning or precipitation.

2.6.1 Analytical techniques

Various techniques can be used to analyse the products of electrodisolution or chemical oxidation, such as inductively-coupled plasma optical emission spectroscopy (ICP-OES), scanning electron microscopy (SEM) and energy dispersive X-ray

spectroscopy (EDAX), cyclic voltammetry (CV) and UV-visible spectroscopy (UV-Vis).

ICP is an analytical technique for the detection of trace metals, which uses inductively coupled plasma to produce excited ions and atoms that emit characteristic X-rays for a particular element. Samples sent for ICP analysis were first filtered to remove any particulate matter, using a 0.45 μm -pore filter and the ICP machine used was a JY Ultima 2 ICP-OES. Samples were calibrated against standard solutions containing known amounts of either copper or gallium chloride.

The SEM is a type of electron microscope which images the surface morphology of a sample by scanning a high energy electron beam over it in a raster pattern. The electrons from this beam interact with the atoms that make up the sample surface and will produce two different electron signals: back-scattered electrons and secondary electrons, both of which can be used to image the sample surface.

EDAX is an analytical technique, used in conjunction with SEM, for elemental analysis of determination of the chemical composition of a sample. This technique relies on the observation of characteristic X-rays which are emitted from an element when a core shell electron is ejected from an atom and an outer or core shell electron relaxes back into the hole. By collecting all the different X-ray wavelengths emitted, an elemental analysis of the sample can be done.

Prior to SEM/EDAX analysis, metallic samples were rinsed in deionised water, followed by acetone, to remove any trace ionic liquid residues. Powdered material was stuck to nickel strips, chosen because the semiconductor samples should contain no nickel, with sticky carbon pads.

The SEM machine used was a Philips XL30 ESEM, with INCA software for EDAX analysis. All EDAX results will be reported in atomic weight % in the results chapters.

2.6.2 Anodic dissolution

As was shown in *Figure 1.1* in the introduction, there are two methods for solubilising metals: electrolytic dissolution or chemical oxidation. In this section, the methods for the electrolytic (or anodic) dissolution of copper-gallium scrap will be explored. This method of dissolution simply involves using the metal to be dissolved as the anode and a suitable substrate for electrowinning the individual metals as the cathode. Any metals that cannot be electrowon in this manner can instead be recovered *via* any of the other methods described in *Figure 1.1*. Methods of electrochemical oxidation will be discussed further in **Section 2.6.3**.

Copper-gallium dissolution

In a beaker of Ethaline (~250 ml), samples of copper-gallium scrap (obtained from MCP group, Wellingborough) were connected into an electrochemical cell as the anode, with a nickel plate as a cathode. A constant voltage of 1.75 V was applied over an 11 day period, at *approx.* 50°C, although this voltage did decrease during the process as the current became limited by the power source. Samples of the solution and the cathodic deposit were collected at daily intervals. The final solution was an opaque blue-green colour.

As energy dispersive X-ray spectroscopy (EDAX) showed that there were trace gallium deposits in the copper recovered from the cathode and it was not possible to determine whether the deposits at the bottom of the beaker had come from the anode,

the cathode, or a combination of both, the experiment was repeated with an altered setup: a crystallising dish was placed within the main beaker to catch any electrodeposits falling from the cathode, a small beaker was placed within this to catch any material that broke off the anode, and a filter paper was used to prevent any particulate matter from the anode reaching the cathode, as shown in **Figure 2.8**. This time, the cathode was an iridium oxide-coated titanium mesh, bent in a ring around the anode, to allow an even flow of current. The voltage was raised to 5.0 V, however the voltage dropped to 2.8 V during the electrodisolution, as the current became limited by the power pack. The Ethaline solution after this second method of electrodisolution was clear and dark brown.

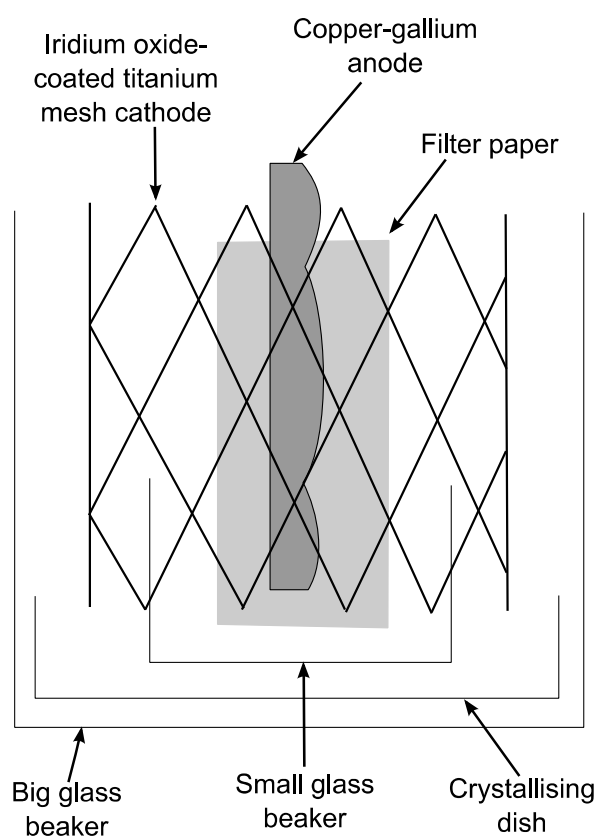


Figure 2.8 Schematic of the new and improved set-up for copper-gallium dissolution.

After both methods of dissolution, the anode was washed first with Ethaline, followed by water, to both clean it in preparation for further dissolution and remove any loose material from the surface.

Upon disassembly of this electrodisolution set-up, copper was found to have crystallised onto the filter paper membrane, most likely due to contact between the membrane and the cathode or cellulose reducing copper to form seed crystals.

The inner beaker was removed from the bulk solution and copper was plated out onto a copper cathode at 2.5 V for 4 days, using an iridium oxide-coated titanium mesh as an anode. After all the copper was removed, the solution turned a clear, very pale yellow from an original dark yellow-brown liquid with white lumps in it. This was repeated for the bulk solution, however only minimal powdery black copper was obtained and the solution remained brown.

As minimal gallium was observed in any of the precipitates via EDAX and none observed in the electrowon copper, ICP analysis of both inner and outer beaker solutions was done to determine where the gallium was present.

To recover the gallium, 1 M aqueous potassium hydroxide solution or 1 M aqueous ammonia solution were added to the inner beaker solution. This precipitated a gelatinous white substance which was almost impossible to filter, either by gravity or by suction filtration. Upon air drying, the precipitate became creamier coloured, yet was still quite gelatinous. The resulting liquid from this treatment was boiled to remove the ammonia and water and afterwards, the recovered Ethaline was returned to the bulk solution. In an attempt to ensure that all DES was removed from the precipitate, it was washed with a 1:1 solution of ethanol and deionised water.

Repeating this electrodisolution process with the same bulk Ethaline solution and the Ethaline recovered from the precipitation produced a similar set of results to fresh

Ethaline. The only exception was that slightly more of the anode was dissolved, potentially due to remainder water making the solution less viscous or trace ammonia making the solution more aggressive.

As an ammonia solution was required to precipitate out the gallium as a gelatinous white compound, this dissolution process was repeated using Reline. Reline contains a significant quantity of urea, which decomposes into ammonia with time and heat. The theory was that the presence of ammonia in the solution would aid gallium recovery. However, dissolution was much slower, most likely due to the higher viscosity. A blue solution formed in the outside beaker and a blue-brown solution inside the inner beaker. Electrowinning of copper from of the inner beaker liquid was unsuccessful and, hence, gallium recovery was not achievable.

Copper-indium-gallium dissolution

In a beaker of Ethaline, a sample of copper-indium-gallium scrap (CIG) was connected to the anode, with an iridium oxide-coated titanium mesh as the cathode. The CIG sample was electrolytically dissolved over three days, with a potential of 0.5 V being applied the first day, 0.75 V the second and 1.0 V the third. This change in voltage was to determine if the constituent metals would dissolve electrolytically at different voltages. The electro-dissolution was carried out at around 60°C. After each 24 hours, a sample was taken of the solution, and it was noted that the solution gradually became milky as the dissolution progressed and the voltage was increased. After the dissolution had been ended, the milky precipitate began to settle, leaving a clear solution behind. EDAX analysis of the white precipitate confirmed it as containing indium, with no trace of copper or gallium. A silvery grey coating present on the cathode was also confirmed as indium metal.

2.6.3 Electrochemical oxidation using iodine

The second method of metal solubilisation, as depicted in *Figure 1.1* in the introduction, is chemical oxidation. This involves the addition of an oxidising agent to the solution containing the sample to be dissolved and once the sample has been oxidised, the individual components can then be recovered *via* any of the four recovery methods, also detailed in *Figure 1.1*. The advantage of using an electrochemical oxidising agent instead of simple anodic dissolution is that the sample to be dissolved does not need to be in direct contact with the anode. The regeneration of the oxidation agent at the anode completes the circuit instead and as it can be regenerated, smaller amounts can be used.

In the high chloride environment of DES media, the higher oxidation states of several of the late transition metals have been stabilised and several of the more oxophilic metals have been destabilised, as seen in **Chapter 3, Figure 3.7**. Iodine is a powerful oxidising agent as it has a much higher redox potential than the majority of these metals. In aqueous media, it has a very low solubility of 0.29 g iodine per kg of water. In Ethaline, however, it has a much greater solubility of up to more than 200 g of iodine per kg of solvent.

Chemical oxidation of copper-gallium shavings

Shavings of copper-gallium alloy (~5 g) were partially dissolved in Ethaline (65 ml) with iodine (100 mM) as an oxidising agent, using the method depicted in *Figure 2.9*. Initially the solution was heated and stirred at 60°C until all of the iodine had been depleted (*approx.* 1 hour), as seen by the solution turning from red-brown to green. A

potential of 2.6 V was then applied over 19 days, using an iridium oxide-coated titanium mesh anode and a nickel cathode, to electrowin the copper (~4 g).

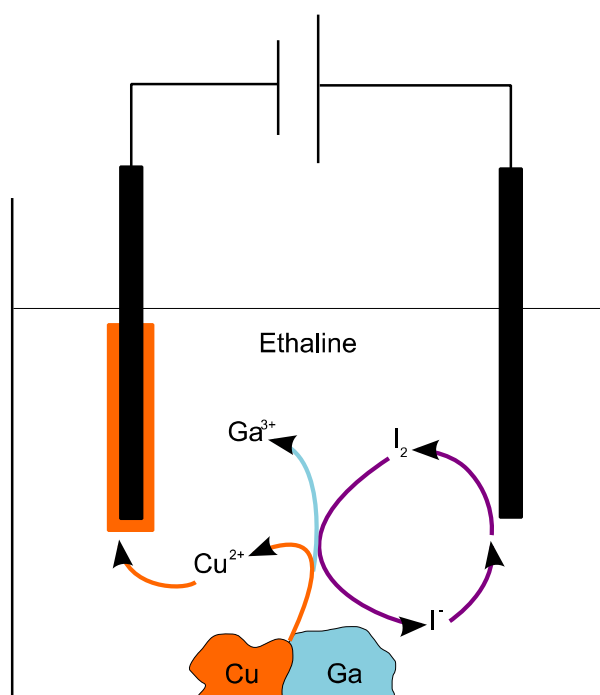


Figure 2.9 Schematic diagram of the dissolution of copper-gallium shavings in Ethaline, using iodine as an electrochemical oxidation agent.

Samples of the CG shavings were removed at intervals to identify whether both metals were being oxidised simultaneously or if one metal was being selectively oxidised. EDAX analysis of these shavings showed that the copper was preferentially oxidised from the sample and that the cathodic deposit was not as pure as from the non-iodine dissolved samples.

The addition of aqueous ammonia solution (1 M) to precipitate the gallium, as was used to recover the gallium from the electrolytic method described in **Section 2.6.2**, resulted in a clear blue solution. The expected gelatinous white gallium compound was not observed after this method of CG dissolution.

Recovery of gold-coated microfossils²⁵

When a sample is being imaged in the SEM, the sample must be either electrically conductive or electrically grounded to prevent localised build-up of charge on the surface otherwise the image will be blurred. If a non-conducting sample is to be used, it can be coated in a thin sputtered layer of gold foil to provide this electrically conducting layer. A gold layer also helps to limit the penetration of the electron beam due to its high density, which will improve spatial resolution of the specimen surface. Valuable paleontological microfossil samples which have been imaged in this method need recovering and the gold coating removed. The current method involves a cyanide-based process²⁶ and, whilst highly effective, a less hazardous method is desirable.

Iodine is a powerful, yet more benign, oxidising agent than cyanide but has a very low solubility in water. Ethaline, however, can dissolve iodine up to more than 200 g of iodine per kg of solvent and is therefore a good matrix for iodine-based dissolution. In addition, the higher oxidation states of gold are stabilised in the high chloride environment, making oxidation more likely to proceed.

Calcareous and phosphatic microfossils which had been adhered to aluminium stubs with carbon adhesive pads, gum tragacanth or dilute PVA and sputter coated with approximately 30 nm thick gold (Emitech K500X and Bio Rad Microscience Division SC650) were obtained from the Department of Geology, University of Leicester. Solutions of iodine in Ethaline were made up to concentrations of 0.02, 0.05 and 0.1 mol dm⁻³, with stirring at 60°C until all the iodine was dissolved.

The gold-coated samples were carefully placed into a sample tube containing approx. 20 ml of the iodine in Ethaline solution using tweezers and heated to 60°C, for times varying from 30 minutes to 12 hours. Iodine was always present in excess to ensure that the gold dissolved and solution volume was dependant on the size of the

sample, rather than the amount of gold to be removed. After oxidation of the gold, the samples were carefully dipped into a solution of saturated aqueous potassium iodide (Fisher, $\geq 99\%$) in deionised water to rinse off the iodine, followed by a second rinse of deionised water. The potassium iodide was used to reduce staining of the samples by iodine precipitation by raising the solubility of iodine in water *via* the formation of I_3^- .

Optical photomicrography was used to image the samples both before gold-coating and after removal, using optical microscopy with either a Leica Microsystems DFC425C camera mounted on a Leica M205C microscope, or a Qimaging camera mounted on a Leica M8 microscope. Smaller areas of the specimens were also imaged at high magnification with SEM to ensure there was no fine-scale damage.

2.7 References

1. K. Izutsu, *Electrochemistry in Nonaqueous Solutions*, Wiley-VCH, 2002.
2. A. P. Abbott, G. Frisch, S. J. Gurman, A. R. Hillman, J. Hartley, F. Holyoak and K. S. Ryder, *Chemical Communications (Camb)*, 2011, **47**, 10031-10033.
3. U. Wietelmann and R. J. Bauer, *Lithium and Lithium Compounds*, *Ullmann's Encyclopedia of Industrial Chemistry*, 2000.
4. A. P. Abbott, G. Capper, D. L. Davies, K. J. McKenzie and S. U. Obi, *Journal of Chemical and Engineering Data*, 2006, **51**, 1280-1282.
5. A. P. Abbott, J. C. Barron, G. Frisch, S. Gurman, K. S. Ryder and A. Fernando Silva, *Physical Chemistry Chemical Physics*, 2011, **13**, 10224-10231.
6. C. Hardacre, in *Annual Review of Materials Research*, 2005, vol. 35, pp. 29-49.
7. B. Ravel and M. Newville, *Journal of Synchrotron Radiation*, 2005, **12**, 537-541.
8. S. Tomic, B. G. Searle, A. Wander, N. M. Harrison, A. J. Dent, J. F. W. Mosselmans and J. E. Inglesfield, in *CCLRC Technical Report*.

9. H. E. Swanson, R. K. Fuyat and G. M. Ugrinic, *Standard X-ray Diffraction Powder Patterns: Data for 42 inorganic substances*, National Bureau of Standards, 1955.
10. J. A. Oberteuffer and J. A. Ibers, *Acta Crystallographica Section B Structural Crystallography and Crystal Chemistry*, 1970, **26**, 1499-1504.
11. A. W. Hull, *Physical Reviews*, 1917, **10**, 661-696.
12. A. W. Hull, *Physical Reviews*, 1921, **17**, 571-588.
13. W. P. Davey, *Physical Reviews*, 1925, **25**, 753-761.
14. H. E. Swanson, E. Tatge and U. S. N. B. o. Standards, *Standard X-ray Diffraction Powder Patterns: Data for 54 inorganic substances*, National Bureau of Standards, 1953.
15. J. Häglund, A. Fernández Guillermet, G. Grimvall and M. Körling, *Physical Review B*, 1993, **48**, 11685-11691.
16. B. Brehzer, *Die Naturwissenschaften*, 1959, **46**, 106-106.
17. A. S. Cooper, *Acta Crystallographica*, 1962, **15**, 578-582.
18. M. Marezio, *Acta Crystallographica*, 1966, **20**, 723-728.
19. B. Kamenar and D. Grdenic, *Journal of the Chemical Society*, 1961, 3954-3958.
20. F. Pertlik, *Czechoslovak Journal of Physics*, 1978, **28**, 170-176.
21. P. Cortona, *Physical Review B*, 1992, **46**, 2008-2014.
22. C. E. Housecroft and A. G. Sharpe, *Inorganic Chemistry*, Pearson Prentice Hall, 2008.
23. B. Gupta, N. Mudhar and I. Singh, *Separation and Purification Technology*, 2007, **57**, 294-303.
24. J. Cui and L. Zhang, *Journal of Hazardous Materials*, 2008, **158**, 228-256.

25. D. Jones, J. Hartley, G. Frisch, M. Purnell and L. Darras, in *Palaeontologia Electronica*, 2012, vol. 15.
26. S. A. Leslie and J. C. Mitchell, *Palaeontology*, 2007, **50**, 1459-1461.

Chapter 3 Ideal solutions and redox potentials

Chapter 3	Ideal solutions and redox potentials.....	78
3.1	Reference electrode.....	79
3.1.1	Review of reference electrodes in ILs	80
3.1.2	Novel reference system for use in DES systems	84
3.2	Activity coefficients in ionic liquids.....	87
3.2.1	Activity coefficients in imidazolium liquids	89
3.2.2	Activity coefficients in DESs	92
3.3	Redox potentials of metal salts in DESs ⁴⁸	95
3.3.1	Redox potentials in Ethaline vs. H ₂ O.....	96
3.3.2	Cyclic voltammetry of metal salts in Ethaline.....	98
3.4	Conclusions.....	107
3.5	References.....	108

3.1 Reference electrode

Hydrometallurgical techniques for the recovery and separation of metals are heavily relied upon by technological societies. These methods commonly and routinely use strong mineral acids and bases to dissolve oxides and use oxidising acids (*e.g.* H₂SO₄ and HNO₃) to solubilise metals.¹ The reactivity of the electrolyte and complexity of the oxide/hydroxide chemistry of most metals makes a significant proportion of these processes inefficient, providing strong motivation for more energy efficient and environmentally sustainable chemistries.

DESs can be used for the selective dissolution^{2, 3} and electrowinning⁴ of metals from ores⁵ and wastes. For instance, a 1:2 molar mixture of choline chloride and urea (Reline) can be used to process a mixed metal oxide matrix from an electric arc furnace⁶ by selectively dissolving zinc and lead, whilst Ethaline can be used to electropolish steel.⁷ Ionic fluids allow the manipulation of the speciation of soluble metal salts through the elevated concentrations of coordinating anions. Properties of these metal species, such as redox potentials, can therefore be adjusted through the composition of the liquid.⁸ However, unlike the corresponding aqueous processes, underlying fundamentals such as metal speciation and redox chemistry in the high chloride environment of DESs are currently poorly understood. Some redox potentials have been found to shift considerably in ILs and DESs, compared to aqueous solution⁹ but more practical difficulties with reference electrodes and junction potentials have impeded the quantitative analysis.

Electrochemical studies using ionic liquids as electrolytes are well studied but a ubiquitous issue is still the definition of a reference potential.¹⁰ This is a common issue with non-aqueous solutions and stems from the lack of knowledge of standard

thermodynamic properties in any media other than water. It also results in part for the inability to gain reliable information about liquid junction potentials.

In this chapter, the development of a new reference electrode for use in deep eutectic solvent (DES) and ionic liquid (IL) media will be discussed, followed by its application to the determination of activity coefficients *via* the Nernst equation and application to the construction of a scale of redox potentials for a range of different metal chloride salts in a 1:2 molar mixture of choline chloride and ethylene glycol (Ethaline). Cyclic voltammetry will be used to identify the redox couples and an average of the onset values for the oxidation and reduction peaks will be used to determine formal redox potentials.

3.1.1 Review of reference electrodes in ILs

According to Koryta *et al.*¹¹ there are three different types of reference electrode. The first type of reference electrode is based on potential determining equilibria, where equilibrium is established in solution between the atoms of the electrode and their corresponding cations or anions. An example of this is the Ag/Ag^+ electrode.

The second type is based on a three-phase system, where a metal wire is coated in a layer of a sparingly soluble salt of that metal and then immersed in a solution containing a known concentration of the corresponding anion of the salt. For instance, the $\text{Ag}/\text{AgCl}/\text{Cl}^-$ electrode and the $\text{Hg}/\text{Hg}_2\text{Cl}_2/\text{Cl}^-$ (SCE) electrode are both of this type.¹²

The final type described by Koryta is based on soluble redox couples. An inert metal, such as platinum or gold, is immersed in a solution containing both the reduced and oxidised species of a redox couple and the potential of that redox couple is then measured with respect to the inert wire. The ferrocene/ferrocenium and

cobaltocene/cobaltocenium couples are commonly used as reference couples in non-aqueous solutions.^{13, 14}

By convention the H^+/H_2 redox couple is used to define the standard electrode potential and is assumed to have a voltage of 0.00V in aqueous media with 1 mol kg⁻¹ activity of HCl and 1 bar hydrogen pressure. It is necessary that the electrochemical processes to reach equilibrium must have fast kinetics, therefore in the case of the SHE the platinum electrode must be platinised with platinum black to provide a suitably large surface area for the hydrogen to adsorb to.

Reference electrode potentials are mostly unreliable in ILs and there is currently no accepted standard reference potential. When using an aqueous electrode of the first or second type as a reference electrode in ionic liquids, an additional factor must be taken into consideration when determining electrode potentials. Liquid junction potentials (LJPs) can arise between a traditional aqueous reference and a non-aqueous solution in three different ways.¹⁵ Firstly, a concentration gradient is formed at the junction between the two solutions and differences between the mobilities of the cationic and anionic components will exacerbate this. Secondly, the ions in the different solutions will have different solvation properties. Finally, if the reference solution is in contact with the bulk solution, cross-contamination of the reference and bulk solutions can occur, therefore altering the reference potential, either via solvent-solvent interactions, ion-solvent interactions or ion-ion interactions. This can be minimised by using the same electrolyte/solvent in the reference electrode as is used in the bulk solution or by using a glass frit to prevent solvent mixing. Combined, these three issues can cause a large LJP, which does not necessarily remain constant over the course of the whole measurement, and therefore leads to inaccurate electrode potential data.¹⁰

One method for avoiding an LJP in non-aqueous metal-containing solution is through the use of a pseudo reference electrode. In this case, an inert electrode or a metal wire is immersed directly into the solution and the reaction at this electrode is therefore considered to be the reference potential. With this method, the reference potential is always fixed at zero for the deposition and dissolution of the metal wire. However, this method is not necessarily ideal for all metal-containing solutions, as some redox couples can be kinetically hindered in solution and the test solution can become contaminated with dissolved species from the pseudo reference wire. In addition, the exact identity of the reference reaction may not be completely defined in the solution of choice and can vary considerably in different electrolytes.

Whilst the pseudo-reference electrode potential may be stable in one specific experiment, it is difficult to place it on a standard scale. When the reference electrode is in direct contact with the test solution, interactions between the reference electrode and solutes in IL can cause a change in reference potential and surface species on the reference electrode and the variability of the oxidised component of the reference redox couple in solution may also affect the reference redox potential.¹⁶ In IL media, the most commonly used pseudo reference electrodes are often made of silver^{17, 18} or platinum,¹⁹ however magnesium²⁰ and aluminium²¹ wire have also been employed.

Another method is by using an internal reference, such as FeCp₂ or CoCp₂,¹⁸ as a calibrating agent, *i.e.* an internal standard as described above, in combination with a pseudo reference electrode. If there is no solvent-solvent boundary, then there can be no junction to cause problems. The reference potential is therefore the potential of a solvent independent redox couple, at least one component of which must be dissolved in the solution. The potential of this reference couple can then be determined by voltammetric methods and used as a marker for any other processes occurring in the

solution. The most common internal references used in non-aqueous solutions are the ferrocene/ferrocenium, cobaltocene/cobaltocenium and bis(biphenyl)chromium(0/1) redox couples.^{13, 14} Other common internal references include the I^-/I^{3-} redox couple.¹⁵ However, the redox potential of $FeCp_2$ is highly dependent on solvation effects by both the solvent and the supporting electrolyte²² and there are solubility issues associated with the dissolution of $FeCp_2$ in ionic liquids and deep eutectic solvents. Both the cationic and anionic components of the IL can interact with $FeCp_2$ ²³ and in polar organic solvents decomposition of $FeCp_2$ can occur with the presence of molecular oxygen.²⁴

De Vreese *et al.*²⁵ have tested out ferrocene, cobaltocene and bis(biphenyl)chromium tetraphenylborate as internal references in [BMIM][NTf₂] and [EMIM][ES] and also in Ethaline vs. Pt, Au and glassy carbon working electrodes. They found that the redox couple of $CoCp_2$ on Pt was not in the electrochemical window of Ethaline, but aside from that, the separations of all three references peak potentials were constant in all three liquids, on all three working electrodes. These were found to be 1.337 V between $FeCp_2$ and $CoCp_2$ and 1.114 V between $FeCp_2$ and bis(biphenyl)chromium(0/1), which is similar to the differences between the same redox couples in organic solvents, and suggests that they may be suitable for use in IL studies.

The silver Ag^+/Ag redox couple is a common choice in pseudo and second kind reference electrodes and has been studied by several different groups. For instance, Saheb *et al.*²⁶ have used an Ag^+/Ag electrode of the first kind with $AgNO_3$, and an $Ag/AgCl/M^+Cl^-$ electrode of the second kind using tetrabutylammonium chloride (Bu_4NCl) dissolved in acetonitrile to compensate for its low solubility in IL media. Both of these electrodes were compared against $FeCp_2$, however there are issues associated

with the unknown solubility of redox couples in ILs²⁷ and a general assumption that the potential of a redox process is independent of solvent.

Solvent-based variation in E^0 tends to be smaller for the larger, coordinatively saturated reagents such as CoCp_2 . Smaller ions, like Ag^+ or NO^+ , have potentials which are more highly affected by the choice of solvent²² and it has been suggested that some of these differences in potential may be caused by a slow Ag^+/Ag interconversion.²⁸

3.1.2 Novel reference system for use in DES systems

Currently for DES systems, a silver wire pseudo reference electrode is commonly used, however this reference potential cannot be considered as stable as the silver can be oxidised by more electronegative species in solution. Therefore, instead of a simple silver wire in solution, the decision was made to return to the more traditional silver/silver chloride electrode, but modified for use in DES media.

Coating the silver wire in AgCl is highly unlikely to keep the reference potential constant, as in Ethaline AgCl has a solubility of up to 0.2 mol dm^{-3} in contrast to $\sim 1.3 \times 10^{-5} \text{ mol dm}^{-3}$ in aqueous solution. This means that a specific AgCl concentration is needed in the reference solution itself and the reference equilibrium will then be between Ag^+ in solution and the Ag metal wire. The concentration of AgCl chosen for this reference electrode was 100 mM to prevent any solubility issues that could be associated with being near the saturation point at 200 mM and to ensure that small changes in the concentration will not affect the reference potential as much as they would at lower concentrations. Also, a high metal concentration in solution will make dissolution of the silver wire into the reference solution less favourable. By using the same DES or IL inside the electrode as used outside in the bulk solution, LJPs can be

minimised. A Vycor glass frit was used to prevent cross-contamination of reference and bulk solution, yet still allow ion transfer.

Two complementary types of potential measurement were made to ensure that the reference potential for the Ag/AgCl electrode was stable – cyclic voltammetry and equilibrium potential measurements. In some ILs, diffusion is a very slow process due to their high viscosities and this can affect the reference potential. By allowing the reference electrode to equilibrate in solution for 5-10 minutes, or by using a slow sweep rate (10 mV s^{-1}) for cyclic voltammetry, this is no longer likely to be a factor in the final potential. For a stable reference electrode, any reversible couples would be expected to remain at a constant potential.

Each solvent has a potential window, where the solvent is stable and does not decompose with the application of potential. This decomposition can be observed by an increase in the magnitude of current at the ends of the CV, where no redox couples for the solutes are expected. The potential window of Ethaline is found between +1.3 V and -0.8 V, on a Pt working electrode *vs.* a silver wire pseudo reference electrode, hence the choice of potential range for these experiments. These potential windows, especially the cathodic end, are dependent on the choice of working electrode. By examining cyclic voltammograms of the reversible $\text{Cu}^{2+/+}$ couple from concentrations of 1 to 100 mM in Ethaline *versus* an Ag wire pseudo reference electrode or the AgCl/Ag reference electrode (see **Section 2.2**), the stability of both reference electrodes can be observed.

When the pseudo reference is used, the peak potential of this reversible couple is not stable over the range of concentrations used. Significant variations between the height of the peak reduction and oxidation currents ($i_{\text{p,red}}$ and $i_{\text{p,ox}}$) can also be seen, as shown in **Figure 3.1**. If the AgCl/Ag reference electrode is used instead, the peak potentials for the reversible $\text{Cu}^{2+/+}$ couple remain at a constant potential throughout the

concentration series and, for the higher concentrations, $i_{p,red}$ and $i_{p,ox}$ appear to be visually consistent in height with each other. This shows that this electrode is redox stable during the experimental time frame. The $Cu^{0/+}$ couple, on the other hand, shows variation over the range of concentrations with both types of reference electrode.

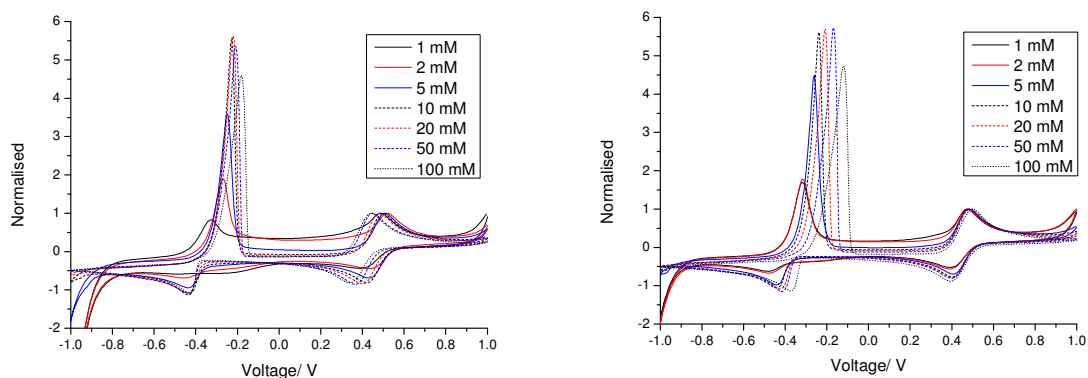


Figure 3.1 Normalised cyclic voltammograms of $CuCl_2$ (1 to 100 mM) in Ethaline vs. Ag wire pseudo reference electrode (left) and vs. Ag^+/Ag reference electrode (right). Scans have been normalised to the peak oxidising current for the reversible $Cu^{2+/+}$ couple.

The shift in the relative redox potential of the $Cu^{2+/+}$ couple observed between the Ag wire reference and the $AgCl/Ag$ electrode may be a side effect of the test solution oxidising the Ag wire pseudo reference or of the presence of a LJP forming between the $AgCl/Ag$ reference electrode and the test solution.

To see if the $AgCl$ reference electrode is stable with respect to the internal standard for the redox potential measurements that will be carried out in **Section 3.3.1**, it is necessary to examine the response of $K_4[Fe(CN)_6]$ vs. both of these reference electrodes. It was seen that the CVs of $K_4[Fe(CN)_6]$ vs. an Ag wire pseudo reference showed consistent $i_{p,ox}$ peak positions, but the position of $i_{p,red}$ were seen to gradually

shift towards more anodic potentials with further scans, as can be seen in **Figure 3.2**.

This suggests an oxidation of the Ag wire, even though it is not visibly tarnished.

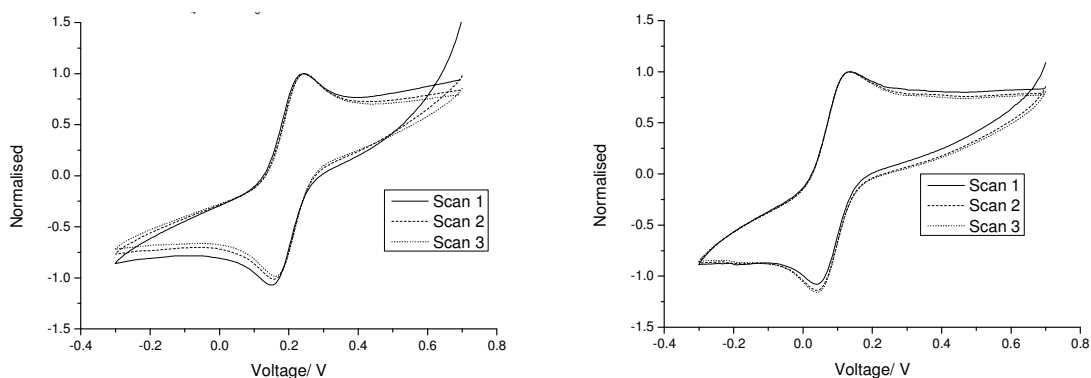


Figure 3.2 Normalised cyclic voltammograms of $K_4[Fe(CN)_6]$ (20 mM) in Ethaline vs. Ag wire pseudo reference electrode (left) and vs. Ag^+/Ag reference electrode (right).

When the AgCl/Ag reference electrode is used instead, the potentials of both $i_{p,red}$ and $i_{p,ox}$ are consistent for all scans. The slight difference between the first scan and the other subsequent scans, along with a slight discrepancy between $i_{p,ox}$ and $i_{p,red}$ on the first scan may be down to the choice of sweep direction (+ve to -ve).

In conclusion, the AgCl/Ag reference electrode is stable in Ethaline at the slow scan rates used and can now be used as a reference for various electrochemical techniques, such as the determination of activity coefficients (**Section 3.2**) and the determination of redox potentials of a range of metal salts (**Section 3.3**). The Ag wire is suitable for determination of the presence of redox couples; however it is a less accurate reference electrode for determining the values of the redox couples themselves.

3.2 Activity coefficients in ionic liquids

Ionic liquids are amongst the fastest growing research themes and the rapid progress from academic interest to industrial applications has been documented in a recent review by Pletchkova and Seddon.²⁹ The synthetic and electrochemical

applications, including phase transfer catalysis, solar cells, electrodeposition and lithium batteries, are comprehensively covered in recent books.^{1, 10} Underpinning these applications is a wide range of literature on the physical and chemical properties of ILs and DESs. However, some of the more fundamental issues, such as activity coefficients, still need to be fully understood.

The concept of activity has been clearly developed in a number of ways, all of which are well documented.^{30, 31} It has been proposed that the high coulombic density in ILs shield solute molecules and ions from each other³² and supporting evidence has been obtained from solvatochromic indicators.³³ This growth in the application of ILs to metal deposition¹⁰ and metal processing⁵ means that it is important to understand the activity of the metal ions in solution. Activity coefficients at infinite dilution have been determined by Heintz *et al.* for molecular solvents but this particular approach is unsuitable for solutions containing metal salts due to their lack of vapour pressure.^{34, 35}

One method for the determination of activity coefficients for metal ions in ionic liquids is through redox potential measurements. The equilibrium cell redox potential, E , for the process $\text{Ox} + e^- \rightarrow \text{Red}$, is given by the Nernst equation:³⁶

$$E = E^0 + \frac{RT}{nF} \ln \left(\frac{a_{\text{ox}}}{a_{\text{red}}} \right) \quad \text{Equation 3.1}$$

$$= E^0 + \frac{RT}{nF} \ln \left(\frac{m_{\text{ox}}}{m_{\text{red}}} \right) + \frac{RT}{nF} \ln \left(\frac{\gamma_{\pm \text{ox}}}{\gamma_{\pm \text{red}}} \right)$$

where E^0 is the standard cell potential, R is the gas constant, T is the absolute temperature, F is the Faraday constant, n is the number of electrons, $\gamma_{\pm} = \sqrt{\gamma_+ \gamma_-}$ is the mean activity coefficient and a and m are the activity and molality of the solute, respectively. The third summand of this equation can be omitted when the solute ions behave independently (*i.e.* $\gamma_{\pm} = 1$, and therefore $a = m$) and exhibit ideal properties. Usually, solute ions can only be considered as behaving independently if there are no

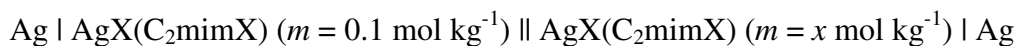
solute ion-ion interactions, which will only happen if the solution is very dilute, *i.e.* less than ~ 0.01 M.³⁷ Deviations from this ideal behaviour are often modelled using the Debye-Hückel limiting law (DHLL):³⁶

$$\ln\gamma_{\pm} = \frac{-(z_+^2 z_-^2 q^3 N_A^{1/2})}{4\pi(\epsilon_0 \epsilon_r k_B T)^{3/2}} \sqrt{\frac{I}{2}} = -A|z_+ z_-| \sqrt{I} \quad \text{Equation 3.2}$$

where z_+ and z_- are charges of the solute ions, I is the ionic strength of the solution, A is a solvent specific constant that depends on its dielectric constant, q is the elementary charge, T is temperature, k_B is the Boltzmann constant, ϵ_0 is the permittivity of a vacuum, ϵ_r is the relative permittivity of the solvent (*i.e.* the dielectric constant) and N_A is Avogadro's number. The DHLL describes the distribution of ions around a given ion and the net effect that these neighbouring ions will, in turn, have upon the ions of the solution. From this equation, theoretical values of activity coefficients can be calculated and the DHLL predicts significant deviations from ideal behaviour at low solute concentrations (*e.g.* for CuSO_4 in water at 298 K, a 0.01 mol kg^{-1} solution has $\gamma_{\pm} = 0.41$ and a solution of 0.1 mol kg^{-1} has $\gamma_{\pm} = 0.16$).³⁷ The DHLL is based on dielectric continuum models which might not be entirely appropriate to describe an ionic matrix and the DHLL does not predict correct activities for solutes in ionic liquids.

3.2.1 Activity coefficients in imidazolium liquids

The activity of silver ions was determined by measuring the reduction potential of silver ions over a range of concentrations, in imidazolium-based ILs with different anions and in Ethaline. The activity coefficients of Cu^{2+} and H^+ were also measured in Ethaline. **Figure 3.3** shows the change in redox potential as a function of molality for the imidazolium IL solutions, along with the Nernstian line which assumes that both the working and reference couples are ideal solutions ($\gamma_{\pm} = 1$, $a = m$), for the cell



where X is either chloride (Cl^-), acetate (OAc^-) or thiocyanate (SCN^-). During repeat measurement, the cell potentials tend to stay relatively constant, which leads to relatively small error bars. When the molalities of both the reference and the sample solutions are similar, the cell potentials exhibit a Nernstian behaviour but as the difference in molalities increases, so do deviations from ideality. For this particular cell shown in *Figure 3.3* the deviations would occur at low molalities, as the reference cell has a molality of 0.1 mol kg^{-1} of the relevant silver salt. Due to the potential for increased dilution errors for the lower concentration data points (1 and 2 mM of silver salt), it is possible that these points may be less accurate than originally thought.

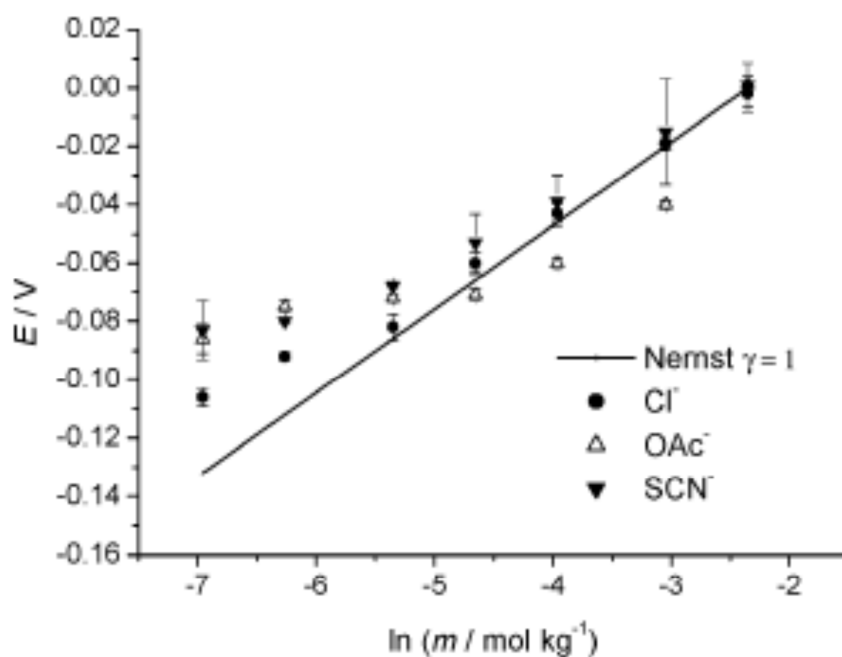


Figure 3.3 Graph of potential vs. $\ln(\text{molality})$ for the three imidazolium IL solutions.³⁸

By assuming that in these solutions concentrations of $0.001 \text{ mol kg}^{-1}$ are approximately ideal, activity coefficients can therefore be calculated from the Nernst equation:

where 1 refers to the reference cell and 2 refers to the test cell.

Figure 3.4 shows the activity coefficients for AgOAc in [EMIM][OAc] and AgSCN in [EMIM][SCN] as a function of silver salt molality, calculated from the data shown above in **Figure 3.3**, using the **Equation 3.3**. These solutions were found to deviate from ideality as the molality of the solute increased. Despite all of the salts being 1:1 electrolytes present in similar ionic liquids where the concentration of ions is roughly similar (6.9 to 7.3 mol dm⁻³), the different salts do not have identical activity coefficients at high silver concentrations. The silver salts with the highest charge density anions follow the Nernstian trend line more closely. With [BMIM][Cl] as the ionic liquid, the solution of AgCl is almost ideal.

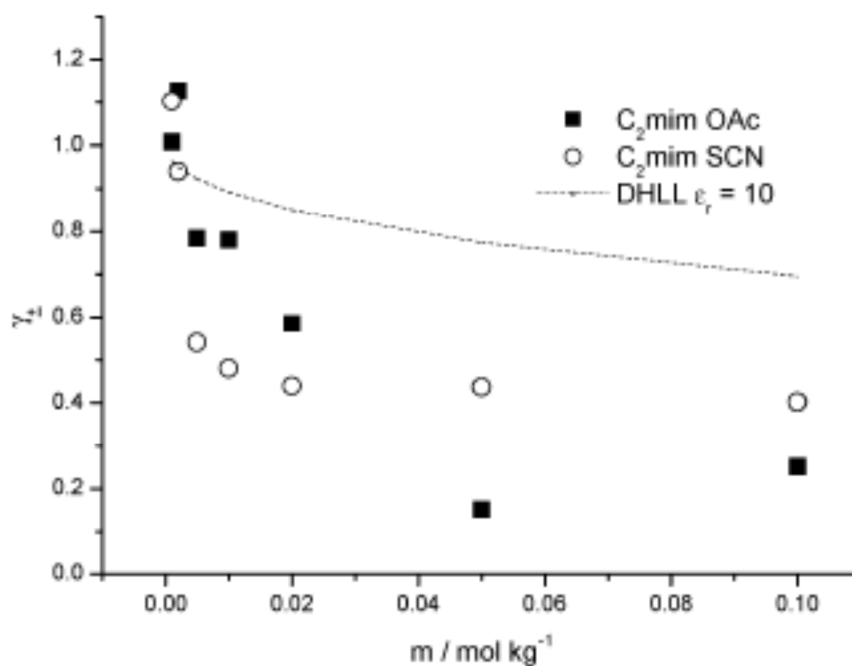


Figure 3.4 Activity coefficient as a function of molality for the systems AgOAc in [EMIM][OAc] and AgSCN in [EMIM][SCN]. The dashed line shows the DHLL values calculated from Equation 3.3, assuming $\epsilon_r = 10$.³⁸

There are several methods for the calculation of activity coefficients, all of which are based on a dielectric constant model. Although these methods are not appropriate for accurate modelling in IL media, approximate values of γ_{\pm} can be obtained from **Equation 3.2**. The determination of dielectric constants in ILs has been studied by Wakai *et al.* and Izgorodina *et al.* these were found to be in the range of 8 to 15.^{39, 40} If a dielectric constant of 10 is used, the trend predicted by the DHLL can be shown as the dashed line in **Figure 3.4**. If the value of the dielectric constant is changed to either 8 or 15, *i.e.* the literature limits, there is no significant effect seen on this plot. This is suggestive that these experimentally determined values show an approximate trend and are comparable to other electrolyte systems. Electrochemical cells as a method to determine activity coefficients has been previously proposed by Mihichuk *et al.*⁴¹ and these results show it to be a viable method that should be applicable to most metal salts.

3.2.2 Activity coefficients in DESs

DESs have previously been found to show behaviour with similar properties to ionic liquids with discrete anions.^{42, 43} As the chloride-based imidazolium ionic liquid [BMIM][Cl] shows close to ideal behaviour, it would be interesting to see if the same holds true for activity coefficients in the high chloride DES environment.

Figure 3.5 shows E vs. $\ln(m)$ for the following cells in Ethaline vs. an AgCl reference electrode of Ag | AgCl(DES) ($m = 0.1 \text{ mol kg}^{-1}$).

Cell 1 ref. || AgCl(DES) ($m = x \text{ mol kg}^{-1}$) | Ag

Cell 2 ref. || CuCl/CuCl₂(DES) ($m(\text{Cu}^+) = 0.01 \text{ mol kg}^{-1}$ $m(\text{Cu}^{2+}) = x \text{ mol kg}^{-1}$) |

Pt

Cell 3 ref. || F₃CSO₂H(DES) ($m = x \text{ mol kg}^{-1}$) | H₂(1 atm) | Pt

The Nernst equation (*Equation 3.1*) is used to find the equilibrium electrode potential of a half cell or the total voltage for a full electrochemical cell. From the change in redox potential with molality, it can be seen that all three of these solutes obey the Nernst equation for an ideal solution. For instance, the AgCl cell shows a line with a gradient value of 24.3(4) mV, which is close to the predicted value of 25.7 mV at 298 K. Close to ideal behaviour is observed for this cell, which indicates that the activity of the silver ions is close to unity, up to the saturation concentration of *c.a.* 0.2 mol kg⁻¹. The high solubility of AgCl in Ethaline is due to the formation of the [AgCl₂]⁻ species and is comparable to the high solubility of AgCl in concentrated HCl. These silver ions are therefore shielded from each other by the ionic matrix of the liquid, ensuring that they behave independently. Similarly close to ideal behaviour was also observed for the CuCl (10 mM)/CuCl₂ cell (gradient 30.3(8) mV at 20°C) up to a concentration of 1 mol kg⁻¹, despite the nominally higher charge on the ion. In Ethaline, the CuCl₂ is present as [CuCl₄]²⁻ and the CuCl as [CuCl₂]⁻.⁴⁴ The concept of coulombic shielding in ionic liquids has previously been demonstrated by Takahashi *et al.* through use of the diiodide anion radical.⁴⁵ In dilute solutions it was found that the rates of reaction between the I₂⁻ radicals in the ionic liquid were similar to those for neutral reactants in solution, indicating that the charge on the anion radical was, in effect, shielded, *i.e.* the solute species show ideal behaviour.

For the systems in *Figure 3.5* the potential difference between the silver and copper redox couples is approximately constant at any particular molality, which indicates the ideality and additivity of electrode potentials in DESs and opens the way for standard thermodynamic data to be obtained, along with standard redox potentials. [BMIM][Cl] is seen to behave in a similar manner to Ethaline, showing that the anion is the dominant species affecting the activity coefficient, which suggests that complex

equilibria between various ionic species, such as bridging effects by the ligand creating multinuclear complexes, might be the cause of deviations from ideality with other anions.

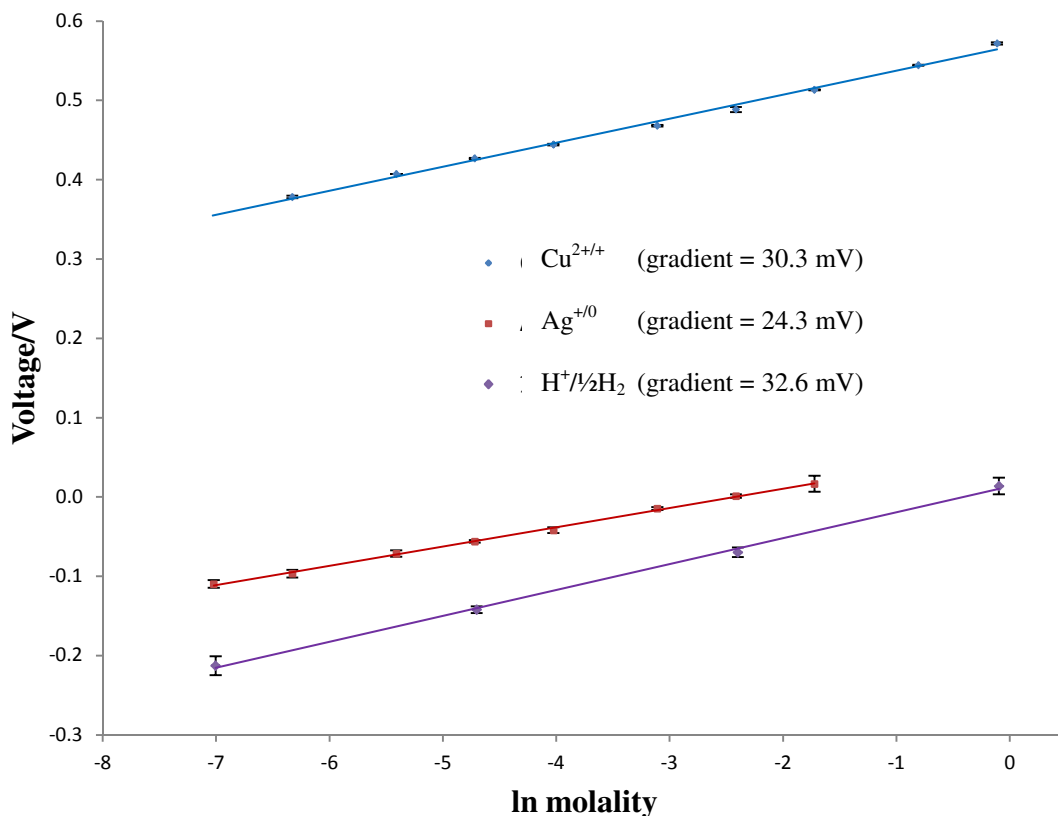


Figure 3.5 Nernst plot for the redox couples $\text{H}^{+}/\frac{1}{2}\text{H}_2$, $\text{Ag}^{+/0}$ and $\text{Cu}^{2+/+}$ vs. 0.1 mol kg^{-1} AgCl reference electrode, measured from equilibrium potential measurements.

To obtain standard potentials for metal salts it is necessary to measure the redox potential for the $\text{H}^{+}/\frac{1}{2}\text{H}_2$ redox couple, *i.e.* a DES standard hydrogen electrode (SHE) (cell 3). A SHE is defined as having a H_2 pressure of 1 atm. with a proton activity of 1 mol kg^{-1} . The dissociation of acids in DES is currently poorly understood⁴⁶ but the use of triflic acid as a proton source should ensure complete dissociation of the acid in solution. Triflic acid is a superacid, *i.e.* it has an acidity of greater than 100% pure sulphuric acid⁴⁷ and has a pKa of ~ 15 . Once again, ideal behaviour was observed at

molalities of up to 1 mol kg^{-1} of triflic acid, which indicates that the acid is mainly dissociated and there are no interactions of protonated species. If it can be assumed that the independence of the protonated species is also true for weaker acids, it should theoretically be possible to get true pH measurements and construct pKa scale for solutes in ILs.

Using the standard DES hydrogen electrode as a reference point and assuming that it has a redox potential of 0.00 V, the standard redox potential for the $\text{Ag}^{+/0}$ system can be calculated as $E^0 = +0.034 \text{ V}$ and for $\text{Cu}^{2+/+}$ it is $E^0 = 0.543 \text{ V}$. When the redox potentials for these systems *vs.* the AgCl reference electrode are compared to their CVs, it can be seen that both of these methods share similar values. These values are very different to the aqueous potentials of +0.80 and +0.158 V, respectively.⁴⁸ This difference is thought to be due to a change in speciation of the metals in the two solvent systems.⁴⁹ This observed ideal behaviour from coulombic shielding in the DES helps to reinforce the notion that DESs behave like molten salts and can be considered as ILs.

3.3 Redox potentials of metal salts in DESs⁴⁹

Before DESs can be applied to any specific electrochemical applications the relative positions of the redox couples for various metal salts must first be understood, with respect to the reference electrode. Once an electrochemical redox series in DES has been created, it can be used to aid the dissolution and recovery of scrap metal, as will be seen in **Chapter 6**. The similarities and differences to aqueous redox behaviour will also be discussed and compared. Once this electrochemical series has been created, the correct conditions then can be carefully chosen to selectively drive metal dissolution and deposition in practical applications.

3.3.1 Redox potentials in Ethaline vs. H₂O

The formal redox potentials, determined from averages of redox couple onset potentials, as described previously in **Section 2.4**, for 17 couples with [Fe(CN)₆]^{3-/4-} reference in Ethaline and aqueous solution are shown in **Figure 3.6**. The formal electrode potentials, E^0 , were determined from the 20 mM metal salt solutions and compensation for differences in concentration and temperature were made using the Nernst equation. Through the centre of the plot is the line of equivalence, where the formal potentials in Ethaline are the same as those from aqueous solution. Generally, for the metal couples above the line of equivalence the higher oxidation state is destabilised in relative terms compared to the lower oxidation state. Below the line of equivalence, the reverse is true: the higher oxidation state is stabilised compared to the lower oxidation state. Where the couple involves elemental metal as the reduced half, the absolute activity of the metal is defined as unity.

Couples which involve the oxophilic p-block elements, such as gallium and antimony, show the largest positive deviations from the line of equivalence and chlorophilic late transition metals, such as silver, gold and palladium, show the largest negative deviations. A reduced oxidising power is therefore indicated for these chlorophilic late transition metal species in DESs.

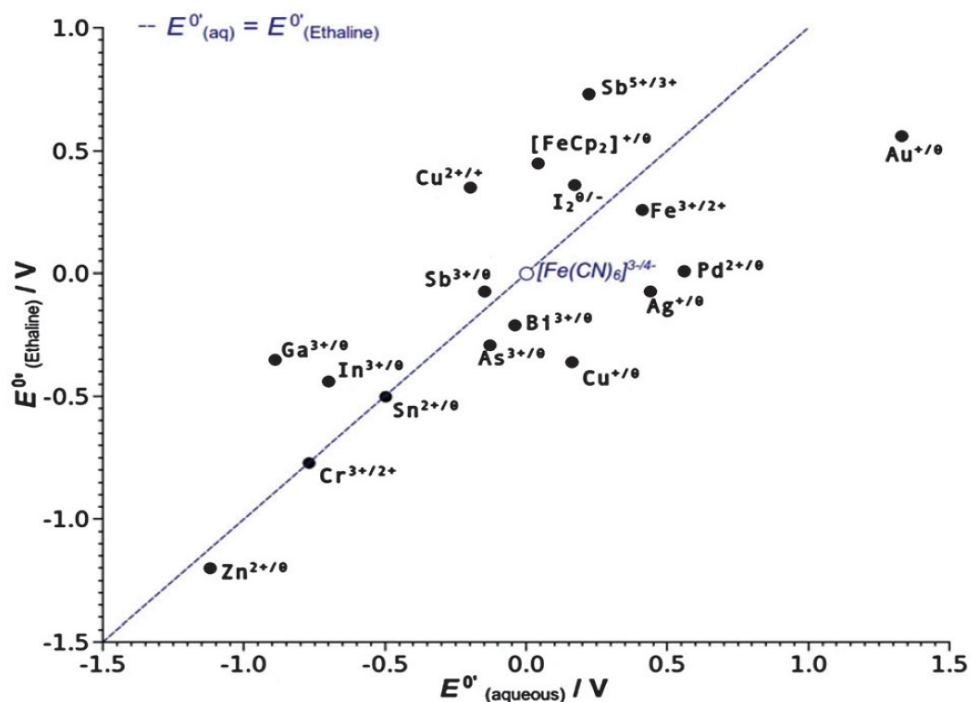


Figure 3.6 Formal electrode potentials of a selection of metal species in Ethaline compared with potentials in aqueous solution, corrected for temperature and concentration. Through the centre of the graph is the line of equivalence, where electrode potentials would be identical in both solutions.

When determining the redox potentials for the various metal salts, three types of redox response for metal deposition and stripping were observed: reversible, semi-reversible and irreversible. The metals included in **Figure 3.6** have been chosen because they showed well defined oxidation and reduction peaks which could be averaged as per the method described in **Section 2.4**. Metals which did not show clear redox couples from cyclic voltammetry, such as nickel or platinum, were not included, however they will be discussed further in **Section 3.3.2**.

3.3.2 Cyclic voltammetry of metal salts in Ethaline

A particularly interesting case is that of the two copper couples. The above **Figure 3.6** shows that, in aqueous solution, the $\text{Cu}^{+/0}$ couple has a more anodic redox potential than the $\text{Cu}^{2+/+}$ couple ($E^0 = +0.52$ vs. $E^0 = +0.16$ V, respectively), leading to disproportionation of the Cu^+ ion to Cu^{2+} and metallic copper and hence the Cu^+ ion is generally not seen in aqueous solution. In the DES Ethaline, this is not the case, as the $\text{Cu}^{2+/+}$ couple shows a positive deviation from the line of equivalence and the $\text{Cu}^{+/0}$ couple shows negative deviation. The Cu^+ ion is stabilised by the high chloride environment, allowing it to be detected in the cyclic voltammetry, as shown in **Figure 3.7**, where two distinct redox couples are visible. The couple at more positive potentials is clearly a reversible couple, which can be attributed to the reduction and oxidation of the $\text{Cu}^{2+/+}$ species. At more negative potentials, the voltammetric shape of the redox couple suggests plating of copper metal and stripping of this deposit into a soluble (and stable) form of Cu^+ .

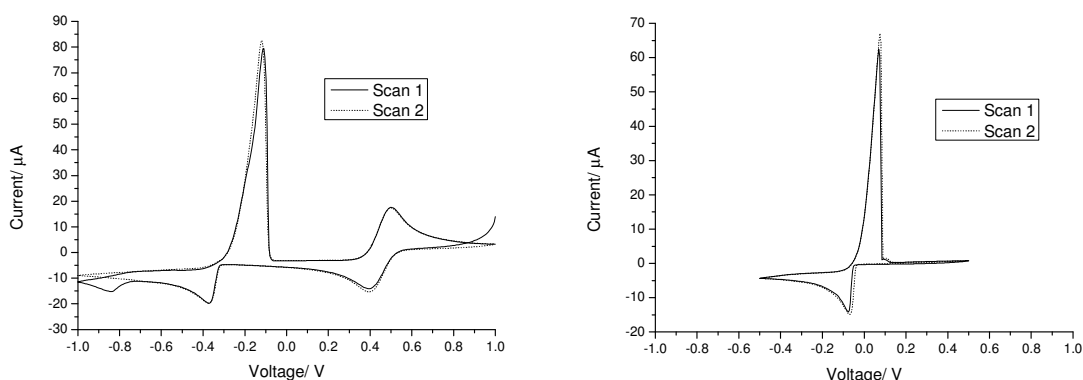


Figure 3.7 Cyclic voltammograms of 100 mM metal salts in Ethaline: CuCl_2 (left) and AgCl (right). Scans recorded on 1 mm Pt disc working electrode vs. Ag/AgCl in Ethaline reference, at a scan rate of 10 mV s^{-1} .

Cyclic voltammetry of silver chloride (**Figure 3.7**) and tin (II) chloride (**Figure 3.8**) both show a clear pair of redox peaks for the $\text{Ag}^{+/0}$ and $\text{Sn}^{2+/0}$ couple, respectively.

However, whilst silver has been made easier to oxidise in the high chloride environment, the redox potential for the $\text{Sn}^{2+/0}$ couple remains the same as it would be in aqueous media. As would be expected vs. a silver wire reference electrode, a single redox couple for $\text{Ag}^{+/0}$ is seen centred about the zero potential.

Continuing this theme of clear redox behaviour is bismuth trichloride (**Figure 3.8**). A clear pair of deposition and stripping peaks is observed, with a similar structure to the redox couples of either silver or tin, which most likely corresponds to the $\text{Bi}^{3+/0}$ couple. However, in this case there is an additional oxidation peak at *approx.* 0.5 V more positive than the initial oxidation, with no corresponding reduction peak.

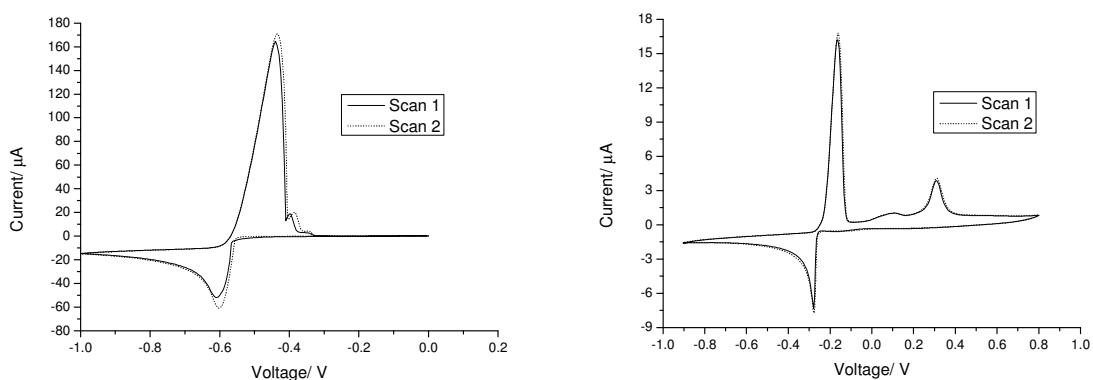


Figure 3.8 Cyclic voltammograms of metal salts in Ethaline: 100 mM SnCl_2 (left) and 20 mM BiCl_3 (right). Scans recorded on 1 mm Pt disc working electrode vs. Ag/AgCl in Ethaline reference, at a scan rate of 10 mV s^{-1} .

As this extra oxidation peak is at a significant distance away from the main redox couple, it is unlikely to be due to an alternative structure of metal deposit, and the lack of a corresponding reduction peak rules out the presence of the $\text{Bi}^{5+/3+}$ couple. An alternative argument is that the bismuth species produced from oxidation of the metal is different to the preferred speciation in solution.

As has been explained above, the higher oxidation states of palladium and gold have both been stabilised in the high chloride environment and are therefore much

easier to oxidise in DES media. AuCl shows a single redox event within the potential window of this experiment; however the deposition and stripping peaks are widely separated on the first scan. There are several arguments for the origin of this hysteresis: the presence of a small amount of gold being left on the working electrode surface, making nucleation of new gold easier; a higher concentration of gold chloride (or other gold complexes) remaining close to the electrode surface after the first round of dissolution enabling quicker deposition; or even that there is a difference in speciation of the gold before deposition and after reoxidation.

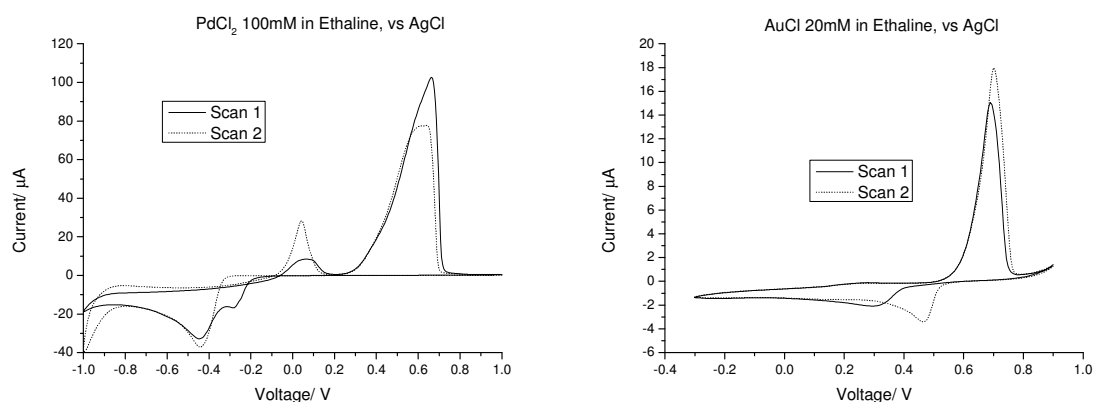


Figure 3.9 Cyclic voltammograms of 100 mM metal salts in Ethaline: PdCl₂ (left) and AuCl (right). Scans recorded on 1 mm Pt disc working electrode vs. Ag/AgCl in Ethaline reference, at a scan rate of 10 mV s⁻¹.

Palladium (II) chloride, on the other hand, has a particularly unusual CV shape, compared to the other metal salts examined so far. The deposition and stripping peaks, similar to gold, have a large potential separation between them. As the potential is swept in a reducing direction, deposition occurs in several stages. The first scan shows two reductions events, along with a nucleation. At very low potentials, it is possible there is hydrogen evolution from the presence of trace amounts of water absorbed by the Ethaline and if the scan is shortened, the nucleation loop becomes more visible and

the oxidation peaks are decreased. Within the potential range used, two oxidation peaks are seen, a broad one for the bulk deposit at approximately +0.2 V vs. AgCl reference and a smaller one which could possibly be assigned to the nucleation loop deposit at approximately -0.1 V.

Interestingly, the second scan and any further scans are different to the first scan, in that the nucleation loop is less prominent, along with the more negative oxidation peak, and the more positive oxidation peak is increased in current. This suggests that the properties of the freshly prepared Pt working electrode surface are different compared to after the first scan and that there is a possibility that not all of the palladium is stripped off in the oxidising wave, potentially due to slow diffusion of the palladium complex away from the working electrode or of slow diffusion of chloride towards the electrode.

From the slightly more unusual redox behaviour of these two metals, it could be suggested that different speciation from either copper or silver may be affecting the redox properties of the bulk solution.

Nickel and platinum chloride salts, which are not included in the redox series depicted in *Figure 3.6*, are shown here in *Figure 3.10* because they show unusual redox behaviour. Palladium chloride, as shown above, has clear, yet widely-spaced redox peaks. Neither nickel nor platinum behaves in this manner, despite being in the same group as palladium. If any nickel or platinum deposition is taking place on the Pt working electrode, the low currents observed suggest that it is minimal. In addition, deposition may coincide with solvent breakdown, as for the PtCl₂ solution it was necessary to truncate the potential range to avoid this.

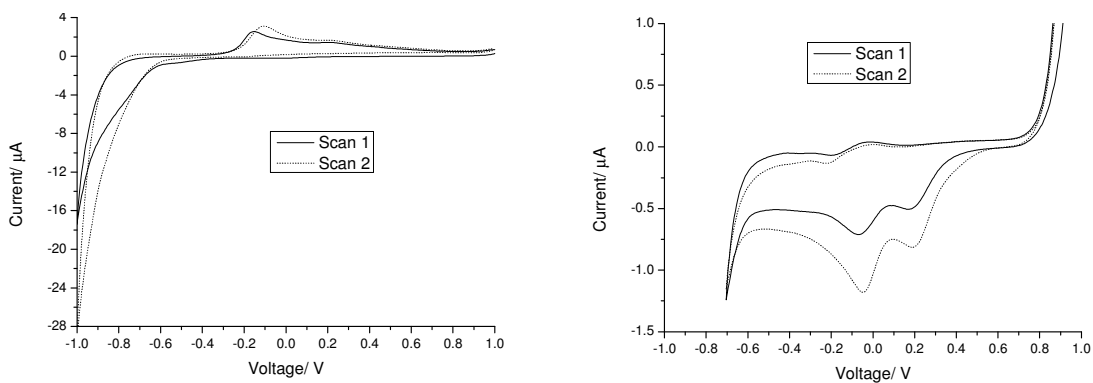


Figure 3.10 Cyclic voltammograms of 100 mM metal salts in Ethaline: NiCl_2 (left) and PtCl_2 (right). Scans recorded on 1 mm Pt disc working electrode vs. Ag/AgCl in Ethaline reference, at a scan rate of 10 mV s^{-1} .

The CV of nickel chloride in Ethaline shows very few features. Deposition, if any occurs, is at the low potential edge of the CV window and may coincide with solvent breakdown. A small oxidation bump is observed at large separation from where deposition would be expected. There may be some kind of surface effect on the Pt electrode preventing proper Ni deposition and therefore a native metal electrode may show clearer redox processes and this line of investigation will continue further in **Chapter 5**. A dependence on temperature has previously been observed for the reoxidation of the nickel deposit.⁵⁰ As the temperature of the solution was increased, the oxidation peak also increased. At 120°C , clear reduction and oxidation peaks were observed, along with a solution colour change from green to blue.

The deposition of platinum from a solution of platinum (II) chloride in Ethaline appears to coincide with breakdown of either the DES or of absorbed water. Hydrogen evolution may also be catalysed at the more negative potentials, despite no visible bubbles being formed. The relatively low temperatures involved in this experiment may be causing slow kinetics and hence why no visible redox behaviour is observed at the scan rates and temperatures used in these experiments. From the substantial difference

in redox behaviour observed for both nickel and platinum, it could be hypothesised that the salts of these metals may have completely different speciation in the DES environment compared to metals such as copper or silver, which have clear and concise redox behaviour. The speciation of these salts will be discussed further in **Chapter 4**.

Certain others of the d-block elements, such as chromium, manganese and cobalt, or p-block metals, such as indium, also show voltammetric responses where any redox couples are difficult to distinguish, similarly to nickel or platinum. These are shown below in *Figure 3.11*.

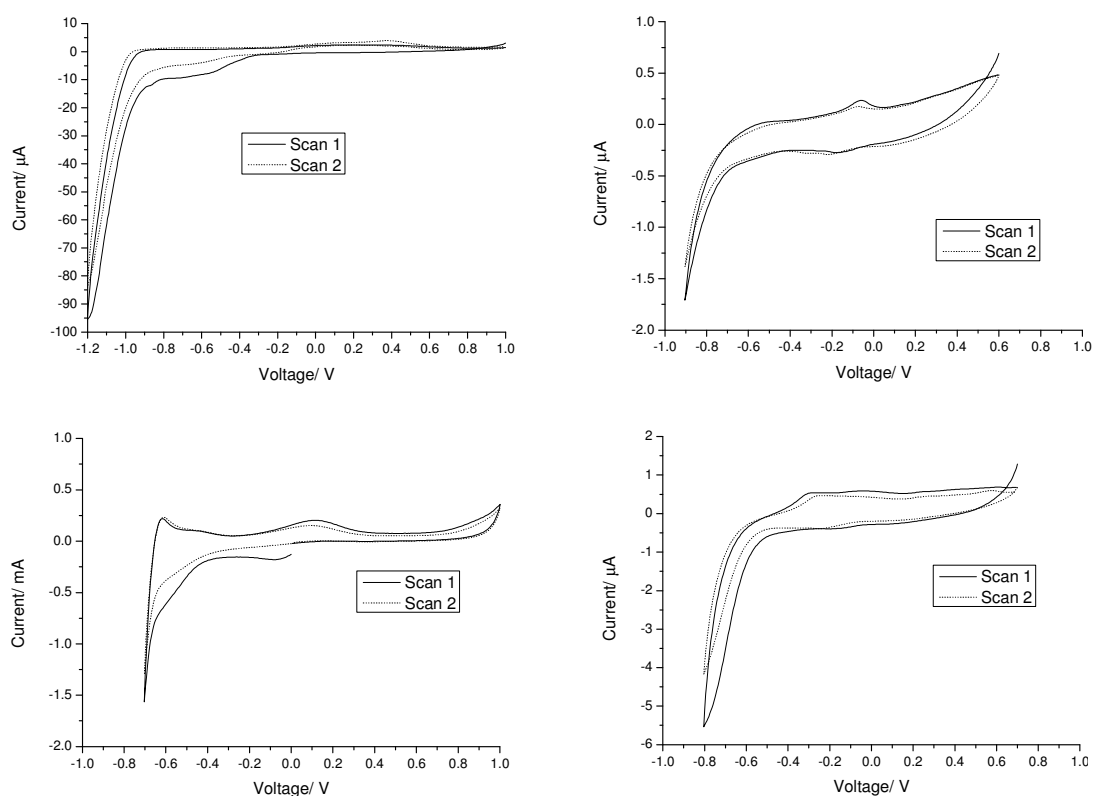


Figure 3.11 Cyclic voltammograms of 100 mM metal salts in Ethaline: CrCl₃ (top left), MnCl₂ (top right), CoCl₂ (bottom left) and InCl₃ (bottom right). Scans recorded on 1 mm Pt disc working electrode vs. Ag/AgCl in Ethaline reference, at a scan rate of 10 mV s⁻¹.

The cyclic voltammetry of the solutions of chromium (III), manganese (II), cobalt (II) and indium (III) chloride in Ethaline all show a similar voltammetric response onto

a Pt working electrode, where there is either minimal metal deposition or an indication of solution breakdown and the expected corresponding stripping peak is either minimal or non-existent. The cause of this voltammetric response is likely to be either a speciation or surface effect, or a combination of the two. For instance, if the metal species is not a purely chloride complex and is instead a complex formed with part of the HBD *e.g.* ethylene glycol in Ethaline, redox behaviour may not be seen within the potential window of the solvent as it could cause solution breakdown. If instead a surface effect is the issue, *e.g.* oxide formation, then the metal to be deposited may not be able to be reduced. The speciation of these metal salts in a range of different DESs will be discussed further in **Chapter 4** and the effects of surface behaviour (if any) will be discussed in **Chapter 5**.

Other unusual redox behaviour is seen for iron and zinc chloride solutions. In an iron (III) chloride solution in Ethaline, two different redox processes are seen. A reversible redox couple, probably $\text{Fe}^{3+/2+}$, is visible at the more positive potentials and this behaves similarly to the $\text{Cu}^{2+/+}$ couple, as would be expected. However, in the region where the iron deposition and stripping couple would be expected, only a small amount of Fe deposition is observed, followed by an unusually shaped oxidation that continues with a reducing current. One possibility is that Fe^{3+} from the bulk solution is oxidising the Fe^0 at the same time as it is being deposited from Fe^{2+} , hence only a small deposition current is seen, and continues to oxidise concurrently with the oxidation of Fe^0 by loss of electrons at the working electrode. The negative current increases as all of the Fe^0 has been oxidised to Fe^{2+} , and continues in this manner until the potential is positive enough to oxidise Fe^{2+} to Fe^{3+} again. Another possibility is that the Ethaline itself is chemically reacting with any metallic iron deposit.

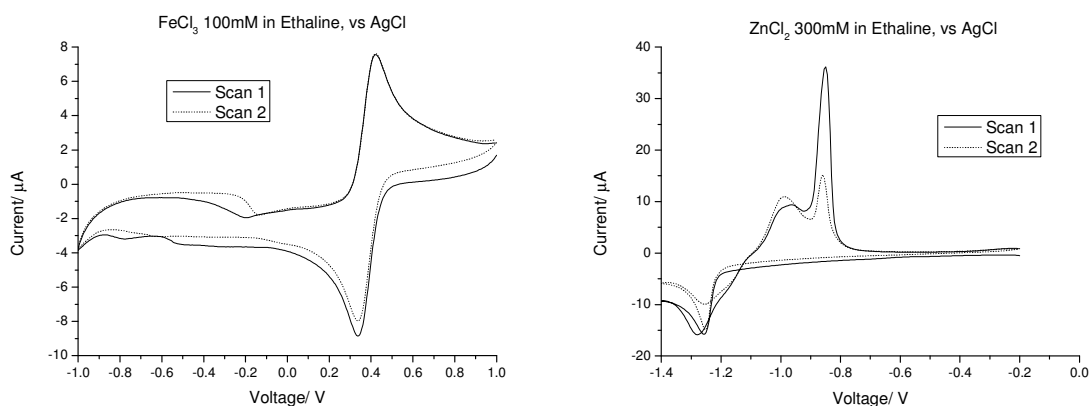


Figure 3.12 Cyclic voltammograms of metal salts in Ethaline: 100 mM FeCl_3 (left) and 300 mM ZnCl_2 (right). Scans recorded on 1 mm Pt disc working electrode vs. Ag/AgCl in Ethaline reference, at a scan rate of 10 mV s^{-1} .

At 100 mM, zinc (II) chloride in Ethaline produces a CV which is similar to that reported by Barron.⁵¹ Slow deposition is seen at approximately -0.6 V with two stripping peaks which have previously been assigned to two different zinc morphologies.⁵¹ Raising the concentration of ZnCl_2 to 300 mM causes the more positive stripping peak to increase in area (**Figure 3.12**). A nucleation loop can be seen at the low potential end of the scale and two separate stripping peaks are observed in the oxidation scan. The more positive stripping peak was shown by AFM to be due to micron sized nuclei growing on the electrode surface whereas the less positive overpotential peak is associated with nano deposits. It would be logical that an increase in ZnCl_2 concentration should lead to larger scale metal nuclei.

Gallium and iodine are both higher in redox potential than most of the other couples studied, therefore they are less easy to oxidise in the high chloride environment of Ethaline but more easy to reduce. This makes iodine in particular a much stronger oxidising agent in DES media than it would be in aqueous media. Combining this

oxidising ability with a substantially higher solubility in Ethaline, iodine can be applied as a benign, yet powerful, oxidising agent to different metallurgical processes.

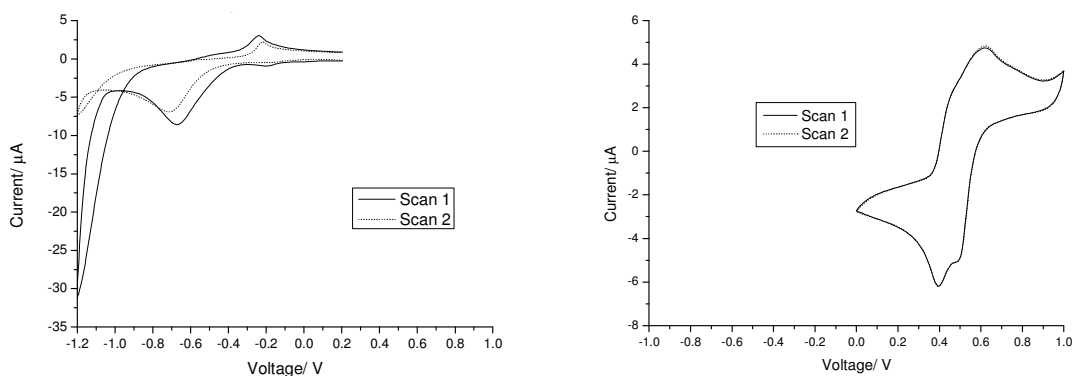


Figure 3.13 Cyclic voltammograms of 100 mM metal salts in Ethaline: GaCl_3 (left) and I_2 (right). Scans recorded on 1 mm Pt disc working electrode vs. Ag/AgCl in Ethaline reference, at a scan rate of 10 mV s^{-1} .

Voltammetry of iodine (20 mM) in Ethaline shows two reversible redox couples, with similar redox potentials to each other, one of which will be the I_2/I^- couple. The second redox couple suggests that another species is also formed in solution – possibly a trihalide species, such as I_3^- or I_2Cl^- . A speciation determining technique, such as EXAFS, could be used to determine which combination of halides is present and will be explored further in **Chapter 5**. The position of the iodine redox couples at much more positive potentials with respect to the majority of the other metal deposition and oxidation couples (as seen in **Figure 3.6**) reinforces the potential for iodine to be used as an oxidising agent in DES media.

Gallium (III) chloride, on the other hand, shows two reduction peaks, one of which is a nucleation loop at very low voltages. The stripping peak current seems too small for the amount of Ga deposited, unless the first reduction peak is due to Ga^{3+} then the nucleation loop is of Ga^{+0} . This suggests that the gallium complex in solution may be particularly difficult to reduce *via* electrolytic methods. If so, this information

could potentially be exploited for the separation of gallium from other metals which will be explored later in this thesis.

3.4 Conclusions

A new Ag/AgCl reference electrode has been developed for use in DES media and its stability was tested with both potentiometric and equilibrium measurements and has subsequently been applied to determining activity coefficients in IL and DES media.

From equilibrium measurements as a function of concentration, it has been seen that ionic association in the ILs and DESs examined does not appear to shift the redox potentials of the metal salts and their ions exhibit an ideal Nernstian response. It was found that the $\text{Ag}^{+/0}$ couple exhibited ideal behaviour (*i.e.* activity \approx concentration) in ILs and DESs with Cl^- as the anion, whereas the same redox couple had significant deviations from ideality with other anions, such as SCN^- or OAc^- , possibly due to the formation of multinuclear complexes *via* bridging of the anion. Ideal behaviour is also observed at up to 1 mol kg^{-1} for the $\text{Cu}^{2+/+}$ couple in Ethaline and for the H^+/H_2 couple for Triflic acid in Ethaline, suggesting that the acid is fully dissociated, which could potentially allow a measure of pH to be determined in DESs. The above results show that coulombic shielding of the solute by the IL or DES allows independent behaviour of the ions in solution and may allow standard thermodynamic behaviour to be applied to ionic solutions.

The first set of standard redox potentials has been obtained for a range of metal salts in DESs. In addition, an electrochemical series for metal redox couples in Ethaline has been created and it can be seen that, for some redox couples, significant deviations in potential occur compared to in aqueous media. For example, the higher oxidation states of the chlorophilic late transition metals are stabilised in the DES environment

and the oxophilic p-block elements are destabilised. This can be seen by a decrease or an increase of formal potentials in Ethaline, respectively, compared to formal aqueous electrode potentials. These deviations can potentially be explained by speciation effects caused by the high chloride activity of the DES, as will be shown by the use of EXAFS in *Chapter 4*.

In the DES electrochemical series, the location of iodine couple with respect to the other metal couples makes it an effective oxidising agent, which can be used for metal dissolution and recovery. By employing iodine in high enough concentrations even thermodynamically unfavourable oxidations, such as the oxidation of gold, can be achieved and will be discussed further in *Chapter 6*.

3.5 References

1. P. Wasserscheid and T. Welton, *Ionic liquids in synthesis*, Wiley-VCH, Weinheim, 2008.
2. A. P. Abbott, D. Boothby, G. Capper, D. L. Davies and R. K. Rasheed, *Journal of the American Chemical Society*, 2004, **126**, 9142-9147.
3. A. P. Abbott, G. Capper, D. L. Davies, K. J. McKenzie and S. U. Obi, *Journal of Chemical and Engineering Data*, 2006, **51**, 1280-1282.
4. A. P. Abbott, G. Capper, D. L. Davies, R. K. Rasheed and P. Shikotra, *Inorganic Chemistry*, 2005, **44**, 6497-6499.
5. A. P. Abbott, G. Frisch, J. Hartley and K. S. Ryder, *Green Chemistry*, 2011, **13**, 471-481.
6. A. P. Abbott, J. Collins, I. Dalrymple, R. C. Harris, R. Mistry, F. L. Qiu, J. Scheirer and W. R. Wise, *Australian Journal of Chemistry*, 2009, **62**, 341-347.

7. A. P. Abbott, G. Capper, K. J. McKenzie, A. Glidle and K. S. Ryder, *Physical Chemistry Chemical Physics*, 2006, **8**, 4214-4221.
8. A. P. Abbott, G. Frisch and K. S. Ryder, *Annual Reports on the Progress of Chemistry, Section A: Inorganic Chemistry*, 2008, **104**, 21-45.
9. A. P. Abbott, G. Capper, D. L. Davies and P. Shikotra, *Mineral Processing and Extractive Metallurgy*, 2006, **115**, 15-18.
10. F. Endres, D. MacFarlane and A. Abbott, *Electrodeposition from Ionic Liquids*, Wiley-VCH, 2008.
11. J. Koryta, J. Dvořák and L. Kavan, *Principles of Electrochemistry*, Wiley, 1993.
12. E. Gileadi, *Physical Electrochemistry*, John Wiley & Sons, 2011.
13. G. Gritzner and J. Kuta, *Pure and Applied Chemistry*, 1984, **56**, 461-466.
14. R. S. Stojanovic and A. M. Bond, *Analytical Chemistry*, 1993, **65**, 56-64.
15. K. Izutsu, *Electrochemistry in Nonaqueous Solutions*, Wiley-VCH, 2002.
16. G. A. Snook, A. S. Best, A. G. Pandolfo and A. F. Hollenkamp, *Electrochemistry Communications*, 2006, **8**, 1405-1411.
17. F. Endres and W. Freyland, *The Journal of Physical Chemistry B*, 1998, **102**, 10229-10233.
18. J. Zhang and A. M. Bond, *Analytical Chemistry*, 2003, **75**, 2694-2702.
19. U. Schroder, J. D. Wadhawan, R. G. Compton, F. Marken, P. A. Z. Suarez, C. S. Consorti, R. F. de Souza and J. Dupont, *New Journal of Chemistry*, 2000, **24**, 1009-1015.
20. Y. NuLi, J. Yang, J. L. Wang, J. Q. Xu and P. Wang, *Electrochemical and Solid State Letters*, 2005, **8**, C166-C169.
21. D. M. Ryan, T. L. Riechel and T. Welton, *Journal of the Electrochemical Society*, 2002, **149**, A371.

22. N. G. Connelly and W. E. Geiger, *Chemical Reviews*, 1996, **96**, 877-910.
23. A. Lewandowski, L. Waligora and M. Galinski, *Electroanalysis*, 2009, **21**, 2221-2227.
24. J. P. Hurvois and C. Moinet, *Journal of Organometallic Chemistry*, 2005, **690**, 1829-1839.
25. P. De Vreese, K. Haerens, E. Matthijs and K. Binnemans, *Electrochimica Acta*, 2012, **76**, 242-248.
26. A. Saheb, J. Janata and M. Josowicz, *Electroanalysis*, 2006, **18**, 405-409.
27. V. M. Hultgren, A. W. A. Mariotti, A. M. Bond and A. G. Wedd, *Analytical Chemistry*, 2002, **74**, 3151-3156.
28. E. I. Rogers, D. S. Silvester, S. E. WardJones, L. Aldous, C. Hardacre, A. J. Russell, S. G. Davies and R. G. Compton, *Journal of Physical Chemistry C*, 2007, **111**, 13957-13966.
29. N. V. Plechkova and K. R. Seddon, *Chemical Society Reviews*, 2008, **37**, 123-150.
30. H. S. Harned and B. B. Owen, *The Physical Chemistry of Electrolytic Solutions*, Reinhold Pub. Corp., 1958.
31. R. A. Robinson and R. H. Stokes, *Electrolyte Solutions*, Dover Publications, 2002.
32. J. P. Hallett, C. L. Liotta, G. Ranieri and T. Welton, *Journal of Organic Chemistry*, 2009, **74**, 1864-1868.
33. M. Y. Lui, L. Crowhurst, J. P. Hallett, P. A. Hunt, H. Niedermeyer and T. Welton, *Chemical Science*, 2011, **2**, 1491-1496.
34. A. Heintz, *Journal of Chemical Thermodynamics*, 2005, **37**, 525-535.
35. Q. Li, F. Xing, Z. Lei, B. Wang and Q. Chang, *Journal of Chemical & Engineering Data*, 2008, **53**, 275-279.

36. K. J. Laidler, J. H. Meiser and B. C. Sanctuary, *Physical Chemistry*, Houghton Mifflin, 2003.
37. G. M. Barrow, *Physical Chemistry*, 1988.
38. A. P. Abbott, G. Frisch, S. J. Gurman, A. R. Hillman, J. Hartley, F. Holyoak and K. S. Ryder, *Chemical Communications (Camb)*, 2011, **47**, 10031-10033.
39. C. Wakai, A. Oleinikova, M. Ott and H. Weingartner, *The Journal of Physical Chemistry. B*, 2005, **109**, 17028-17030.
40. E. I. Izgorodina, M. Forsyth and D. R. Macfarlane, *Physical Chemistry Chemical Physics*, 2009, **11**, 2452-2458.
41. L. M. Mihichuk, G. W. Driver and K. E. Johnson, *Chemphyschem*, 2011, **12**, 1622-1632.
42. D. Lloyd, T. Vainikka, L. Murtomaki, K. Kontturi and E. Ahlberg, *Electrochimica Acta*, 2011, **56**, 4942-4948.
43. A. P. Abbott, R. C. Harris and K. S. Ryder, *The Journal of Physical Chemistry B*, 2007, **111**, 4910-4913.
44. A. P. Abbott, K. El Ttaib, G. Frisch, K. J. McKenzie and K. S. Ryder, *Physical Chemistry Chemical Physics*, 2009, **11**, 4269-4277.
45. K. Takahashi, S. Sakai, H. Tezuka, Y. Hiejima, Y. Katsumura and M. Watanabe, *The Journal of Physical Chemistry B*, 2007, **111**, 4807-4811.
46. K. E. Johnson, R. M. Pagni and J. Bartmess, *Monatshefte für Chemie - Chemical Monthly*, 2007, **138**, 1077-1101.
47. N. F. Hall and J. B. Conant, *Journal of the American Chemical Society*, 1927, **49**, 3047-3061.
48. A. J. Bard and L. R. Faulkner, *Electrochemical Methods: Fundamentals and Applications*, Wiley, 1980.

49. A. P. Abbott, G. Frisch, S. J. Gurman, A. R. Hillman, J. Hartley, F. Holyoak and K. S. Ryder, *Chemical Communications (Camb)*, 2011, **47**, 10031-10033.
50. C. M. Ip, MChem, University of Leicester, 2012.
51. J. C. Barron, PhD, University of Leicester, 2010.

Chapter 4 Speciation and EXAFS

Chapter 4	Speciation and EXAFS	113
4.1	Theory of EXAFS	114
4.1.1	Generation of X-rays	115
4.1.2	Absorption edges	116
4.1.3	Generation of EXAFS spectra	117
4.1.4	The different regions of EXAFS spectra	120
4.1.5	Methods and modes	122
4.2	The speciation of metal salts in DES media.....	123
4.2.1	Speciation of metal chloride salts in glycol-based DESs	124
4.2.2	Speciation of metal chloride salts in Reline.....	132
4.2.3	Nickel: A special case.....	136
4.2.4	Speciation of iodine in DES media.....	141
4.3	Speciation in imidazolium liquids.....	142
4.3.1	Speciation of metal salts in [HMIM][Cl].....	142
4.3.2	Other ILs with different anions.....	146
4.4	Conclusions	148
4.5	References	150

4.1 Theory of EXAFS

In **Chapter 3**, it was seen that metal salts such as silver, gold, tin and copper chloride in Ethaline and Propaline show a simple and clear voltammetric response for each set of redox couples. Other metals, such as nickel or palladium show semi-reversible behaviour. Some metals, such as cobalt or manganese, were even seen to display irreversible deposition behaviour. The hypothesis was that if simple redox behaviour was observed, then a single species is also present. Conversely, if complex redox behaviour was observed, then a more complex species is theorised to be present. If speciation and redox behaviour can be directly linked, then the redox behaviour of a solute could be controlled simply by modifying the solvent to alter the speciation. This would have implications for metal processing as it would mean that the effects of the solvent alone would be sufficient to obtain the desired speciation, without the need for additional complexation agents. The particular method chosen for this determination of metal salt speciation in deep eutectic solvent (DES) media is Extended X-ray absorption fine structure (EXAFS).

EXAFS is the oscillatory variation in X-ray absorption beyond an X-ray absorption edge, as a function of increasing photon energy E .¹ This absorption occurs when a core shell electron in an atom is excited and can be found from the measurement of X-rays transmitted through a sample and their consequent attenuation. Their attenuation is often expressed as the absorption coefficient, μ . Interference caused by the scattering of the emitted photoelectron wave off of the surrounding atoms results in an oscillation in the absorption coefficient and from this interference pattern, the local arrangement of atoms around the absorbing species can be determined.² EXAFS is a useful technique for the structural analysis of both ordered and disordered chemical and biological systems where conventional diffraction methods are not applicable, for

instance in liquid samples. As EXAFS needs a continuous tuneable monochromatic X-ray spectrum to obtain data, it necessitates the use of a synchrotron as a light source.

4.1.1 Generation of X-rays

Synchrotrons generate electromagnetic radiation by forcing charged particles, often electrons, which are moving close to the speed of light to change direction in a magnetic field. The electrons are first produced by an electron gun and are then sped up by a series of accelerators. Once the electrons have reached just under the speed of light, they are introduced to the storage ring, where they will pass through a series of bending magnets or wigglers, both to steer the electrons around the ring and to make the synchrotron radiation. As the electrons pass through each magnet, they lose energy in the form of light. As this radiation spans a wide frequency range, it must then be passed through a monochromator to obtain the specific X-ray wavelengths needed, which are then focussed onto the sample.

To be able to measure the intensity of the X-rays before and after they have interacted with the sample, a combination of three ion chamber detectors filled with a specific gas mix is employed. The first of these ion chamber detectors (I_0) measures the intensity of the X-rays before hitting the sample, the second measures the intensity after transmission or fluorescence (I_T or I_F) and the final chamber measures the intensity after the X-rays have passed through a reference foil for the specific element edge for the absorbing atom (I_R). This array is depicted in *Figure 4.1*.

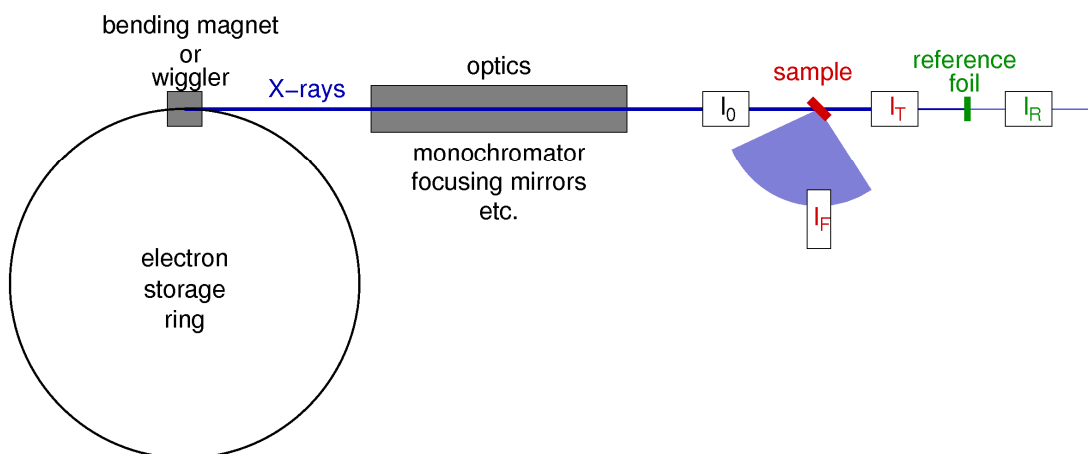


Figure 4.1 Schematic diagram of the synchrotron beamline.

4.1.2 Absorption edges

To generate the EXAFS spectra, hard X-rays of greater than 3-4 keV are utilised and photon absorption within this range is determined by core electron excitations. When the energy of an X-ray photon matches that of the binding energy of a core shell electron in a sample, a sharp increase in absorption coefficient, μ , occurs as the electron is excited and ejected into the environment. This is known as the absorption edge. For single isolated atoms, the absorption decreases monotonically as a function of energy after the edge. For molecules or condensed phases, any variation of the absorption coefficient at energies above the edge displays EXAFS. These spectra are usually visible at 40-1000 eV above the absorption edge and tend to have amplitudes of a few tenths of the edge step magnitude.^{1, 3}

In X-ray absorption spectroscopy the absorption edges observed have a characteristic energy which corresponds to the relevant atomic core orbitals. For instance, excitation of the 1s orbital gives rise to the K-edge, the 2s, 2p_{1/2} and 2p_{3/2} correspond to the L_{I-III} edges respectively and the 3s, 3p_{1/2} and 3p_{3/2} orbitals to the M edges (see **Figure 4.2**).

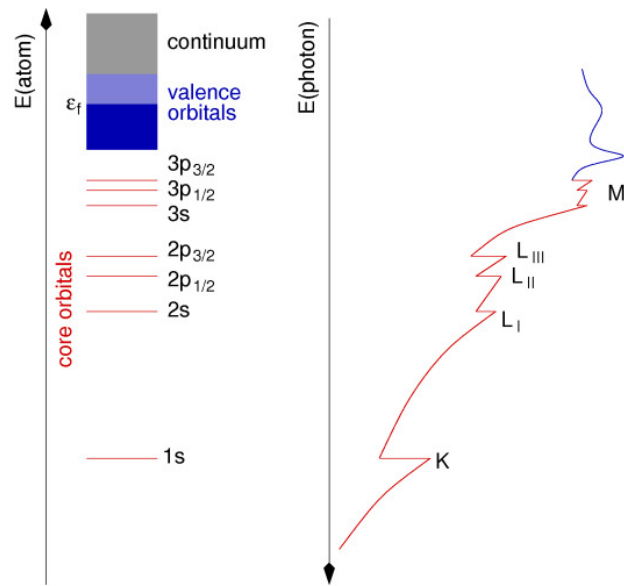


Figure 4.2 Schematic diagram showing the core orbitals of a 3d-element atom and their corresponding X-ray absorption edges.

4.1.3 Generation of EXAFS spectra

Once an outgoing photoelectron wave has been generated by absorption of an X-ray and ejection of a core shell electron from the absorbing species, this photoelectron wave is then backscattered from any neighbouring atoms in the sample (**Figure 4.3**) and the interference between these two waves produces a distinctive pattern which is known as the fine structure.

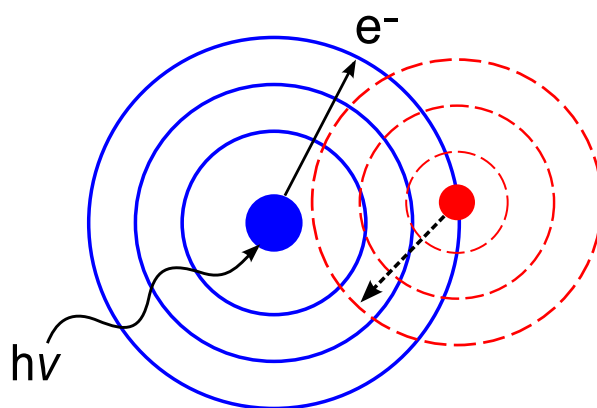


Figure 4.3 Schematic diagram showing how EXAFS arises for a simple diatomic molecule. The solid coloured circle in the middle is the atom and the coloured lines surrounding are the photoelectron waves.

This interference, *i.e.* the EXAFS, can be defined as the fractional oscillation of the absorption coefficient above the edge with respect to the atomic background absorption, shown in **Equation 4.1**,

$$\chi(k) = \frac{\mu(k) - \mu_0(k)}{\Delta\mu_0(k)} \quad \text{Equation 4.1}$$

where $\chi(k)$ is the EXAFS as function of photoelectron wavevector k ; $\mu(k)$ is the absorption above the edge; $\mu_0(k)$ is a smoothly varying atomic-like background absorption, which will include contributions from other edges if necessary, and $\Delta\mu_0$ is a normalisation factor which arises from the net increase in the total atomic background absorption at the examined edge. It can then be defined as a function of the photoelectron wavevector (**Equation 4.2**). The wavevector, k , is defined as photon energy, E , above the edge, E_0 , with respect to the mass of an electron, m_e .

$$k = \sqrt{\frac{2m_e}{\hbar^2} (E - E_0)} \quad \text{Equation 4.2}$$

The EXAFS can then be related to the wavenumber by the equation

$$\chi(k) \approx \sum_i \frac{N_i f_i(k)}{kr_i^2} e^{-2\sigma_i^2 k^2} e^{-2r_i/\lambda} \sin[2kr_i + \alpha_i(k)] \quad \text{Equation 4.3}$$

where $\chi(k)$ is the sum over N_i back scattering atoms i ; f_i is the scattering amplitude; $\exp(-2\sigma_i^2 k^2)$ is the Debye-Waller factor for the thermal vibration of the atoms; r_i is the distance of the scattering atom from the absorber atom; λ is the mean free path of the photoelectron and α_i is the phase shift of the spherical photoelectron wave as it rebounds off the back scattering atoms.²⁻⁵ Fourier transform of the fine structure $\chi(k)$ will produce a real space radial distribution function for the back scattering atoms around the central absorbing atom. An example of this is shown in **Figure 4.4**.

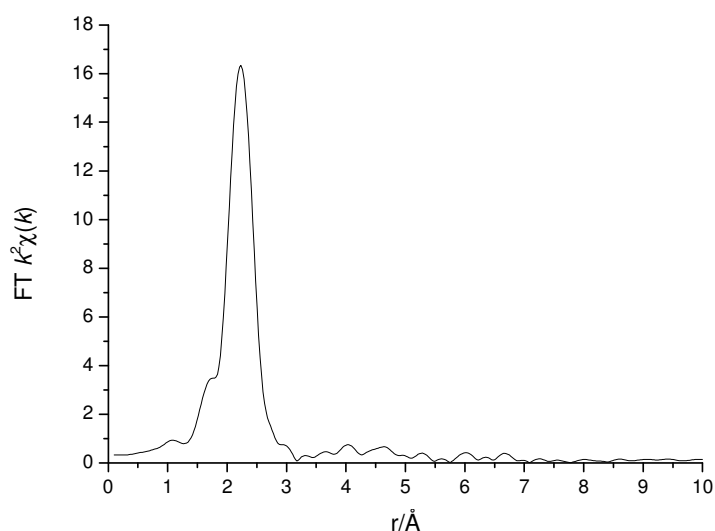


Figure 4.4 Example of a Fourier transform for a solution of 100 mM CoCl_2 in Ethaline. This plot is related to the electron density of a nearby ligand as a function of distance away from the absorbing atom.

However, this equation only describes the EXAFS for single scattering atoms and not for multiple scattering atoms. Single scattering is sufficient for most of the samples used in this project however certain linear molecules, such as SCN, can show strong multiple scattering effects. This is particularly significant when one atom lies directly behind the

emitting atom and any contributions to the EXAFS from it are greatly affected by the forward scattered photoelectron waves.⁶

4.1.4 The different regions of EXAFS spectra

Different regions of the EXAFS spectrum can be interpreted for different sets of information and these regions are shown in **Figure 4.5**. From the energy of the edge information on the absorbing atom, such as structure and oxidation state can be extracted. From the interference after the edge, information about the local short-range environment around the absorbing atom can be determined, such as the number of scattering neighbouring atoms, their identities and distances away from the absorbing atom.⁷

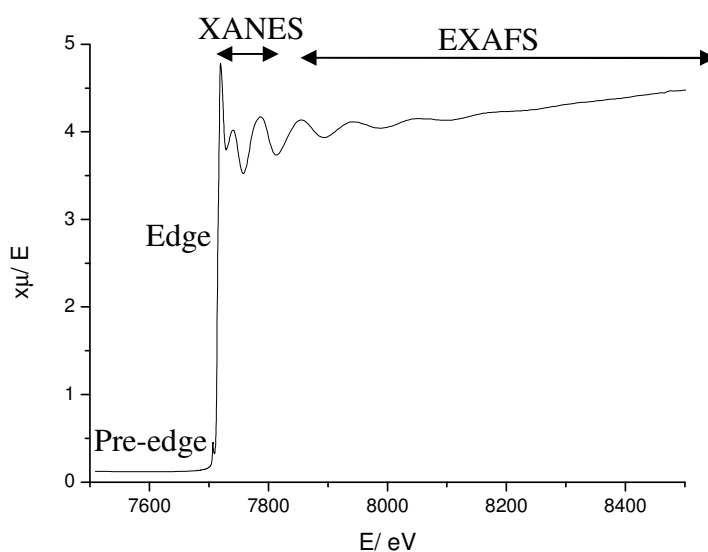


Figure 4.5 Example of a transmission X-ray absorption spectrum, $x\mu$ vs. E , for the Co- K absorption edge (CoCl_2 in Ethaline), where E is the energy of the X-ray beam.

Near or below the edge are absorption peaks due to the excitation of core electrons. This pre-edge region shows the bonding information for orbitals which are unoccupied in the ground state, electronic configurations and site symmetry. Between

the pre edge and EXAFS regions is the XANES region, which is caused by multiple scattering, many-body interactions, distortion of excited state wavefunctions by Coulomb field, band structures, *etc.*

The advantage to EXAFS is that elements of interest can be selectively investigated by exciting an electron from a core shell. EXAFS usually only shows the direct coordination of ligands to the excited atom and other uncoordinated compounds in the sample will not contribute to the spectral features of the signal. The electron scattering amplitude is reduced with distance as the ligand atoms get further away and the distance determination of these atoms is restricted to $\sim 6 \text{ \AA}$ away from the absorber,³ although greater distances (6-8 \AA) can be obtained by a slightly different method that involves the use of high energy X-ray scattering.⁷ However, the higher energies mean that all of the atoms in the sample will contribute to the scattering signal, resulting in complicated spectra unless high atomic number elements and high concentrations are used to increase contrast against background noise.

When using EXAFS, it must be understood that the amplitude of the fine structure of μ vs. E is dependent on the type and bonding of neighbouring atoms, whilst the frequency is dependent on the distance away the neighbouring atom is from the absorbing atom, although these neighbouring atoms do not necessarily need to be bonded to the absorbing atom. Errors in coordination number will depend on the particular system and can be high depending on the structure of the coordinating ligands, e.g. a linear molecule can cause multiple scattering in the EXAFS. If the sample contains multiple potential absorbers, precise determination of the speciation can be obtained by studying all of these absorbing atoms.^{2, 3} To obtain the best results, EXAFS should be used in conjunction with other speciation techniques to be certain of a realistic interpretation of the structure of the species of interest.

4.1.5 Methods and modes

The two most common modes of EXAFS measurements are transmission and fluorescence. A transmission experiment records

$$\mu x = \ln \frac{I_0}{I_t} \nu S E_{\text{photon}} \quad \text{Equation 4.4}$$

where μ is the absorption coefficient, x is the thickness of the sample, I_0 is the intensity of the incoming X-ray beam and I_t is the intensity of the transmitted beam. It is most useful for solid or concentrated samples where the signal is strong but care must be taken to ensure that it does not cut off all signal to the ion chamber detectors. For powder samples this can be achieved by diluting the sample with boron nitride powder.

When using dilute samples or ones which suffer from a high amount of background absorption, fluorescence mode is a more suitable method as it minimises the signal from the matrix. For transmission experiments in DESs, the signal from the solvent itself will swamp the signal from the comparatively low concentration of metal and will substantially reduce the quantity of X-rays being detected. The fluorescence mode involves the placement of the sample at *ca.* 45° to the beam and the measurement of fluorescence radiation at *ca.* right angles to the incident beam. This is given by

$$\mu x = \frac{I_f}{I_0} \nu S E_{\text{photon}} \quad \text{Equation 4.5}$$

where I_f is intensity of the fluorescence. A concern with the transmission mode is that the samples need to be uniformly thick if multiple measurements from different points on the sample are needed, as the signal strength will change if not. For fluorescence mode, radiation fluorescing from the top few layers of the sample is detected and the precise thickness of the sample is less of an issue.

In order to be able to calibrate the energy of the spectra prior to fitting the data, a reference sample must be used. This can be expressed as

$$\mu x = \ln \frac{I_t}{I_r} \text{ vs } E_{\text{photon}} \quad \text{Equation 4.6}$$

where I_r is the intensity of the beam after the reference sample. The reference sample is often a metal foil or a boron nitride diluted solid sample of a salt corresponding to the absorbing atom which has been targeted.

4.2 The speciation of metal salts in DES media

As seen in above in **Section 3.4**, the redox potentials of several of the late transition metals in Ethaline have been shifted towards more cathodic potentials, *i.e.* the higher oxidation states have been stabilised in DES solution, compared to aqueous solution. It is thought that this may be due to the *ca.* 5 M chloride environment of the DES inducing metal chloro-complexes to form. The speciation of metal salts in DESs has previously been studied by Abbott *et al.* using fast atom bombardment-mass spectroscopy (FAB-MS)⁸ and EXAFS.^{9, 10} Comparing the data gathered with these methods for Zn^{2+} , it can easily be seen that there is a mismatch between the proposed speciation. For instance, FAB-MS suggests that complex anions are formed in Ethaline, such as $[\text{ZnCl}_3]^-$, $[\text{Zn}_2\text{Cl}_5]^-$ and $[\text{Zn}_3\text{Cl}_7]^-$,¹¹ whilst EXAFS indicates the presence of a single tetrachloro species, $[\text{ZnCl}_4]^{2-}$.¹⁰

FAB-MS is unlikely to provide a complete representation of the solution phase due to potential fragmentation of the metal chloro-complexes in the gas phase. By using EXAFS to study speciation instead, an *in situ* analysis of the species of interest can therefore be made, without destruction of the sample or breakdown of the solution species.

In general, for the DESs used, it was found that the M^+ salts tended to form $[\text{MCl}_2]^-$ complexes, whilst the M^{2+} salts tended to form $[\text{MCl}_4]^{2-}$ complexes, with a few special exceptions for the more oxophilic metals and particularly strong ligands.

4.2.1 Speciation of metal chloride salts in glycol-based DESs

Metal salts such as silver, gold, tin and copper chloride in Ethaline and Propaline have been seen to show a simple and clear voltammetric response for each set of redox couples. The hypothesis was that if simple redox behaviour was observed, then a single species is also present. In this section, the speciation of metal chlorides will be discussed.

4.2.1.1 Speciation of the metal (I) chloride salts

The speciation of three metal (I) chloride salts; AgCl, AuCl, and CuCl, were studied in the glycol-based DESs, Ethaline and Propaline. In all cases, chloride species were observed. The EXAFS data fits for these metal salts in Ethaline and Propaline are shown in **Table 4.1**, along with proposed species.

Table 4.1 EXAFS fits of a range of metal (I) chloride salts in Ethaline (top) and 1,2-Propaline (bottom).

Metal salt	M-X, where X = ?	Number of atoms, n	Distance from centre, r (Å)	Debye-Waller factor, a (Å ²)	Fermi energy, EF (eV)	Fit index, R(min)	Proposed species
AgCl	Cl	2.5(2)	2.484(7)	0.017(2)	-6.3(6)	4.3 %	[AgCl ₂] ⁻
AuCl	Cl	1.9(2)	2.262(6)	0.006(2)	-7(1)	5.5 %	[AuCl ₂] ⁻
CuCl	Cl	2.4(3)	2.19(1)	0.016 (3)	-6.0(9)	10.9 %	[CuCl ₂] ⁻
AgCl	Cl	2.4(2)	2.486(6)	0.016(2)	-5.6(6)	4.2 %	[AgCl ₂] ⁻
AuCl	Cl	1.8(1)	2.265(6)	0.007(1)	-7(1)	6.8 %	[AuCl ₂] ⁻

An example of this single species coordination is shown in **Figure 4.6** for the solution of AgCl in Ethaline. In this particular case, a single peak is visible in the Fourier transform (FT) of the EXAFS, with an electron density suggesting the presence

of two to three chloride atoms at a distance of ~ 2.48 Å away from the excited silver atom. Translating this data to a structure infers that there is a mixture of both the $[\text{AgCl}_2]^-$ and the $[\text{AgCl}_3]^{2-}$ species present in solution, similarly to what would be expected for the dissolution of AgCl in strong aqueous chloride solutions.¹² This similarity in speciation is also highlighted by a consistent DW factor of ~ 0.016 Å².

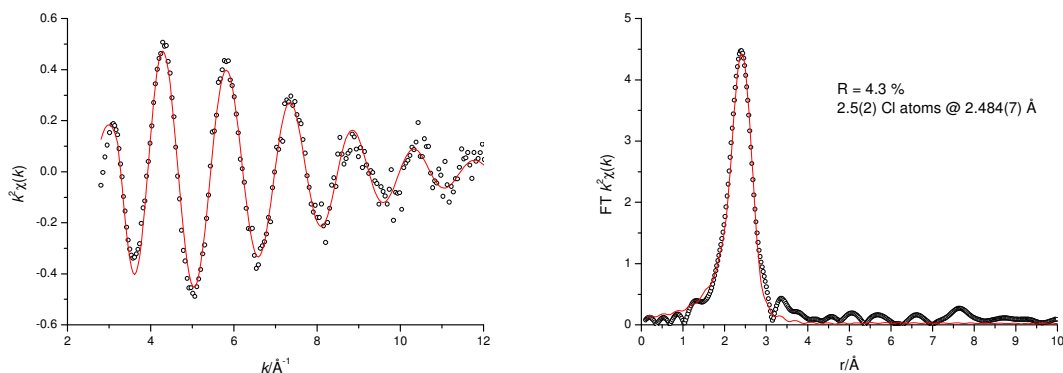


Figure 4.6 EXAFS (left) and Fourier transform (right) of 100 mM AgCl in Ethaline. Data is black circles, data fit is red line.

The other two metal chloride salts, AuCl and CuCl, also showed a similar response in the Fourier transform of the EXAFS spectra, where a single peak was visible that corresponded to between two and three chloride atoms. No variation in speciation was observed when the solvent was changed from Ethaline to Propaline.

4.2.1.2 Speciation of the metal (II) chloride salts

If the MCl_2 salts are considered instead, it can be seen that these tended to form tetrachloro complexes in the glycol-based DESs, rather than the dichloro species, as can be seen in **Table 4.2**. The presence of water in the form of hydration shells in the salts used did not appear to affect the speciation significantly. The formation of tetrachloride species in DES media has been previously proposed by Abbott *et al.* from studies of

UV-vis spectra of copper (II) chloride and its hydrated form in Ethaline,⁹ and also for zinc chloride from EXAFS studies.¹⁰

Table 4.2 EXAFS fits of 100 mM solutions of metal (II) chloride salts in Ethaline.

Metal salt	M–X, where X = ?	Number of atoms, n	Distance from centre, r (Å)	Debye-Waller factor, a (Å ²)	Fermi energy, EF (eV)	Fit index, R(min)	Proposed species
CoCl ₂	Cl	4.0(2)	2.282(3)	0.0062(7)	-6.6(3)	2.2 %	[CoCl ₄] ²⁻
CoCl ₂ ·6H ₂ O	Cl	3.9(1)	2.282(2)	0.0053(6)	-7.0(3)	1.5 %	[CoCl ₄] ²⁻
CuCl ₂	Cl	3.7(2)	2.252(5)	0.008(1)	-7.4(5)	4.5 %	[CuCl ₄] ²⁻
CuCl ₂ ·2H ₂ O	Cl	3.6(3)	2.250(5)	0.007(1)	-7.2(6)	6.2 %	[CuCl ₄] ²⁻
FeCl ₂	Cl	3.8(2)	2.313(3)	0.0065(8)	-7.8(4)	2.9 %	[FeCl ₄] ²⁻
FeCl ₂ ·4H ₂ O	Cl	3.8(2)	2.312(3)	0.0069(8)	-7.6(4)	2.5 %	[FeCl ₄] ²⁻
MnCl ₂	Cl	3.8(2)	2.369(3)	0.0048(8)	-6.2(4)	3.0 %	[MnCl ₄] ²⁻
MnCl ₂ ·4H ₂ O	Cl	3.9(2)	2.370(3)	0.0061(9)	-5.9(4)	3.2 %	[MnCl ₄] ²⁻
PdCl ₂	Cl	4.0(2)	2.313(3)	0.0055(6)	-1.1(4)	1.5 %	[PdCl ₄] ²⁻
PtCl ₂	Cl	3.9(2)	2.309(4)	0.005(1)	-11.4(7)	4.7 %	[PtCl ₄] ²⁻
SnCl ₂ ·2H ₂ O*	Cl	4.2(3)	2.482(7)	0.017(2)	-9.0(7)	5.6 %	[SnCl ₄] ²⁻
ZnCl ₂ *	Cl	4.3(2)	2.278(4)	0.0084(9)	-6.2(4)	2.5 %	[ZnCl ₄] ²⁻

*The concentration of SnCl₂·2H₂O was 50 mM and ZnCl₂ was 300 mM

Tetrachloride species for cobalt and manganese were also suggested by Dent *et al.* for binary molten salt melts of 1-methyl-3-ethylimidazolium chloride [EMIM]₂[MCl₄] with 1-methyl-3-ethylimidazolium chloride aluminium chloride [EMIM][Cl-AlCl₃] under basic conditions (low molar ratio of AlCl₃), where ‘M’ is the metal studied.¹³ Bond lengths of 2.28 Å and 2.38 Å were reported for cobalt and manganese salts, respectively. These bond lengths correspond closely to the M-Cl distances of 2.37 Å and 2.28 Å for Mn and Co, respectively, determined for both the Ethaline and Propaline

solutions. Similar speciation was also seen by Hamill *et al.* for palladium salts in pyridinium chloride-based ILs and in 1,2-dimethyl-3-hexyl imidazolium chloride, where the single species observed in both of these solutions was $[\text{PdCl}_4]^{2-}$, with an M-Cl bond length of 2.33 Å.¹⁴ This data corresponds closely to the data fit obtained here for PdCl_2 in Ethaline, as can be seen from **Table 4.2**.

For the majority of these metals a tetrahedral complex is the most probable, similarly to copper. However, platinum and palladium chloride salts are more likely to form d^8 square planar complexes.¹²

If the closest coordination shells for the solid state M-Cl bond lengths are considered, it can be seen that they vary from almost identical, up to no more than 2 Å longer than the values determined here for the species in solution. For instance, copper in solid anhydrous CuCl_2 displays four M-Cl bonds of 2.351 Å,¹⁵ which are approximately 0.1 Å longer than the bonds seen in DES media. This disparity is most likely due to the ions in solution being spaced further apart or shielded from each other by the solvent, whereas in the crystal all atoms are in close proximity. Similarly, ZnCl_2 ,¹⁶ PtCl_2 ,¹⁷ PdCl_2 ,¹⁸ and tin chloride¹⁹ in DES media show minimal deviations from the solid state structure.

The solid cobalt and manganese chlorides display higher bond lengths (*ca.* 0.2 Å) than the solution-based species, possibly due to the greater number of M-Cl bonds in the crystal structure compared to the solution (six *vs.* four).^{20, 21}

The similarity of the data fits of the EXAFS of the two Propaline variants to Ethaline can be highlighted with the specific example of CoCl_2 . The EXAFS for CoCl_2 in the three diol-based DESs are shown overlaid in **Figure 4.7** to illustrate this point.

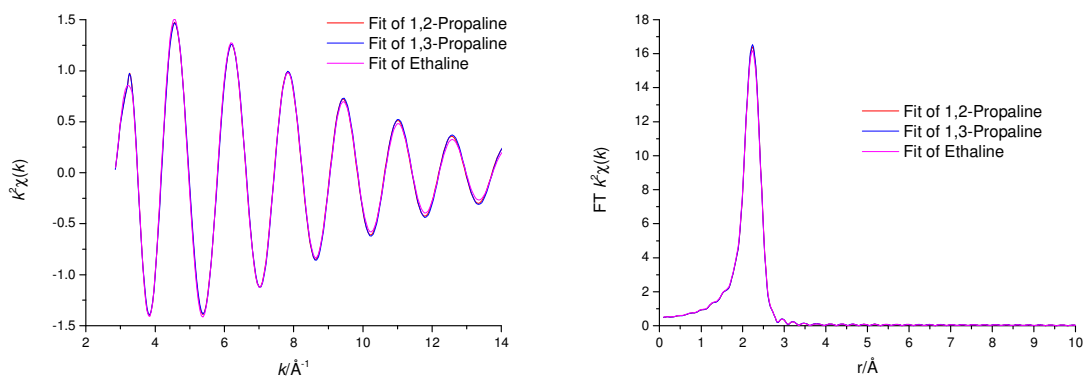


Figure 4.7 Example data fits of the EXAFS (left) and FT of the EXAFS (right) for solutions of 100 mM CoCl_2 in Ethaline, 1,2-Propaline and 1,3-Propaline.

As can clearly be seen, the three different data fits are effectively identical and hence it can be deduced that the speciation in these three solutions is also identical. Therefore, the glycol can definitely be considered to not be playing an active part in the speciation of the cobalt or any of the other salts described here.

4.2.1.3 Hydration shells

To understand the effect that the waters of hydration from the metal salts have on the speciation in DES media, the EXAFS for both the anhydrous and hydrated copper (II) chloride solutions in Ethaline were compared. After fitting, both solutions were found to show identical speciation, *i.e.* a 4-chloride shell at 2.255(4) Å from the copper centre, as shown in **Figure 4.8**. Therefore, it can be assumed that the addition of a significant amount of water to the solution does not affect speciation.

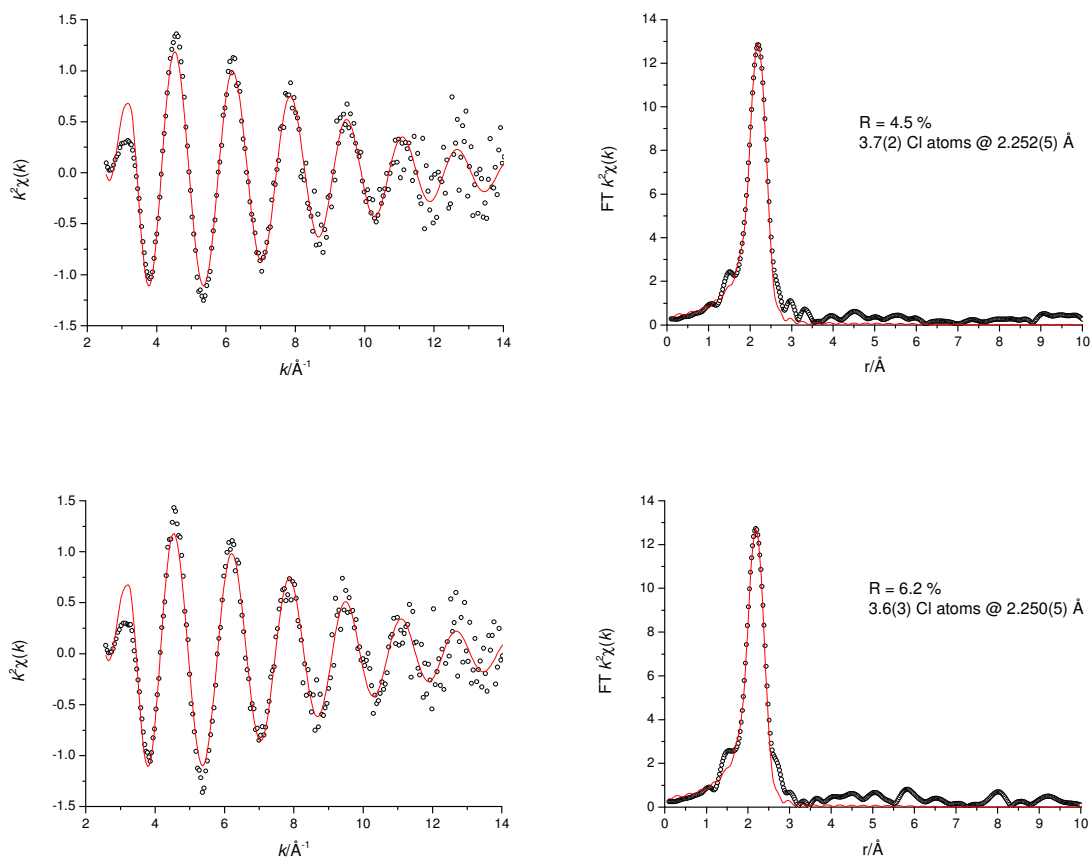


Figure 4.8 EXAFS (left) and Fourier transform (right) of CuCl_2 (top) and $\text{CuCl}_2 \cdot 2\text{H}_2\text{O}$ (bottom) in Ethaline. Data is black circles, data fit is red line.

The UV-vis spectra of Abbott *et al.* also help to confirm this observation, as both the anhydrous and hydrated forms of copper (II) chloride were seen to have almost identical spectra.⁹ In fact, a study by De Vreese *et al.* found that for choline chloride: $\text{CuCl}_2 \cdot 2\text{H}_2\text{O}$ mixtures, it was necessary to add 49 wt% water to the solution to cause a change in speciation from pure chloride to a mixed speciation.²² EXAFS studies by this same group into the speciation of the $\text{CuCl}_2 \cdot 2\text{H}_2\text{O}$ mixtures at 27 wt% water showed a single shell of chloride of 3.6 atoms at an M-Cl bond length of 2.24 \AA from the copper centre. Li *et al.* studied the effect of water on the speciation of CuCl_2 in the imidazolium-based IL [EMIM][Cl] and also observed a chloride coordination of 3.7(2)

atoms, with an M-Cl bond length of 2.255(4) Å.²³ The initialisation of the change from chloride to oxide was also seen at 40 wt% water. Comparing these data to the fits obtained from Ethaline, the presence of [CuCl₄]²⁻ in both of the copper chloride solutions is corroborated.

4.2.1.4 Speciation of metal salts with other anions

With other anions, such as sulphate, nitrate, oxide or perchlorate, copper and silver continue to show a predominantly chloride-based speciation in Ethaline, as can be seen in *Table 4.3*.

Table 4.3 EXAFS fits of 100 mM solutions of a range of metal salts in Ethaline (top) and Propaline (bottom).

Metal salt	M-X, where X = ?	Number of atoms, n	Distance from centre, r (Å)	Debye-Waller factor, a (Å ²)	Fermi energy, EF (eV)	Fit index, R(min)	Proposed structure
Ag ₂ O	Cl	2.1(2)	2.490(7)	0.015(2)	-6.9(7)	6.4 %	[AgCl ₂] ⁻ or complex species
	Cl	1.9(2)	2.478(7)	0.014(2)	-5.0(9)	4.8 %	
	Ag	1.8(9)	2.87(3)	0.05(2)			
AgNO ₃	Cl	2.6(2)	2.482(6)	0.017(2)	-4.9(6)	4.6 %	[AgCl ₂] ⁻
AgAc	Cl	2.4(2)	2.485(7)	0.016(2)	-6.9(7)	6.6 %	[AgCl ₂] ⁻
CuSCN	S	2.6(3)	2.24(1)	0.015(3)	-6.3(9)	11.9%	[Cu(SCN) ₂] ⁻
CuSO ₄ ·5H ₂ O	Cl	3.8(3)	2.252(7)	0.008(2)	-7.1(8)	8.3 %	[CuCl ₄] ²⁻
Cu(ClO ₄) ₂ ·6H ₂ O	Cl	4.0(3)	2.252(6)	0.008(2)	-2.6(7)	7.5 %	[CuCl ₄] ²⁻
AgNO ₃	Cl	2.4(2)	2.484(5)	0.014(2)	-5.6(5)	3.7 %	[AgCl ₂] ⁻
AgAc	Cl	2.0(1)	2.479(5)	0.015(2)	-5.5(7)	2.7 %	complex species
	Ag	2.1(3)	2.822(8)	0.026(3)			

However, major deviations from this simple chloride metal speciation occur for ligands such as acetate or thiocyanate. For instance, silver acetate in Propaline shows an additional shell and copper thiocyanate shows SCN speciation, although multiple scattering makes determination of which end the ligand is binding to the absorbing atom and coordination number less accurate.

When the EXAFS of the solution of AgAc in Propaline is examined and shells fitted to the data, this second shell appears between 2.8 and 3.2 Å away from the absorbing central silver atom (**Figure 4.9**). There are two possible identities for this additional shell: either a second chloride shell or a metal shell. When all of the parameters for these two different data fits are compared, it can be seen that the metal shell is a more realistic fit and probably arises from the formation of a complex anionic species, which is supported by both data fits suggesting a 4-coordinate species in solution.

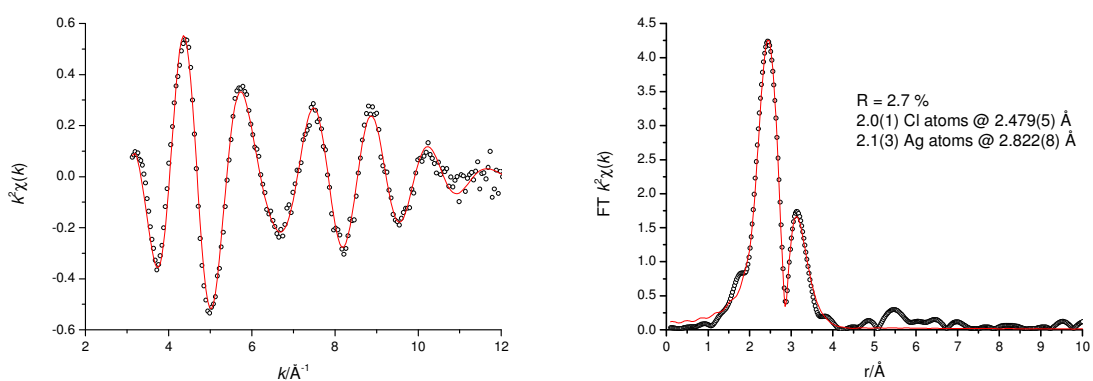


Figure 4.9 EXAFS (left) and FT of the EXAFS (right) for AgAc (100 mM) in Propaline. Data is black circles, data fit is red line.

By examining bond lengths from the data fitting, a second chloride shell can be fitted at 3.197(9) Å away from the Ag central atom, which is rather long for chloride bond, while a silver shell fits at 2.822(8) Å. Two possibilities are: the presence of

another $[\text{AgCl}_2]^-$ ion in close proximity to the studied species, or the formation of silver nanoparticles in solution. By comparing the Ag-Ag bond length calculated here to the Ag-Ag bond lengths in silver foil, it can be seen that they are very similar, *i.e.* 2.822 Å experimental vs. 2.877 Å in the solid metal.²⁴

Similarly to AgAc in Propaline, the EXAFS of Ag_2O in Ethaline shows a much lower coordination number (2.1 chlorides) than the other Ag salts in the same solvent, although the remaining parameters are consistent with all of the other solutions. There is a small peak present after the main peak in a similar position (2.87(3) Å) to the Ag peak in AgAc in Propaline, but it is much less clearly defined. From the voltammetry, it could be expected that a Cl-Ag-O-Ag-Cl species would form in solution; however a mixed chloride-oxide shell produces very high uncertainties in all of the data fitting parameters. Fitting a second shell of either Cl or Ag to the EXAFS data does not alter the parameters of the first shell significantly enough to be able to identify this small peak definitively. The pure chloride coordination that is observed for this solution may be due to the $[\text{AgCl}_2]^-$ complex being more light-stable than $[\text{Ag}_2\text{OCl}_2]^{2-}$, which could explain why there is no second peak in the AgCl Fourier transform of the EXAFS spectrum.

Overall, the information gathered for these salts suggests that metals in similar oxidation states will have similar speciation. For instance, the M^+ salts all appear to have $[\text{MCl}_2]^-$ coordination, mixed with a small amount of $[\text{MCl}_3]^{2-}$ and the M^{2+} salts show a consistent $[\text{MCl}_4]^{2-}$ coordination.

4.2.2 Speciation of metal chloride salts in Reline

The chloride speciation observed for metal salts in the glycol-based DESs, Ethaline and Propaline, also carries through into Reline, although comparatively higher

Debye-Waller factors indicate the possibility of additional, lighter, elements present, *e.g.* nitrogen or oxygen from the urea. However, as the relatively small contribution from this additional element in the EXAFS spectra is dominated over by the chloride contribution, determination of the exact coordination of the metal centre in Reline is a much more complex process.

4.2.2.1 Speciation of the metal (I) chloride salts

Examination of the EXAFS for AgCl and CuCl in Reline indicates a continued chloride speciation, as can be seen from *Table 4.4*. However, the increase in Debye-Waller factor for AgCl in Reline when compared to the Ethaline solution, suggests that another, lighter, element may be present in the coordination. As only a single peak is visible in the Fourier transform, the individual components of this speciation cannot be easily determined due to overlap of any EXAFS signals.

Table 4.4 EXAFS fits of 100 mM solutions of two metal (I) chloride salts in Reline.

Metal salt	M–X, where X = ?	Number of atoms, n	Distance from centre, r (Å)	Debye-Waller factor, a (Å ²)	Fermi energy, EF (eV)	Fit index, R(min)	Proposed structure
CuCl	Cl	2.5(2)	2.224(7)	0.012(2)	-6.6(7)	7.6 %	[CuCl ₂] ⁻
AgCl	Cl	2.9(3)	2.525(8)	0.023(3)	-3.6(7)	7.0 %	[AgCl ₃] ²⁻

Edge shift is another indicator of different oxidation state and, hence, speciation. The majority of the silver salt solutions in glycol-based DES have edges at around 25,522.56 eV, whilst the solution of AgCl in Reline shows an edge at 25,508.93 eV. This energy shift suggests that the silver atoms are not in the same environment, as different energies are needed for excitation. Therefore, combining this information with

the fitted EXAFS data, it can be considered that the silver salts in glycol-based DESs have a slightly different speciation to those in Reline.

4.2.2.2 Speciation of the metal (II) chloride salts

Metal (I) chloride salts in Reline have previously been shown in **Section 4.2.2.1** to take a mainly chloride speciation, but with the potential for other atoms being present in the coordination and this trend continues for the majority of the other metal (II) chloride salts described in this current section, as seen in **Table 4.5**.

Table 4.5 EXAFS fits of 100 mM solutions of metal chloride salts in Reline.

Metal salt	M–X, where X = ?	Number of atoms, n	Distance from centre, r (Å)	Debye-Waller factor, a (Å ²)	Fermi energy, EF (eV)	Fit index, R(min)	Proposed structure
CoCl ₂	Cl	3.4(2)	2.246(4)	0.009(1)	2.4(5)	3.5 %	[CoCl ₄] ²⁻
CuCl ₂	Cl	3.9(3)	2.239(7)	0.013(2)	0.2(7)	6.4 %	[CuCl ₄] ²⁻
CuCl ₂ ·2H ₂ O	Cl	3.8(3)	2.233(6)	0.013(2)	0.8(6)	4.9 %	[CuCl ₄] ²⁻
FeCl ₂	O	4.8(4)	2.08(1)	0.019(3)	1(1)	6.8 %	[Fe(OD) ₅] ²⁺
MnCl ₂	O	5.9(5)	2.16(1)	0.015(4)	2(1)	11.8 %	[Mn(OD) ₆] ²⁺
PdCl ₂	Cl	3.9(2)	2.313(4)	0.008(1)	-1.5(6)	3.2 %	[PdCl ₄] ²⁻
PtCl ₂	Cl	4.7(5)	2.29 (1)	0.024(3)	-8(1)	10.0 %	[PtCl ₄] ²⁻

*Where OD = oxygen donor, *e.g.* water, urea

The solution of manganese chloride in Reline, however, breaks with the above observed trends (that the speciation remains mainly chloride) in that a full six-coordinate oxygen coordination shell is observed at 2.16(1) Å from the absorbing manganese atom (**Figure 4.10**). The early transition metals are more oxophilic than the late transition metals and are therefore more content to form an oxide-based complex.

Another oxophilic metal is iron and this, too, sifts to a pure oxygen shell in Reline for both the Fe^{2+} and Fe^{3+} chloride salts. Iron favours a speciation of 5 oxygen atoms, at a bond length of $\sim 2.07 \text{ \AA}$.

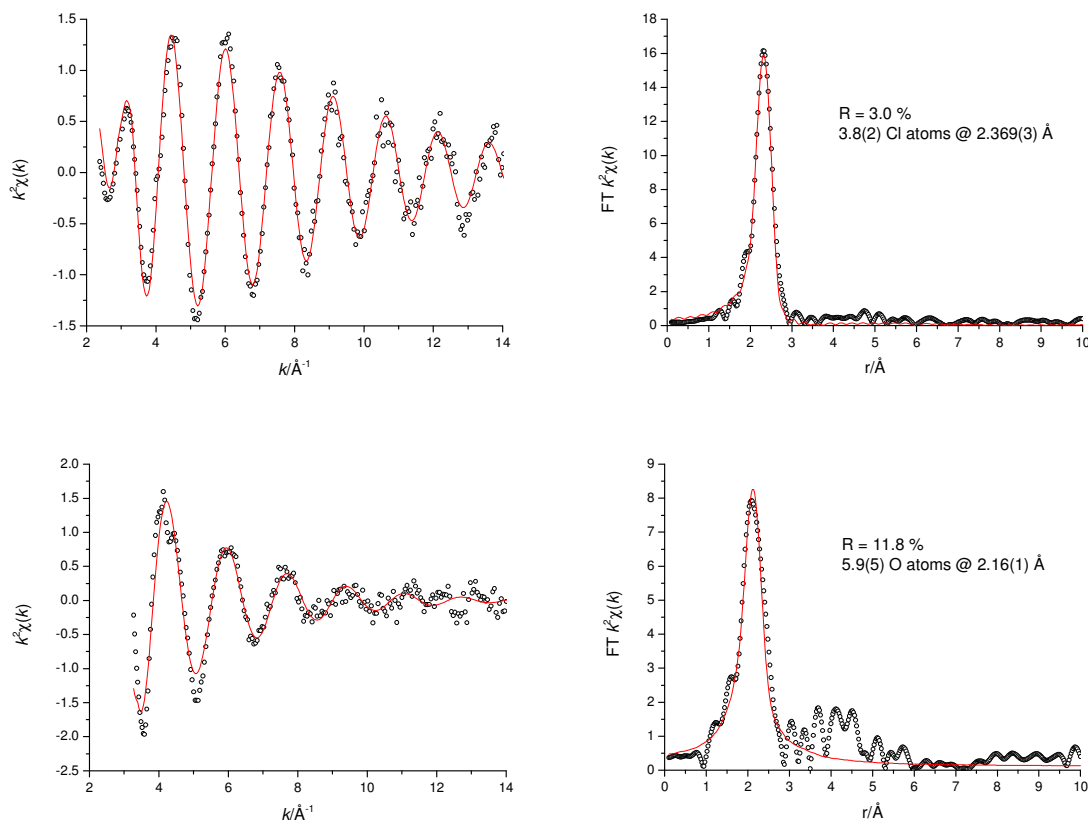


Figure 4.10 EXAFS (left) and Fourier transform (right) of 100 mM MnCl_2 in Ethaline (top) and in Reline (bottom). Data is black circles, data fit is red line.

As can clearly be seen from the difference in the two EXAFS scans in **Figure 4.10** for the MnCl_2 solutions, the two different solvents produce visibly altered responses. For instance, the oscillations in the Reline spectra fade away much more rapidly than for Ethaline. This indicates that a lighter set of atoms are present around the excited manganese ion and gives weight to the proposed oxide coordination shell.

In short, Ethaline gives consistent chloride speciation with M^{2+} giving $[\text{MCl}_4]^{2-}$, as has been suggested in the previous section. The two variants of Propaline (with either

1,2-propylene glycol or 1,3-propylene glycol) also provide consistent chloride speciation, practically identical to the Ethaline solutions. Reline, on the other hand, behaves somewhat differently. Mixed shells are sometimes observed and even a complete speciation change has been seen for at least two metals (manganese and iron).

4.2.3 Nickel: A special case

The speciation of nickel chloride in Ethaline in particular stood out from the speciation of the other metal (II) chloride salts. As it is in group 10, along with platinum and palladium it was expected to have similar redox properties and coordination behaviour, *i.e.* tetrachloride speciation and potentially square planar. However, when the EXAFS spectrum was examined, instead of a simple four chloride speciation, the nickel was found to be chelated by the ethylene glycol component of the ionic liquid (**Table 4.6**). The data for nickel chloride in [HMIM][Cl] is shown as a contrast and will be discussed further in **Section 4.3**.

Table 4.6 EXAFS fits of 100 mM solutions of nickel chloride hexahydrate in a range of DES and IL environments.

DES	M-X, where X = ?	Number of atoms, n	Distance from centre, r (Å)	Debye-Waller factor, a (Å ²)	Fermi energy, EF (eV)	Fit index, R(min)	Proposed structure																								
Ethaline	O	5.9(2)	2.078(8)	0.011(3)	0.8(8)	6.4 %	[Ni(OD) ₃] ²⁺																								
	C	4.4(8)	2.86(2)	0.01(?)				Propaline (1,2)	O	5.2(4)	2.074(7)	0.003(2)	0.3(8)	5.5 %	[Ni(OD) ₃] ²⁺	C	6(2)	2.90(2)	0.01(1)	Propaline (1,3)	O	5.6(4)	2.073(7)	0.006(2)	-6.4(7)	6.4 %	[Ni(OD) ₆] ²⁺	[HMIM][Cl]	Cl	4.1(3)	2.271(6)
Propaline (1,2)	O	5.2(4)	2.074(7)	0.003(2)	0.3(8)	5.5 %	[Ni(OD) ₃] ²⁺																								
	C	6(2)	2.90(2)	0.01(1)				Propaline (1,3)	O	5.6(4)	2.073(7)	0.006(2)	-6.4(7)	6.4 %	[Ni(OD) ₆] ²⁺	[HMIM][Cl]	Cl	4.1(3)	2.271(6)	0.007(2)	-6.2(7)	4.2 %	[NiCl ₄] ²⁻								
Propaline (1,3)	O	5.6(4)	2.073(7)	0.006(2)	-6.4(7)	6.4 %	[Ni(OD) ₆] ²⁺																								
[HMIM][Cl]	Cl	4.1(3)	2.271(6)	0.007(2)	-6.2(7)	4.2 %	[NiCl ₄] ²⁻																								

*Where OD = oxygen donor, *e.g.* ethylene glycol, 1,2-propanediol, 1,3-propanediol

In the Fourier transform of the EXAFS of nickel chloride in Ethaline, two peaks were observed. The first appeared at 2.1 Å away from the excited nickel atom and the second as a shoulder on the main peak at ~2.8 Å (see **Figure 4.11**). This main peak did not fit to pure chloride, as would have been expected, but to oxygen instead (5.9(2) atoms). The second shell could be fitted to carbon (4.4(8) atoms), suggesting coordination by the ethylene glycol (EG) molecules in the solvent and that these molecules could possibly be acting as bidentate ligands to form a complex such as $[\text{Ni}(\text{EG})_2]^{2+}$. The slight bump at 4-5 Å may be caused by a small amount of multiple scattering from the chelated ethylene glycol ligands.

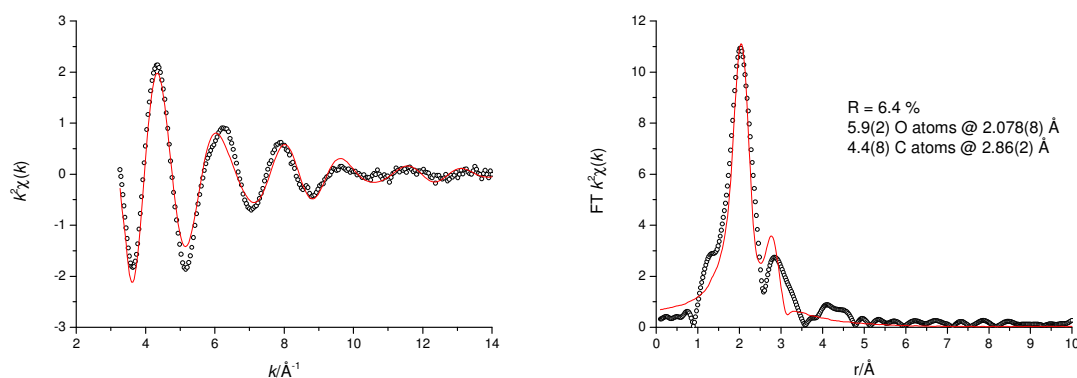


Figure 4.11 EXAFS (left) and Fourier transform (right) of 100 mM $\text{NiCl}_2 \cdot 6\text{H}_2\text{O}$ in Ethaline. Data is black circles, data fit is red line.

To test this theory of ethylene glycol coordination, the nickel chloride solution was made up in two variants of Propaline, using either 1,2-propanediol or 1,3-propanediol. It was expected that the 1,2-Propaline solution would show similar coordination to the Ethaline solution and that the 1,3-Propaline solution would not show a glycol bridge because the angle between the two potential binding centres would be too tight. These three suggested binding methods are shown in **Figure 4.12**.

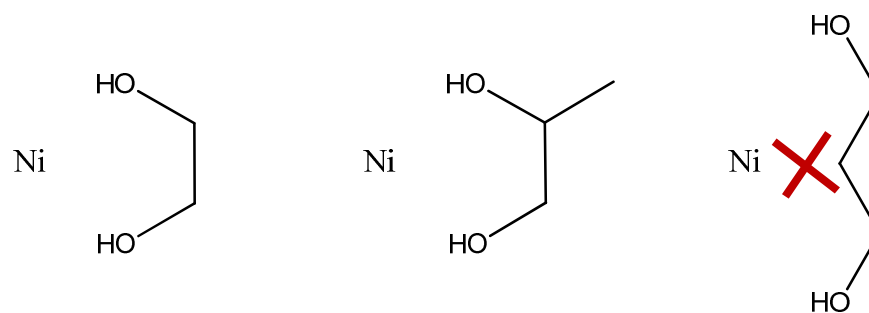


Figure 4.12 Schematic diagram showing the possible configurations for the diol component of the DES to chelate to a nickel centre.

When the three EXAFS spectra were compared, it was clear that the shoulder attributed to the glycol bridge was missing from the 1,3-Propalene spectrum, as can clearly be seen in **Figure 4.13**. All three sets of spectra have the same edge shift (8,342.5 eV), which suggests that the main peak at $\sim 2.1 \text{ \AA}$ is still the same oxide-chloride mix directly coordinated to the nickel centre, as for Ethaline.

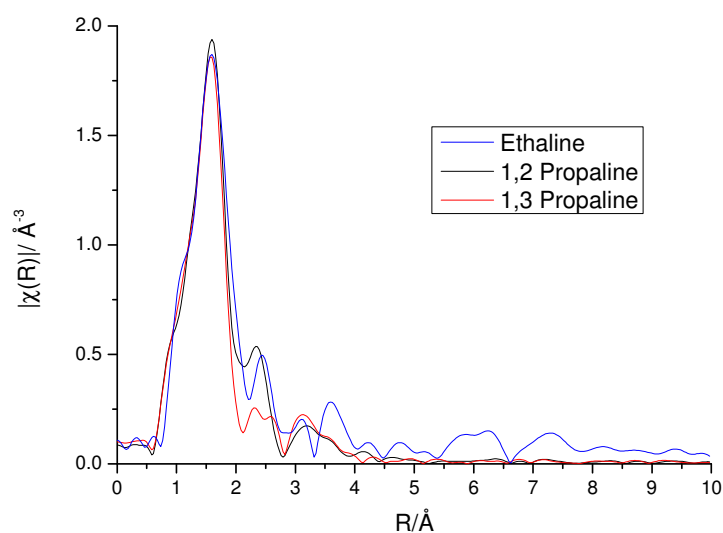


Figure 4.13 Background subtracted Athena overlays of the EXAFS for three nickel chloride hexahydrate solutions in Ethaline (blue), 1,2-Propalene (black) and 1,3-Propalene (red). These spectra have not been adjusted for E_{min} or fitted to any specific coordination shells.

Ethylene glycol coordination to a nickel centre has also been observed in the single crystal x-ray diffraction spectroscopy of a nickel-phenanthroline compound prepared Ethaline.²⁵ In this instance, the neutral EG molecule is bound to the nickel with M-O bond lengths of 2.08 Å. This bond length is effectively identical to the ones determined by EXAFS (**Table 4.6**). Two chloride counter ions were also observed in this crystal, which may be the cause of the additional bump seen in **Figure 4.11**.

Visual examination of these three solutions showed that nickel chloride hexahydrate in Ethaline is apple green, as can be seen in **Figure 4.14**. The two Propaline solutions are a paler, more blue, shade of green, with a greater difference from Ethaline for the 1,3-Propaline solution. Therefore, the general coordination must also be similar, *i.e.* directly bound to oxygen atoms. Comparing these DES solutions to the same nickel salt in [HMIM][Cl], a marked difference can be seen. The nickel complex in the imidazolium-based solution is now a deep turquoise blue, which indicates a profound change in speciation, most likely to the tetrachloride complex (discussed further in **Section 4.3**).

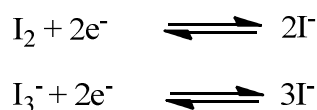


Figure 4.14 Solutions of NiCl_2 (100 mM) in (from left to right): Ethaline, 1,2-Propaline, 1,3-Propaline, and [HMIM][Cl].

This data shows clearly that the HBD component of the DES can also play a significant part in the coordination of metal ions in solution and that the contribution from the anionic components is not the sole governing factor for metal speciation in DES media. If the nickel is effectively changing the composition of the DES by complexing the ethylene glycol, then in order to electrodeposit the nickel from this solution one must either change the speciation to something more reactive, such as a chloride complex, or destroy the solution in the process of electrowinning. Further implications are for separation and recovery processes: if two different metals with different coordination complexes are present in solution, then the glycol complex may have a different stability to a chloride complex. This would make it easier to selectively electrowin or precipitate one of these complexes.

4.2.4 Speciation of iodine in DES media

In **Section 3.4**, cyclic voltammetry of iodine was seen to show two different redox couples almost superimposed on each other. It was suggested that a trihalide species, such as I_2Cl^- or I_3^- , is present and these redox couples might be due to the two processes



Application of EXAFS to the solutions of I_2 in Oxaline and in Ethaline (both 200 mM) showed that the absorbing iodine atom was coordinated by two other iodine atoms, which agrees with the theory suggested in **Section 3.4** that there is a trihalide species present. However, there being two iodine atoms as ligands in a solution, with no metals for them to oxidise, suggests that the iodine may be breaking down the DES, unless it is a side effect of a diatomic molecule being excited at both ends simultaneously.

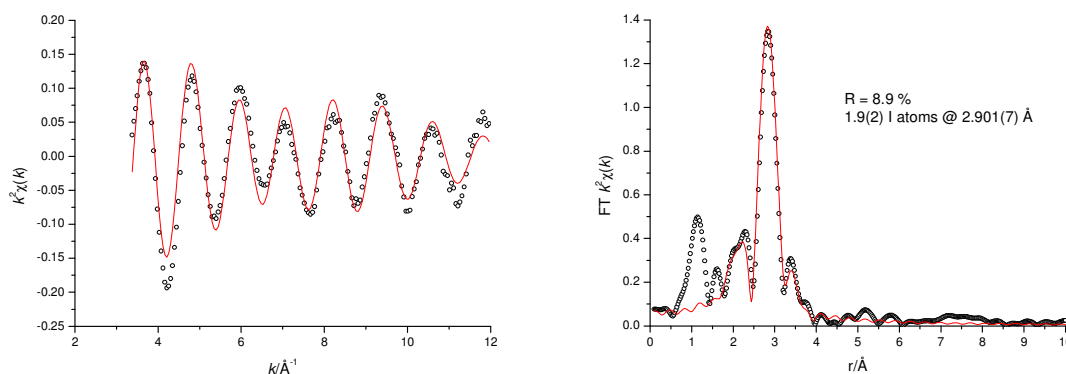


Figure 4.15 EXAFS (left) and Fourier transform (right) of 200 mM I_2 in Oxaline. Data is black circles, data fit is red line.

An additional peak at lower bond length ($\sim 1 \text{ \AA}$) is present in the EXAFS spectra for both Ethaline and Oxaline but this is most likely attributed to either noise in the

spectrum, as 1 Å is much too short a distance to be a real bond, or multiple scattering across a triiodide species. It should be noted that the iodine K-edge (32.3 keV) was outside of the specifications of the ESRF beamline limits (4 to 32 keV) and this data should be viewed with a certain degree of caution.

4.3 Speciation in imidazolium liquids

The studies above in **Section 4.2** are all based on DESs with a high chloride activity. By using imidazolium ILs, which have the potential for a greater range of anions other than chloride, the effects of the anions from the IL can then be compared with the effect of anions from the dissolved metal salt and their hydration shells. By utilising information acquired from studying the EXAFS of metal salts in DESs, chelate ligands can be identified by a shoulder peak, as shown previously for the ethylene glycol bridge on nickel, at 2.7 to 3.0 Å in the Fourier transform. If a complex anion is bound to the metal centre, then further coordination shells will be seen at longer bond lengths, as was observed for the additional silver shell for AgAc in Propaline.

Of the six different imidazolium-based ionic liquids, the speciation appeared to be based on the anionic species from the IL and not the ligand initially bound to the metal salt, depending on its ligand strength compared to that of the metal salt ligands. Liquids with less coordinating anions, such as the NTf₂-based liquid, did not dissolve the metal salts very well, resulting in EXAFS data with a worse signal-to-noise ratio.

4.3.1 Speciation of metal salts in [HMIM][Cl]

All of the metal salts studied in the neat [HMIM][Cl] liquid were found to display a fully chloride coordination shell. With the addition of a substantial amount of water (5 %) to these solutions, the greater part of the speciation for the majority of the metal salts

studied remains based on chloride although there is the potential for mixed shells to occur. However certain salts, such as nickel acetate and chromium chloride, start to include a significant proportion of oxygen in their coordination shells. These data are displayed in *Table 4.7*.

Table 4.7 EXAFS data fits for 100 mM solutions of metal salts in [HMIM][Cl].

Metal salt	M–X, where X = ?	Number of atoms, n	Distance from centre, r (Å)	Debye-Waller factor, a (Å ²)	Fermi energy, EF (eV)	Fit index, R(min)	Proposed structure
CrCl ₃ ·6H ₂ O	Cl	5.5(5)	2.347(7)	0.010(2)	-3.1(8)	5.3 %	[CrCl ₆] ³⁻
CrCl ₃ ·6H ₂ O + H ₂ O	Cl	7.8(8)	2.22(1)	0.026(4)	7(1)	7.5 %	[CrCl ₈] ⁵⁻
	O	6.4(8)	2.08(2)	0.013(4)	-6(1)	12.4 %	[Cr(H ₂ O) ₆] ³⁺
CuAc ₂ ·H ₂ O	Cl	3.2(2)	2.226(5)	0.016(1)	-9.9(4)	3.3 %	[CuCl ₃] ⁻
CuAc ₂ ·H ₂ O + H ₂ O	Cl	2.9(2)	2.184(5)	0.019(2)	-8.5(5)	3.2 %	[CuCl ₃] ⁻
CuCl ₂ ·2H ₂ O	Cl	3.1(1)	2.230(4)	0.014(1)	-8.1(4)	2.7 %	[CuCl ₃] ⁻
CuCl ₂ ·2H ₂ O + H ₂ O	Cl	3.1(1)	2.230(4)	0.014(1)	-8.1(4)	2.7 %	[CuCl ₃] ⁻
CuSO ₄ ·5H ₂ O	Cl	3.2(2)	2.224(5)	0.017(2)	-7.4(4)	3.9 %	[CuCl ₃] ⁻
CuSO ₄ ·5H ₂ O + H ₂ O	Cl	2.8(1)	2.190(4)	0.017(2)	-6.8(4)	3.2 %	[CuCl ₃] ⁻
NiAc ₂ ·4H ₂ O	Cl	3.0(2)	2.259(6)	0.011(2)	0.5(7)	4.3 %	[NiCl ₄] ²⁻
NiAc ₂ ·4H ₂ O + H ₂ O	O	5.0(3)	2.070(7)	0.013(2)	13(1)	4.4 %	[Ni(H ₂ O) ₆] ²⁺
NiCl ₂ ·6H ₂ O	Cl	4.1(3)	2.271(6)	0.007(2)	-6.2(7)	4.2 %	[NiCl ₄] ²⁻
NiCl ₂ ·6H ₂ O + H ₂ O	Cl	5.7(4)	2.216(7)	0.018(2)	12.2(7)	4.9 %	[NiCl ₆] ⁴⁻
	O	5.1(3)	2.084(8)	0.007(2)	-1.5(9)	8.4 %	Ni(H ₂ O) ₆ ²⁺

When the behaviour of metal salts in the imidazolium chloride liquid is compared to DES media, it can be seen that similar speciation is observed. This can be seen in particular for the Cu²⁺ salts. For example, in the DES solutions (*Table 4.2*) copper (II)

chloride had a speciation of 3.7(2) chlorides surrounding the metal centre at a distance of 2.252(5) Å, compared to the coordination of 3.1(1) chlorides at a distance of 2.230(4) Å in [HMIM][Cl] (**Table 4.7**). Copper (II) chloride in dry [EMIM][Cl], as studied by Li *et al.* produces a coordination of chloride (3.7(2) atoms) with an M-Cl bond length of 2.255(4) Å.²³ This is somewhat different to the [HMIM][Cl] fit and even with up to 30% water the speciation in [EMIM][Cl] does not change from a tetrachloride complex. It is unlikely that another element, such as oxygen, is taking part in the speciation in the dry [HMIM][Cl] because there is no water for it to originate from. Therefore, the bulky imidazolium cation may be taking place in this reduction in coordination number.

Interestingly, nickel chloride, which showed coordination to the ethylene glycol in the DES Ethaline, now has a full tetra-chloro shell in [HMIM][Cl] with an M-Cl bond length of 2.271(6) Å. From a comparison to the data by Dent *et al.* for [EMIM]₂[NiCl₄] with [EMIM][Cl-AlCl₃] under basic conditions, *i.e.* tetrachloride and a bond length of 2.25 Å, it can be seen that the speciation is similar.¹³ There is no possibility of a glycol bridge in this liquid and the only potential oxygen ligands are from the waters of hydration, which again lends confirmation to the glycol bridge speciation in Ethaline.

Multiple data fits are shown in **Table 4.7** for chromium and nickel with the addition of water for both the pure chloride complex and the pure aqua complex. These two salts highlight the potential for mixed chloride-aqua coordination. If the example of chromium chloride is considered, it can be seen that fitting a pure chloride shell to the data suggests the coordination of eight chloride atoms, with M-Cl bond lengths of shorter than a six-chloride fit (as was seen for the water-free solution in **Table 4.7**). Combined with a substantially larger Debye-Waller factor and EF value, the presence of lighter atoms about the chromium centre is suggested. However, when the pure aqua complex is considered, it can be seen that these parameters suggest a more chemically

sound fit but with a much greater uncertainty in the ‘goodness’ of the data fit. The same also holds true for the nickel chloride solution. Therefore mixed species coordination must be considered, although exact proportions are not yet known.

This difference in speciation between dry samples and those with water can be seen in **Figure 4.16**, with the normalised EXAFS spectra at the Cr K-edge. A clear difference in the shape of the edge step can be seen: in the neat [HMIM][Cl] solution a small white line is present, which is absent in the solution containing water. By comparing this visual information with the two data fits, it can be concluded that the speciation of the 5 % water sample is mainly an aqua complex, but still retains some chloride in the coordination shell.

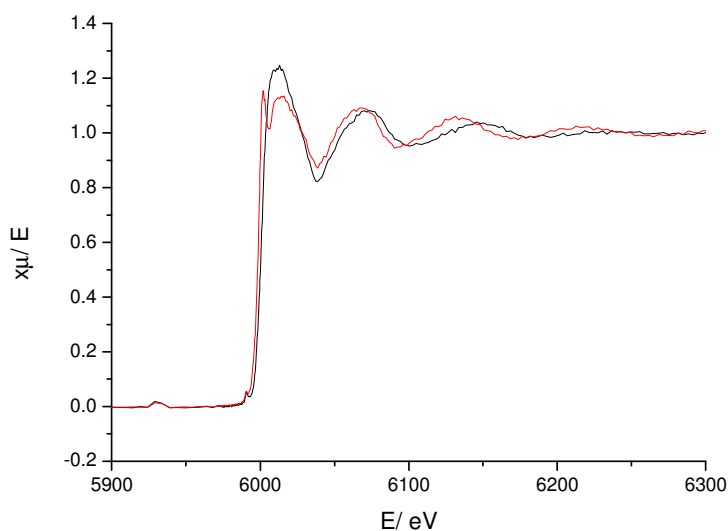


Figure 4.16 Normalised EXAFS spectra for the Cr K-edge for the solutions of 100mM $\text{CrCl}_3 \cdot 6\text{H}_2\text{O}$ in neat [HMIM][Cl] (red) and [HMIM][Cl] with 5% water (black).

Data fits for pure chloride and pure oxygen coordination shells were inconclusive, suggesting the presence of a mixed oxide-chloride coordination shell, although signal overlap prevents the determination of a conclusive speciation. The speciation of these metal salts in ILs appears to be more sensitive to the addition of water than in deep

eutectic solvents, possibly due to the ILs having been kept scrupulously dry before EXAFS analysis.

4.3.2 Other ILs with different anions

Metal salts dissolved in ILs with different anions showed a greater variation in speciation compared to the chloride-based liquid, as can be seen in **Figure 4.17** for chromium chloride hexahydrate. Each of the four solutions displayed here has electron density peaks at different M-X bond lengths, where X is the coordinating ligand. For instance, chromium chloride in [HMIM][Cl] shows a single peak at 2.347(7) Å, which can be fitted to chloride (5.5(5) atoms), whilst the other solutions display peaks at shorter bond lengths.

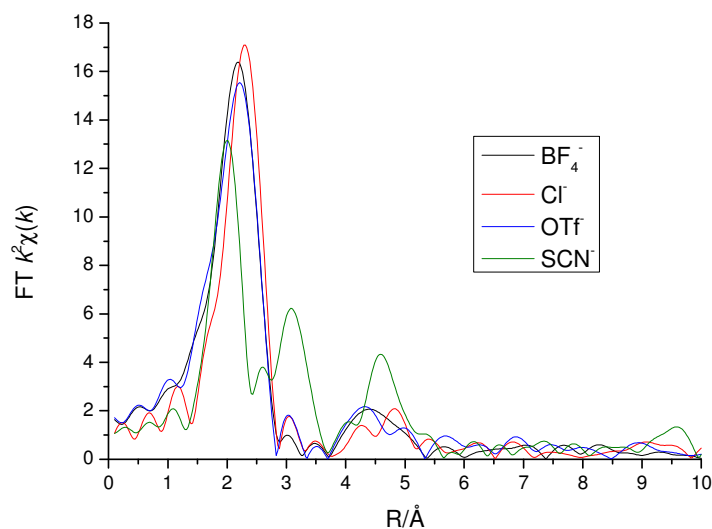


Figure 4.17 Fourier transforms of the EXAFS for $\text{CrCl}_3 \cdot 6\text{H}_2\text{O}$ in four different imidazolium-based ionic liquids. These spectra have not been fitted to any specific coordination shells.

The strength of the anion has a profound effect on the coordination of the metal ions in solution and, as the anion from the ionic liquid becomes less coordinating, the

speciation becomes more complex to identify due to the variety of species in solution. When strong anions are present, such as Cl^- or SCN^- , an identifiable complex is formed, such as



However, when weaker anions are present, such as BF_4^- or OTf^- , a mix of both coordinated and uncoordinated species are seen. For instance, if the $[\text{HMIM}][\text{Cl}]$ solution is taken as 100% chloride speciation, the shorter bond lengths and broader peaks (increasing Debye-Waller factor) of the other systems suggest the presence of lighter atoms in the coordination shell. The other metal salts studied also show mixed coordination when weaker anions are present in the IL, with the more oxophilic metals showing a greater proportion of different anions present in the coordination.

The complexity of the data fitting process is increased further when a linear molecule is present, such as thiocyanate, which has the ability to bind to the metal centre from both ends. Photoelectron waves generated during EXAFS can be propagated forward through the linear molecule, causing multiple scattering, and appearing in the Fourier transform as shoulders on the main peaks (*Figure 4.17*, green line). The multiple scattering effects prevent accurate determination of which end of the thiocyanate is directly binding to the absorbing metal centre, however from the rough length of the M-X bond length, nitrogen is the more likely candidate.

From these experiments it can be seen that by controlling the anionic component of the ionic liquid, the speciation of the metal ions in solution can also be controlled.

4.4 Conclusions

EXAFS has been used to determine the speciation for a wide range of metal chloride salts in four deep eutectic solvent systems (Ethaline, Reline, 1,2-Propaline and 1,3-Propaline). It was observed that the dissolution of these salts in the various DESs tended to produce chloro-complexes and in general, it was found that the M^+ salts showed $[MCl_2]^-$ speciation with a small amount of $[MCl_3]^{2-}$, whilst the M^{2+} salts showed $[MCl_4]^{2-}$ speciation, with a few special exceptions: in the case of nickel, chelation with the glycol component of the DES. The use of strong anionic ligands, such as thiocyanate, allowed different complexes to be produced regardless of other anions present in solution. Exact coordination numbers could not be fitted for thiocyanate coordination, as the linear $S=C=N$ ligand propagates electron waves along the molecule and bridging events can occur, causing uncertainty as to which end of the ligand is binding to the excited metal centre. Chelate ligands, such as the ethylene glycol bridge on nickel in Ethaline, can be identified by a shoulder on the main peak at 2.7-3 Å. The diol-based DESs consistently showed chloride speciation for the majority of the metal salts involved, whilst the same metal salts in Reline hinted at the possibility of mixed species coordination, potentially due to a lower chloride activity.

Therefore, it can be concluded that by replacing aqueous media with DESs, fully chloride speciation can be obtained for the majority of the metal salts studied, without the need for additional complexing agents. By switching away from oxide chemistry to chloride chemistry, a greater range of metals and their salts can be dissolved without the need for additional complexing agents to form the correct species in solution. If the need for additional complexing agents did arise, the overall ligand concentration of the solution is less (~5 M chloride vs. ~55 M water) and less soluble/reactive additives would need to be used.

When a different anionic species is present as part of the liquid, as for the imidazolium-based ILs, the speciation will tend to include the anionic component of the liquid as a ligand, depending on the relative strength of that ligand compared to the one initially on the metal salt. It was noted that the metal salts were less soluble in the liquids that contained less coordinating anions than the ligands already present on the metal salt. Speciation of the metal ions in solution can therefore be altered by careful choice of the anionic component of the liquid.

As has been seen for many of the metal salts in DES, highlighted in the example of copper (II) chloride in Ethaline, the addition of a significant amount of water to a DES solution in the form of a hydration shell will not change the speciation significantly. This is important because it means that any potential applications for these liquids do not need to be carried out in a moisture-free environment.

However, the addition of 5% water to imidazolium-based ILs had a greater effect on the metal speciation, possibly because these liquids had been kept rigorously dry during solution preparation. Metal speciation in ILs with more highly coordinating anions, such as Cl and SCN, is less affected by the inclusion of water. The metal ions retained the same anion as the major part of their coordination shells but reduced in number. The most likely replacement taking effect is an inclusion of either the water or the ligand from the metal salt. Addition of water to ILs with less-coordinating anions, such as OTf⁻, BF₄⁻ and FAP, saw a shift in speciation towards the ligand present in the metal salt or to water, although this cannot be said definitively because of the decidedly lower solubilities in general of the metal salts in these liquids.

The next question to address is how the speciation of metal ions in solution relates to their redox properties and this will be discussed in **Chapter 5**.

4.5 References

1. B. K. Teo, *EXAFS: Basic Principles and Data Analysis*, Springer-Verlag, 1986.
2. A. Filipponi, *Journal of Physics-Condensed Matter*, 2001, **13**, R23-R60.
3. C. Hardacre, in *Annual Review of Materials Research*, 2005, vol. 35, pp. 29-49.
4. P. Wasserscheid and W. Keim, *Angewandte Chemie-International Edition*, 2000, **39**, 3773-3789.
5. J. J. Rehr and R. C. Albers, *Reviews of Modern Physics*, 2000, **72**, 621-654.
6. S. J. Gurman, N. Binsted and I. Ross, *Journal of Physics C-Solid State Physics*, 1986, **19**, 1845-1861.
7. P. Nockemann, B. Thijs, K. Lunstroot, T. N. Parac-Vogt, C. Gorller-Walrand, K. Binnemans, K. Van Hecke, L. Van Meervelt, S. Nikitenko, J. Daniels, C. Hennig and R. Van Deun, *Chemistry-A European Journal*, 2009, **15**, 1449-1461.
8. A. P. Abbott, G. Capper, D. L. Davies, K. J. McKenzie and S. U. Obi, *Journal of Chemical and Engineering Data*, 2006, **51**, 1280-1282.
9. A. P. Abbott, K. El Ttaib, G. Frisch, K. J. McKenzie and K. S. Ryder, *Physical Chemistry Chemical Physics*, 2009, **11**, 4269-4277.
10. A. P. Abbott, J. C. Barron, G. Frisch, S. Gurman, K. S. Ryder and A. Fernando Silva, *Physical Chemistry Chemical Physics*, 2011, **13**, 10224-10231.
11. A. P. Abbott, G. Capper, K. J. McKenzie and K. S. Ryder, *Journal of Electroanalytical Chemistry*, 2007, **599**, 288-294.
12. C. E. Housecroft and A. G. Sharpe, *Inorganic Chemistry*, Pearson Prentice Hall, 2008.
13. A. J. Dent, K. R. Seddon and T. Welton, *Journal of the Chemical Society-Chemical Communications*, 1990, 315-316.

14. N. A. Hamill, C. Hardacre and S. E. J. McMath, *Green Chemistry*, 2002, **4**, 139-142.
15. A. F. Wells, *Journal of the Chemical Society (Resumed)*, 1947, 1670.
16. B. Brehzer, *Die Naturwissenschaften*, 1959, **46**, 106-106.
17. M. T. Falqui and M. A. Rollier, *Annali di Chimica (Roma)*, 1958, **48**, 1154-1159.
18. A. F. Wells, *Phase Transition*, 1992, **38**, 127-220.
19. B. Kamenar and D. Grdenic, *Journal of the Chemical Society*, 1961, 3954-3958.
20. H. Grime and J. A. Santos, *Zeitschrift für Kristallographie, Kristallgeometrie, Kristallphysik, Kristallchemie*, 1934, **88**, 136-141.
21. J. D. Tornero and J. Fayos, *Zeitschrift für Kristallographie*, 1990, **192**, 147-148.
22. P. De Vreese, N. R. Brooks, K. Van Hecke, L. Van Meervelt, E. Mattheijs, K. Binnemans and R. Van Deun, *Inorganic Chemistry*, 2012, **51**, 4972-4981.
23. G. Li, D. M. Camaioni, J. E. Amonette, Z. C. Zhang, T. J. Johnson and J. L. Fulton, *The Journal of Physical Chemistry. B*, 2010, **114**, 12614-12622.
24. L. McKeehan, *Physical Reviews*, 1922, **20**, 424-432.
25. G. Forrest, unpublished work.

Chapter 5 The links between speciation and redox behaviour

Chapter 5	The links between speciation and redox behaviour	152
5.1	Investigating the reversibility of redox processes	153
5.1.1	General redox behaviour	155
5.1.2	The unusual case of nickel	157
5.2	Relation of speciation to redox properties	160
5.2.1	Copper chloride	161
5.2.2	Cobalt chloride	166
5.2.3	Nickel chloride	167
5.2.4	Short summary	169
5.3	Voltammetry in $\text{LiCl} \cdot 2\text{H}_2\text{O}$	169
5.4	DES analogues	172
5.4.1	Copper chloride	173
5.4.2	Iron chloride	176
5.4.3	Short summary	177
5.5	Conclusions	178
5.6	References	180

5.1 Investigating the reversibility of redox processes

In **Section 3.3.1**, it was shown that the voltammetry of metal deposition in DESs could be divided into three categories; chemically reversible, semi-reversible and irreversible. These classes are shown schematically in **Figure 5.1** together with examples of the metals which were found to fall into each category. In **Chapter 4**, it was seen that most of these metals are present as dichloro- or tetrachloro- metallate species in the DES media but this does not necessarily categorise the voltammetric behaviour. What is suggestive from these CVs, however, is that their chemical reversibility may be related to the position of the metals in the periodic table. Elements to the right of the *d*-block tend to be reversible and become increasingly irreversible as the elements move towards the left.

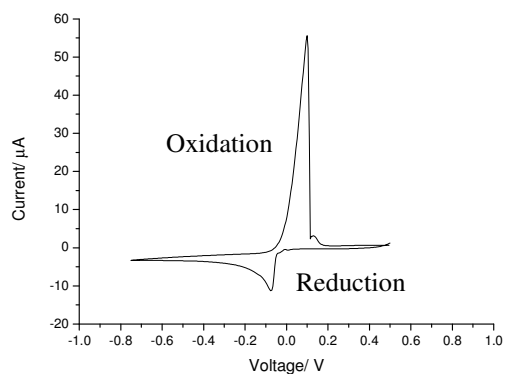
The metals that show an irreversible behaviour on a Pt working electrode, such as Ni, Co and Fe, have deposition and stripping peaks which are not clearly defined. Initially, it was assumed that this response was directly related to the speciation of the metal in solution. However, EXAFS studies of these metal chloride salts in DESs showed that the speciation was not necessarily the cause of the unusual redox properties. For instance, it was discovered in **Chapter 4** that nickel ions were complexed by the ethylene glycol in Ethaline, but cobalt and iron were present as a tetrachloro species.

Chemically reversible

Shown here: Ag

Similar: Cu, Au, Zn

Proposed speciation: $[\text{MCl}_2]^-$

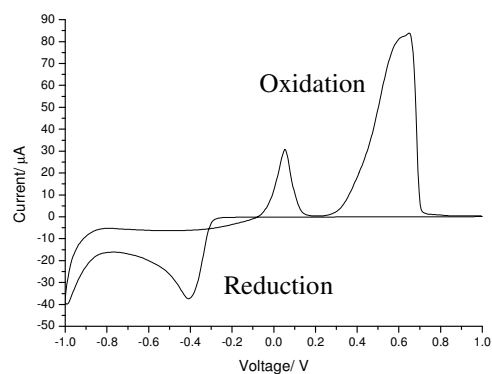


Semi-reversible

Shown here: Pd

Similar: Pt, Ni

Proposed speciation: $[\text{MCl}_4]^{2-}$



Chemically irreversible

Shown here: Mn

Similar: Co, Fe

Proposed speciation: $[\text{MCl}_4]^{2-}$

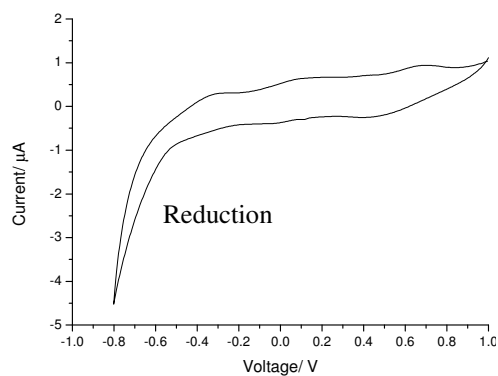


Figure 5.1 The three categories of redox behaviour in DES media, along with the probable speciation of the metal ions in solution.

5.1.1 General redox behaviour

The chemical irreversibility of metal salts, such as nickel, cobalt or iron chloride, in DES media is most likely due to surface effects dominating over speciation effects. To test whether the choice of working electrode is the cause of these surface effects or if it is a side effect of the passivation of a deposited metal layer, cyclic voltammetry of the metal chloride solutions in Ethaline showing chemically irreversible responses was repeated, substituting a native metal working electrode for the Pt working electrode. Metals tend to deposit readily onto themselves and it was expected that reversible or semi-reversible behaviour would be observed on a native metal working electrode. As nickel, cobalt and iron are all more oxophilic than other metals, such as copper or silver, they tend to be affected more by the nature of the cation. All other parameters remained the same. As can be seen in *Figure 5.2*, semi-reversible behaviour was observed on the native metal working electrode, but only after the working electrode had been anodically cleaned in the solution.

If the solution of nickel chloride in Ethaline is considered, minimal deposition onto the freshly prepared native metal working electrode surface is observed in the first reduction scan, as was previously seen with a Pt working electrode. Once this small deposit has been oxidised, stripping of the bulk electrode commences. However, on the second reduction scan, a substantially larger deposition current was observed, as can be seen in *Figure 5.2(b)*, which suggests that a freshly anodised surface is necessary for nickel deposition. Either the working electrode is tarnishing very quickly in the atmosphere or the DES solution, or the higher concentration of metal ions in the double layer after anodic dissolution allows a greater amount of metal to be deposited on the second scan. If more metal has been deposited, a greater concentration of chloride at the working electrode surface will facilitate metal stripping.

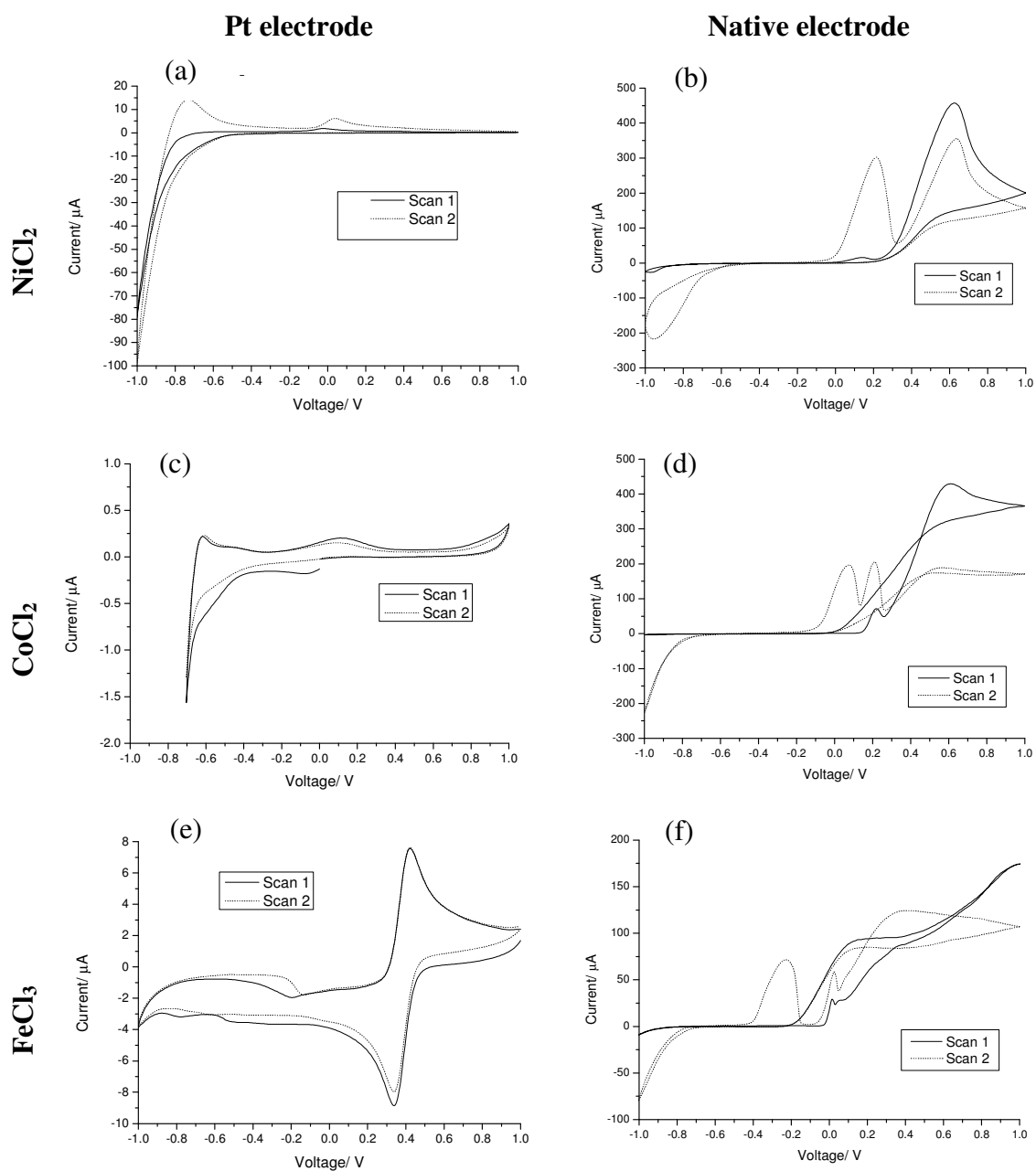


Figure 5.2 CVs of 100 mM metal chloride salts in Ethaline, on a 1 mm diameter Pt disc working electrode (left) and on a 1 or 2 mm native metal disc working electrode (right). From top to bottom: NiCl₂, CoCl₂, FeCl₃. All voltammograms were measured vs. AgCl/Ag in Ethaline reference, at a scan rate of 10 mV s⁻¹.

The first peak of the second oxidation scan appears to be the oxidation of a surface adsorbed species, *i.e.* oxidation of a layer of deposited nickel metal, or the

removal of an insulating salt film. The second peak, however, is clearly diffusion controlled. This separation of the oxidation peaks is indicative that the deposited nickel species has a different morphology to that of the bulk electrode. Integration of the deposition peak and the first stripping peak of the second scan suggests that both of these peaks have the same amount of charge. Therefore, both of them can be considered as being part of the same redox process, confirming that the first stripping peak is related to the deposition and that the second is related to oxidation of the bulk electrode.

The next question to address is whether or not the irreversible voltammetric responses for cobalt and iron on a Pt working electrode are also due to surface effects overwhelming the speciation effects. Instead of Co^{2+} and Fe^{2+} being coordinated by ethylene glycol, EXAFS suggests a tetrachloro-complex. Upon switching to the respective native metal electrode, a generally similar voltammetric response to Ni onto Ni is observed, in that neither metal will deposit onto the working electrode until the surface has been anodically cleaned, as seen in *Figure 5.2(d and f)*. Therefore, the idea that surface effects will dominate over the speciation effects for some metals is once again highlighted. These oxophilic metals are most likely displaying irreversible electrochemistry due to the formation of an oxide or chloride layer on the working electrode surface, insulating any metal deposit from further oxidation. The idea of an insulating layer of chloride hydrates precipitating out onto the electrode surface from a chloride solution has previously been proposed by Rayment *et al.*¹

5.1.2 The unusual case of nickel

When nickel chloride was dissolved in 1,2-Propaline or 1,3-Propaline, the speciation continued to be glycol-based, albeit with different levels of chelation. However, switching to [HMIM][Cl] produced a tetrachloro species. The difference in

voltammetric responses can be seen in **Figure 5.3** for each of these four solutions. All three of the glycol-based liquids show irreversible voltammetric responses. The imidazolium liquid, on the other hand, shows reversible behaviour for the tetrachloro species.

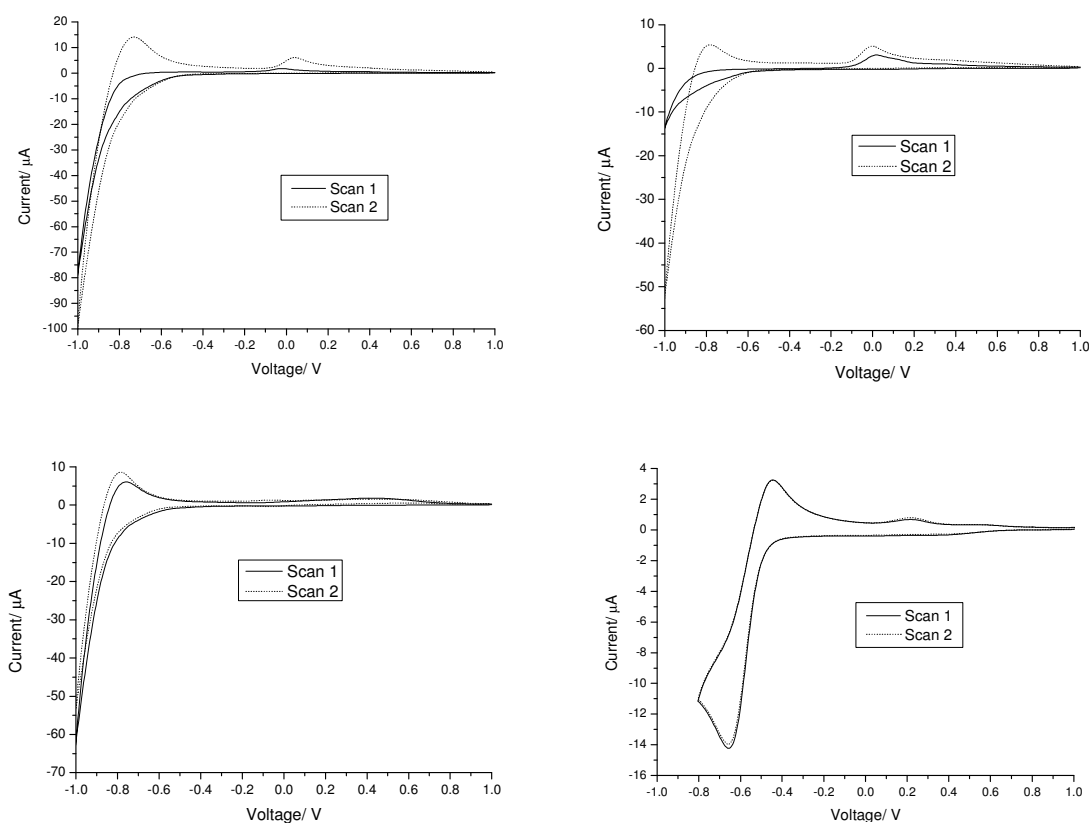


Figure 5.3 Cyclic voltammograms of $\text{NiCl}_2 \cdot 6\text{H}_2\text{O}$ (100 mM) in: Ethaline (top left), 1,2-Propaline (bottom left), 1,3-Propaline (top right) and $[\text{BMIM}][\text{Cl}]$ (bottom right). All scans were made on a 1 mm Pt disc vs. Ag wire reference, at a scan rate of 10 mV s^{-1} .

From comparing these CVs, it is possible that the speciation is having an effect on the redox behaviour of the nickel ions in solution. The $[\text{NiCl}_4]^{2-}$ species has a more anodic redox potential than the $[\text{Ni}(\text{EG})_3]^{2+}$ species. This suggests that the chloro-species is more reactive than the glycol species, hence the appearance of reversible deposition and stripping behaviour. It is possible that there is some form of competition

between the chloride and glycol ligands. A surface effect may be indicated for these metals: after deposition takes place in the DESs, it is possible that an insulating oxide forms on the surface of the working electrode, preventing further stripping of this deposit. It is possible, however, that if the redox potential of nickel chloride in Ethaline was less cathodic, *i.e.* did not overlap with solvent decomposition, then the deposition and stripping currents might be visible and could be quite similar.

In addition, the temperature of the solution may be preventing fully chemically reversible behaviour. It was previously seen for solutions of nickel chloride that had been heated between room temperature and 120°C that quasi-reversible redox behaviour was observed.² Associated with the increasing temperature was a steady colour change from green to turquoise blue. This colour change indicates that a speciation change may be occurring, possibly from the ethylene glycol chelated complex to a chloro species.

EXAFS of NiCl₂ in Ethaline suggests that the nickel centre is being coordinated by three ethylene glycol molecules which form a glycol bridge, and if speciation were the key factor causing the chemically irreversible redox properties of nickel onto a Pt working electrode, then a similar response would also be expected to be observed on a Ni working electrode. However, as this is clearly not the case, (*i.e.* the CV responses are completely different on the two different electrodes) it is therefore suggestive that surface effects are dominating over speciation effects for nickel in the DES environment. The effect of concentration on the speciation of nickel in Ethaline has not yet been studied and if the double layer is indeed becoming supersaturated with nickel ions during dissolution, there may be a speciation change across the concentration gradient.

5.2 Relation of speciation to redox properties

In **Chapter 4**, it was shown that speciation in DESs tends to primarily be chlorometallate. UV-Vis spectroscopy is a good method for qualitatively determining a change in solute speciation and for calculating the proportions of any different complexes present in solution. Molar absorptivity can be used to calculate the relative proportions of these species by changes in the absorbance peak heights and can also be an indicator of the geometry of the species.

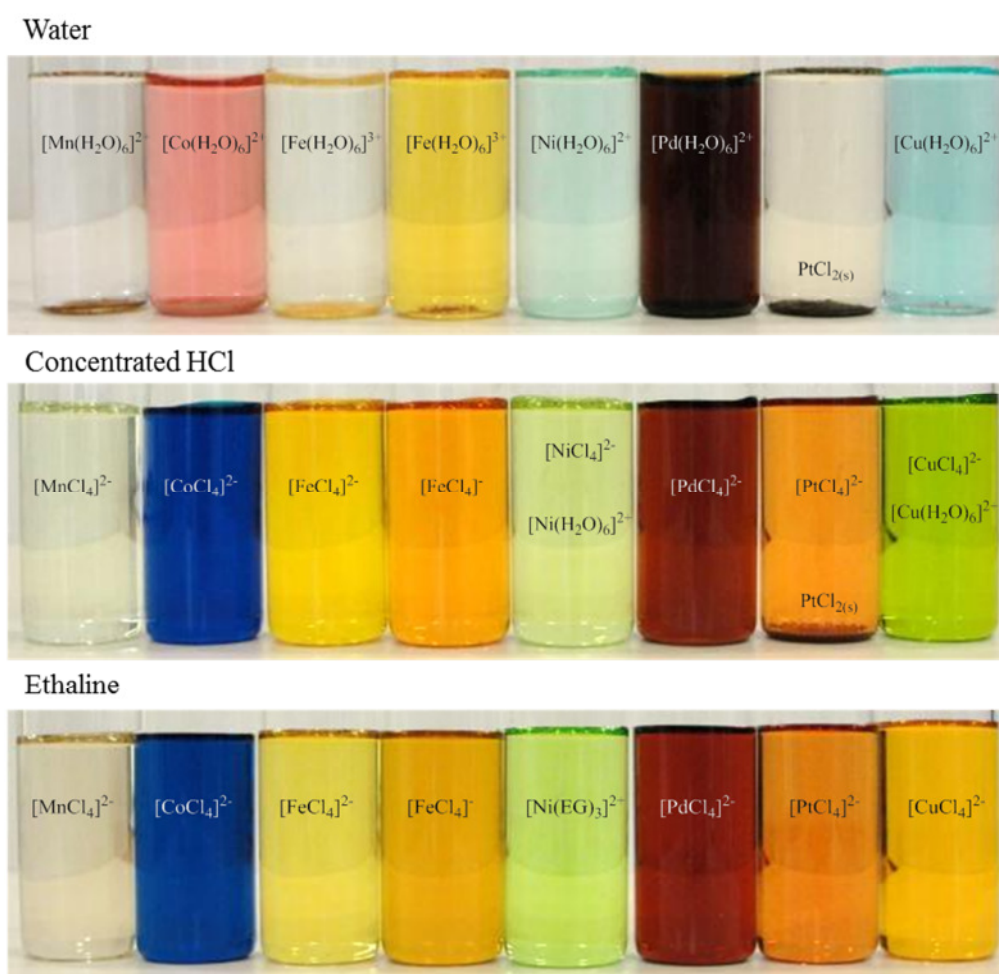


Figure 5.4 Solutions of a range of 100 mM metal salts in water (top), concentrated HCl (middle) and Ethaline (bottom). From left to right: MnCl_2 , CoCl_2 , FeCl_2 , FeCl_3 , NiCl_2 , PdCl_2 , PtCl_2 and CuCl_2 .

To see what difference a high Cl^- concentration makes to metal ions in an aqueous solution and whether the redox behaviour is dependent on the speciation, the speciation was studied in concentrated aqueous chloride solutions *via* cyclic voltammetry and UV-vis spectroscopy. **Figure 5.4** shows how changing the solution from deionised water to concentrated HCl changes the colour, such that it is visually very similar to DES. In the experiments to determine whether redox behaviour is dependent on the speciation, the sources of chloride will be lithium chloride, HCl and choline chloride. Initially, HCl was used as the solvent as it allows a high chloride activity and because the speciation of metal ions is known. LiCl was used for further experiments to limit hydrogen evolution in the electrochemical experiments.

5.2.1 Copper chloride

In water, it is well-known that Cu^+ is unstable and disproportionates immediately to Cu^{2+} and Cu metal, due to the difference in redox potentials (+0.52 V for the Cu^{+0} redox couple *vs.* +0.15 V for the $\text{Cu}^{2+/+}$ redox couple).³ Therefore, it is expected that a cyclic voltammogram for a solution of CuCl_2 in water should only show a single redox couple for the charge transfer reaction



From **Figure 5.5** it can be confirmed that there is no Cu^+ present in the aqueous solution, as there is a single bulk reduction of Cu^{2+} straight to copper metal at -0.2 V, with the possibility of an underpotential deposition beginning at +0.1 V. On the reverse scan, a nucleation loop is observed, followed by three separate oxidation peaks. The two main oxidation peaks can be attributed to the oxidation of Cu metal to an insoluble Cu^+ chloride salt on the electrode surface and then oxidation of this Cu^+ species to a soluble

Cu^{2+} species. The redox couples involving Cu^+ all take place on the surface of the working electrode, as it is present as an insoluble copper (I) chloride salt.

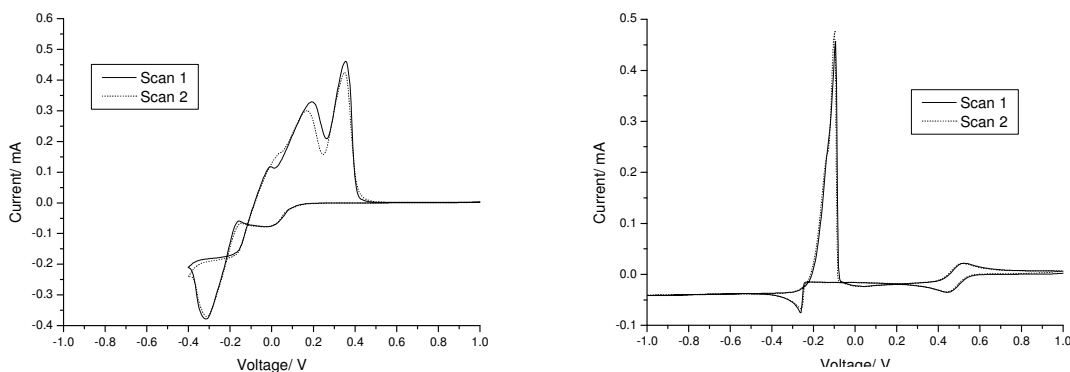
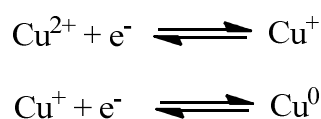


Figure 5.5 CVs of 100 mM CuCl_2 in H_2O (left) and aqueous LiCl 8 mol kg^{-1} (right) on 1 mm Pt disc vs. Ag wire reference, at a scan rate of 10 mV s^{-1} .

As was seen previously in **Section 3.3**, cyclic voltammetry of the same copper salt in Ethaline shows two distinct peaks and that the Cu^+ species in solution is stabilised and the Cu^{2+} species is destabilised by the high chloride environment (see **Figure 3.8**). If the presence of a high concentration of LiCl in an aqueous solution of CuCl_2 also stabilises the Cu^+ in a similar manner to the Ethaline solution, then the two electron transfer processes



should also be present in any voltammograms. As can be seen in **Figure 5.5** for the CV of 100 mM CuCl_2 in 8 mol kg^{-1} $\text{LiCl}_{(\text{aq})}$ solution, this is indeed the case.

The cyclic voltammetry of this LiCl solution shows a marked difference from a simple aqueous solution, as can be seen by comparing the two voltammograms in **Figure 5.5**. With the addition of LiCl , the CV shape resembles that of CuCl_2 in Ethaline. A reversible redox couple at +0.6 V corresponds to the $\text{Cu}^{2+/+}$ redox couple at

+0.45 V in Ethaline (**Figure 3.8**). A deposition/stripping redox couple at -0.2 V in aqueous LiCl corresponds to that of the Cu^{+0} redox couple at -0.4 V in Ethaline, vs. an Ag wire reference. This suggests that the majority of the copper ions have formed chloride species and that the Cu^+ is stabilised, similar to in Ethaline and the reference potential is shifted *ca.* 200 mV. It is highly likely, however, that there is still a small amount of the aqua-complex left in the 8 mol kg^{-1} LiCl solution as it is green rather than yellow, as can be seen in **Figure 5.6**. The slight bump visible in the LiCl voltammogram at approximately +0.1 V in **Figure 5.5** may be an indication of this remaining aqua-complex. If the LiCl concentration is increased sufficiently, then all of the copper should theoretically form the chloro-complex. In actuality, when the concentration of LiCl had been raised to 16 mol kg^{-1} , the small bump seen at +0.0 V had vanished but the solution still remained green. Therefore a portion of the copper must still remain in solution as the aqua-complex, as will be shown *via* UV-vis spectroscopy.



Figure 5.6 CuCl_2 (100 mM) in three different solvents. From left to right: water, aqueous 8 mol kg^{-1} LiCl, and Ethaline.

By examining these solutions with UV-vis spectroscopy it was found that, in general, as the chloride concentration was increased, and two peaks which correspond to the tetrachloro copper complex increased (**Figure 5.7**). The peak maximum for the d-d transition of the chloro-complex was outside the range of the spectrometer and so is not analysed here.

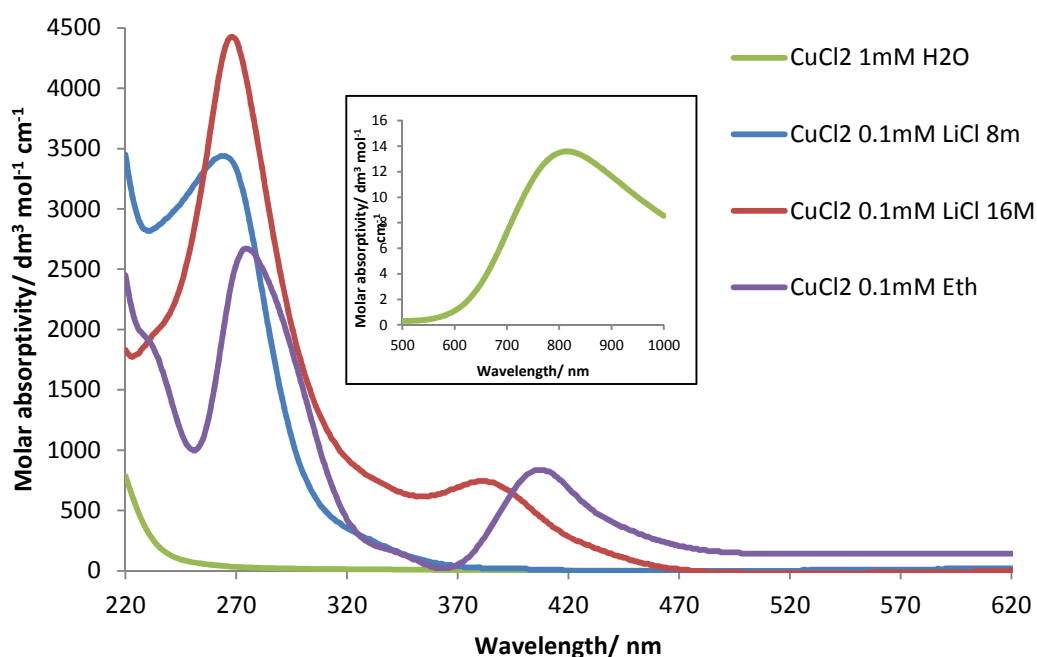


Figure 5.7 UV-vis spectra for solutions of copper chloride in water (green), 8 mol kg⁻¹ LiCl (blue), 16 mol kg⁻¹ LiCl (red) and Ethaline (purple). All CuCl₂ concentrations are 0.1 mM except for the water solution, which is 1 mM. The inserted image is a magnification of the 500 to 1000 nm region for 100 mM CuCl₂ in water.

The main differences between the four copper chloride solutions are highlighted in the low wavelength region of the spectrum between 220 and 520 nm. In pure water the blue copper hexaquo-complex has a strong charge transfer peak at ~220 nm (**Figure 5.7**, green line). A strong peak develops at 264 nm with the presence of 8 mol kg⁻¹ LiCl (**Figure 5.7**, blue line), and the presence of 16 mol kg⁻¹ LiCl (**Figure 5.7**, red line) causes this peak to shift to 268 nm. A second peak at ~380 nm is also observed in

the LiCl solutions. These peaks are likely to be absorbances from the tetrachloro complex, as can be confirmed by comparing the UV-vis spectra of the LiCl-containing aqueous solutions to the spectrum of copper chloride in Ethaline, which is known to be $[\text{CuCl}_4]^{2-}$, as discussed in **Chapter 4**. The low wavelength region of the UV-vis spectrum of Ethaline has the same general shape as the LiCl-containing solutions, with two main charge transfer peaks at 275 and 407 nm (**Figure 5.7**, purple line).

The absorption peak at ~400 nm, in particular, has been attributed to the tetrachloro species by Li *et al.*⁴ and by comparing the molar absorptivities of this peak in the three chloride-containing solutions, the change of copper speciation from purely octahedral to purely tetrahedral can be seen and the percentages of chloro-complex can be calculated.

If the molar absorptivity for the peak at 407 nm in Ethaline is taken as 100% chloride species, then the 16 mol kg⁻¹ LiCl solution has 73% chloro-complex and the 8 mol kg⁻¹ LiCl solution has 7.9% chloro-complex. This is quite surprising considering that the shapes of the LiCl-containing voltammograms are very similar to Ethaline. It appears that even a small amount of $[\text{CuCl}_4]^{2-}$ or $[\text{CuCl}_2]^-$ will dominate the electrochemistry, despite the bulk of the copper ions retaining the aquo complex.

Above 800 nm, a very broad and weak set of *d-d* absorption peaks is visible in all four of the solutions, with the intensity increasing with chloride content. For the tetrahedral chloro-complex, a Jahn-Teller distortion is suggested by the placement of this set of absorption peaks between the absorption peak values suggested by Battaglia *et al.* for tetrahedral (1488 nm) and square planar (615 nm) coordination.⁵

5.2.2 Cobalt chloride

From the UV-Vis spectra of CoCl_2 in H_2O (**Figure 5.8**, green line) a single broad weak peak centred at 520 nm can be seen in the $d-d$ transition region (see insert in **Figure 5.8**). This peak can be assigned to the pale pink octahedral aquo-complex, $[\text{Co}(\text{H}_2\text{O})_6]^{2+}$, which is the main species commonly seen to form in pure water.³ In Ethaline, EXAFS suggests that CoCl_2 will instead form a tetrachloro complex $[\text{CoCl}_4]^{2-}$ (see **Chapter 4**). The observed $d-d$ transition signals shift to longer wavelengths (600 to 720 nm) in Ethaline and the intensity suggests that this complex is tetrahedral, due to the Laporte selection rule. The tetrahedral complex has no symmetry centre of inversion and therefore a dipole moment is caused during inversion, allowing electronic transitions to be made.

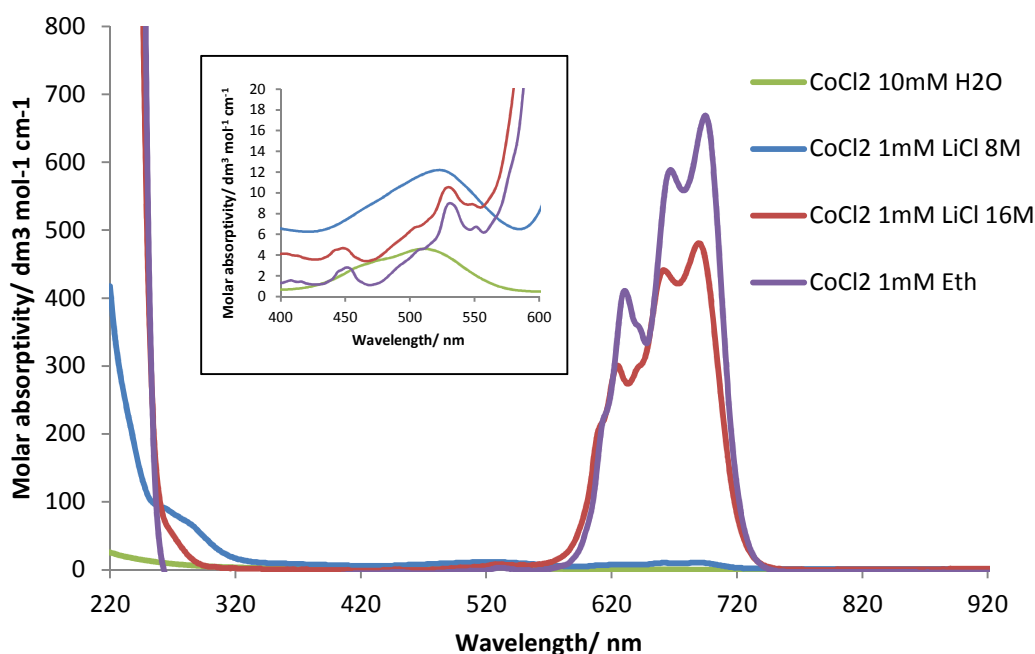


Figure 5.8 UV-vis spectra for solutions of cobalt chloride in water (green), 8 mol kg⁻¹ LiCl (blue), 16 mol kg⁻¹ LiCl (red) and Ethaline (purple). All concentrations of CoCl_2 are 1 mM except for the water solution, which is 10 mM. The inserted image is a magnification of the 400 to 600 nm region (CoCl_2 concentrations are all 100 mM).

When changing to an aqueous chloride environment, *i.e.* 8 mol kg⁻¹ LiCl (**Figure 5.8**, blue line), both of these sets of *d-d* transitions are visible, however they are still very weak. Assuming that the molar absorptivity of the *d-d* transition peak at ~700 nm in the Ethaline solution is 100% chloro-complex, it can be calculated that for the 8 mol kg⁻¹ LiCl solution [Co(H₂O)₆]²⁺ and [CoCl₄]²⁻ are present in a ratio of 98.4% aquo- to 1.6% chloro-complex. Increasing the LiCl concentration to 16 mol kg⁻¹ causes a reduction in the signal from the aquo-complex peak and an increase in the chloro-complex peak to a ratio of 44.2% and 55.8%, respectively. Although the water spectrum can be considered as 100% aquo-complex, this peak cannot be used as a baseline for the other spectra, as the absorption intensity from the chloro-complex peaks merges into the aquo-complex region of the spectrum.

5.2.3 Nickel chloride

In **Chapter 4**, it was seen that nickel ions chelate with the ethylene glycol molecules in Ethaline, and these solutions display unusual redox properties and surface effects. From the behaviour observed for copper and cobalt chlorides in aqueous chloride environments, it was predicted that the aqueous nickel chloride systems would follow a similar trend and also display a steady change from fully aquo-complex (octahedral) to chloro-complex (tetrahedral) with the increasing addition of LiCl, and that a completely different shaped spectra would be observed for the Ethaline solution (most likely still octahedral).

All of these solutions, however, were seen to have a similar general trend: an intense charge transfer band, followed by a sharp (but weak) *d-d* absorption band around 400 to 420 nm and a very broad, double-humped *d-d* transition between 620 and

900 nm, as can be seen from **Figure 5.9**, similarly to that observed by Triest *et al.*⁶ for a solution of $[\text{Ni}(\text{OH}_2)_6]^{2+}$ in water. As the chloride concentration increases, the absorption peaks can be seen to shift to longer wavelengths: from 394 nm in water, through 402 nm with 8 mol kg⁻¹ LiCl, ending at 422 nm with 16 mol kg⁻¹ LiCl. These peaks retain the same shape and relative position to each other and the low molar absorptivity of these solutions infers that they are all octahedral.³ This variation of peak position suggests that a mixture of two different complexes may be present, *i.e.* both aqua and chloride, or that a single complex is present with mixed coordination.

The broad peak at high wavelength between 600 nm and 800 nm appears to be an overlapping series of at least three different weak *d-d* transitions, the intensities and general trends of which are consistent with the other peaks.

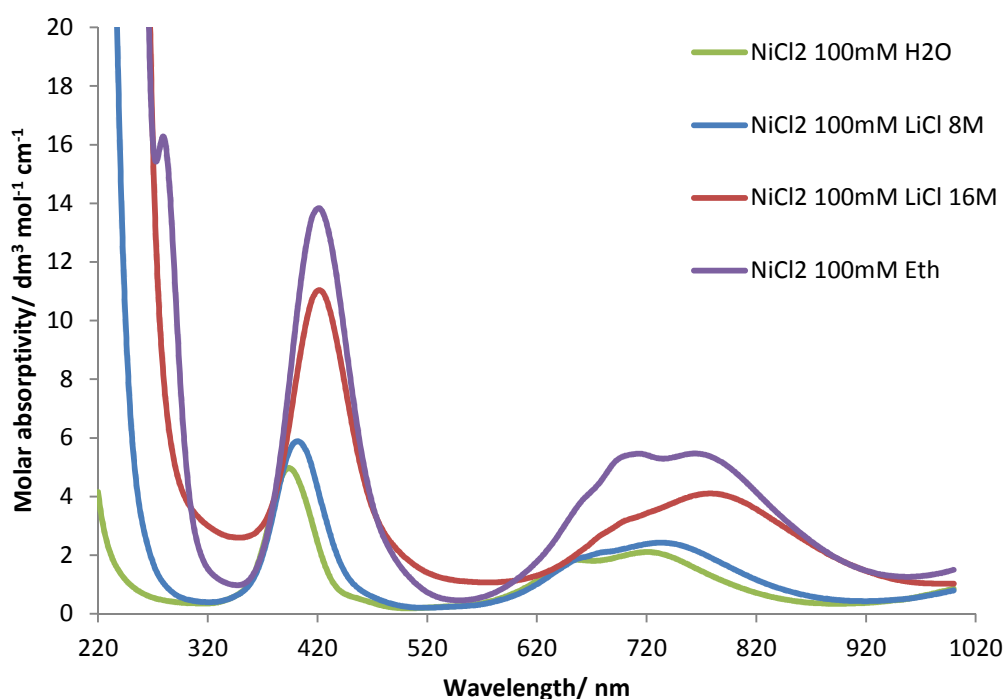


Figure 5.9 UV-vis for solutions of nickel chloride in water (green), 8 M LiCl (blue), 16 M LiCl (red) and Ethaline (purple).

When the Ethaline solution is considered, the general shape of the spectra appears similar to that of the aqueous solution, most likely a result of the complex that forms in Ethaline also being based on an oxygen donor compound, *i.e.* ethylene glycol. On closer inspection, a shoulder is visible at 279 nm on the primary charge transfer band peak. None of the aqueous spectra have this shoulder, which suggests that it may be an effect of the glycol coordination in the Ethaline, as opposed to an effect of the presence of chloride. This would suggest that, even with the addition of a substantial amount of chloride, the nickel prefers to form a mainly oxo-complex.

5.2.4 Short summary

By using a substantial amount of LiCl, metal species in aqueous solution can be converted into chloride complexes, with varying degrees of completion. Visually, the solutions are a similar colour to the equivalent solutions made using concentrated HCl, but without the need for strong acids. Ethaline continues to have a more complete chloride speciation than any of the aqueous solutions, despite the substantial concentrations of chloride added, which suggests that the water molecules are continuing to interfere in the speciation of the metal ions in aqueous systems.

The electrochemistry for these aqueous metal chloride solutions is dominated by the chloride, even if the majority of the metal ions in solution form aquo-complexes.

5.3 Voltammetry in LiCl:2H₂O

In **Chapter 3**, the formal redox potentials of a range of metal chloride salts in Ethaline were compared to the equivalent potentials in aqueous media. These were shown in **Figure 3.7**. As these same metal salts in a 1:2 LiCl:2H₂O analogue (**Figure 5.10**) were seen to have similar redox behaviour to their Ethaline counterparts, it was

theorised that their speciation might also be similar. If speciation and redox behaviour could be linked, then the redox behaviour could be predicted from the speciation and *vice versa*.

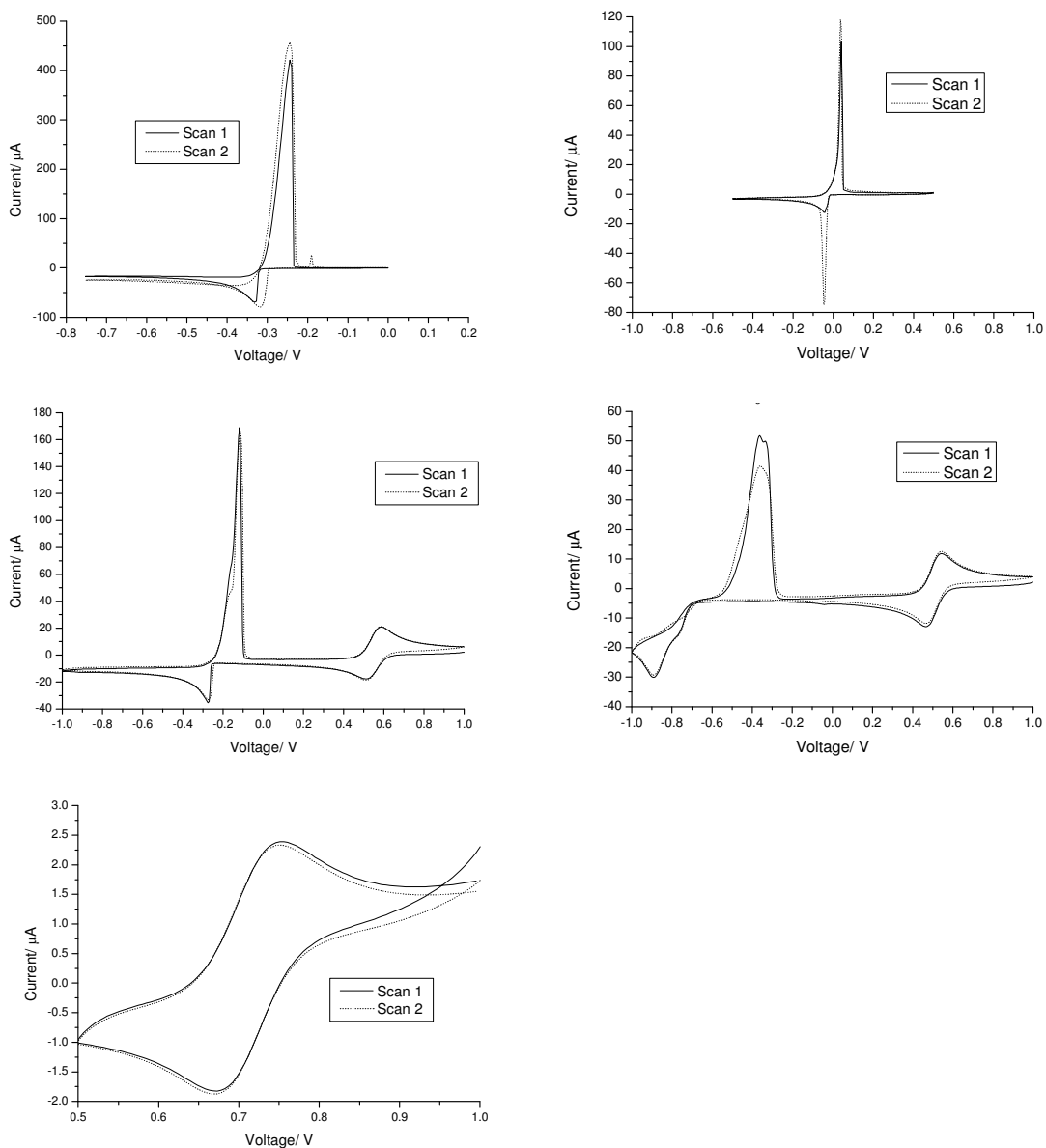


Figure 5.10 Cyclic voltammograms of 100 mM metal salts in LiCl:2H₂O: SnCl₂ (top left), AgCl (top right), CuCl₂ (middle left), FeCl₃ (middle right) and K₄[Fe(CN)₆] (bottom). Scans were made on a 1 mm Pt disc vs. an Ag wire reference, at a scan rate of 10 mV s⁻¹.

Therefore a plot of the formal redox potentials in Ethaline was plotted against the redox potentials from the LiCl-based DES analogue (**Figure 5.11**). As can be seen, these redox values follow a linear trend. However, there is an offset of these values from the line of equivalence, which is most likely an artefact caused by the reference solution.

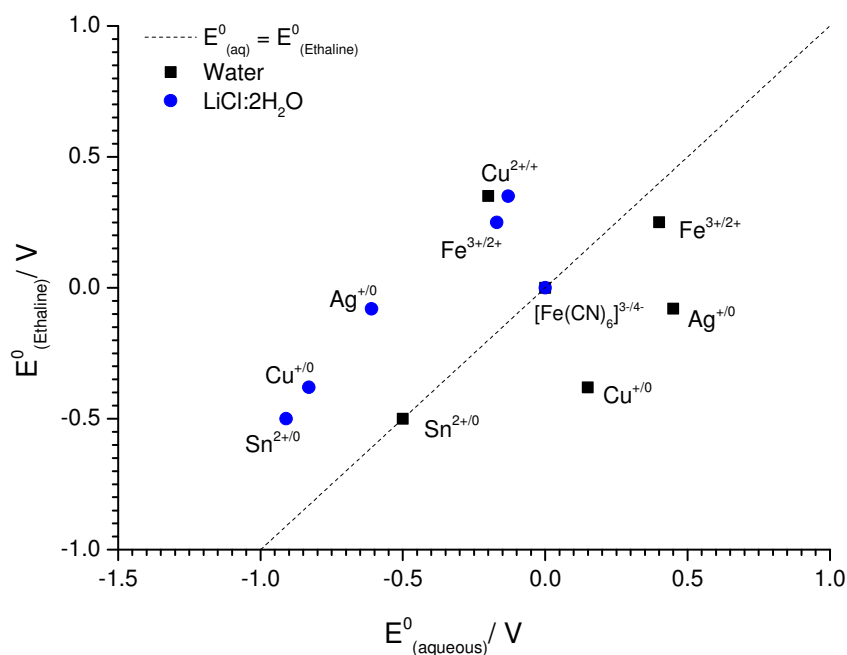


Figure 5.11 Formal electrode potentials of a selection of metal species in Ethaline compared with redox potentials in LiCl:2H₂O (blue) and standard redox potentials in water (black). Through the centre of the graph is the line of equivalence, where electrode potentials would be identical in both solutions.

It is possible that a change in redox potential takes place upon addition of LiCl to the solution, which exceeds the chloro-complex formation effects in Ethaline. However, this is unlikely due to the high chloride activity in both LiCl and Ethaline solution, as can be seen from the UV-vis spectra for these solutions, which show pure chloro-species (**Figure 5.7**). It should also be considered whether there is a bias on the reference potential, and if so, this method may not be suitable to compare LiCl and

Ethaline solutions. The lithium cation may also be affecting the redox potential by binding with the $[\text{Fe}(\text{CN})_6]^{4-/3-}$ species.

5.4 DES analogues

In **Section 5.2**, it has been observed that LiCl (at either 8 or 16 mol kg⁻¹) on its own in water does not have a strong enough chloride activity to completely convert all of the metal salts used into an aqueous chloro-complex. In order to determine what behaves like an aqueous solution, *i.e.* dominated by aquo-complexes, and what behaves like a DES, *i.e.* dominated by chloro-complexes, the next step was to repeat these experiments with solutions composed of 1:2 mixtures of chloride salt to hydrogen bond donor (HBD), where LiCl or choline chloride (ChCl) was the salt and either water or ethylene glycol (EG) was the HDB. These combinations are shown below for clarity:

1 choline chloride: 2 ethylene glycol

1 lithium chloride: 2 ethylene glycol

1 choline chloride: 2 water

1 lithium chloride: 2 water

The effect of the cation on the formation of the chloro complex in DES media is not completely known, and the inorganic and small Li⁺ may have a different stabilising or destabilising effect on the metal chloride species than the organic and comparatively bulky choline.

In addition, the choice of HBD may be having an effect on the solubilisation of the metal salt and may be stabilising the ionic metal species through coordination effects. The HBD is also likely to be interacting differently with different cations. For instance, Li⁺ is likely to have a solvation shell of water molecules around it in aqueous media, but the method of solvation by ethylene glycol is likely to be more complex.

Choline, on the other hand is more likely to interact with the HBD through hydrogen bonding from its OH-group.

The chloride salt used to make Ethaline, choline chloride, may have a higher chloride activity than LiCl and the presence of the organic cation may have a greater stabilising effect on the metal chloride complex than LiCl would.

To determine if it was the chloride salt or the choice of HBD that was helping to form the chloride complex, cyclic voltammetry and UV-vis spectra of these solutions were recorded and compared to the corresponding Ethaline solutions.

5.4.1 Copper chloride

As indicated previously in **Section 3.3.1**, the solution of copper (II) chloride in Ethaline shows two redox couples, which are believed to be $\text{Cu}^{2+/+}$ at the more positive electrode potential and $\text{Cu}^{+/0}$ at the more negative potential. If the Cu^+ species is stabilised in the DES analogues as well, then a similarly shaped voltammogram would be expected. As can be seen in **Figure 5.12**, all three of these analogues show a similar redox shape to the CV of CuCl_2 in Ethaline. However, the relative positions of the redox couples shift towards more positive potentials, compared to the ones in Ethaline.

The voltammetric response of the LiCl-water analogue is almost identical in general shape to that of Ethaline, suggesting that all of the copper is in a chloride complex, although the solution still remains green, visually indicating that this is not the case. The ChCl-water analogue, on the other hand, has similar voltammetry to the LiCl-water solution but is instead yellow in colour, hinting at a fully chloride speciation.⁷ The LiCl-ethylene glycol analogue was also yellow and continued to show both sets of copper redox couples. The solution was particularly viscous and cloudy, suggesting that

not all of the LiCl had dissolved, which could explain the more unusual shape of the voltammogram.

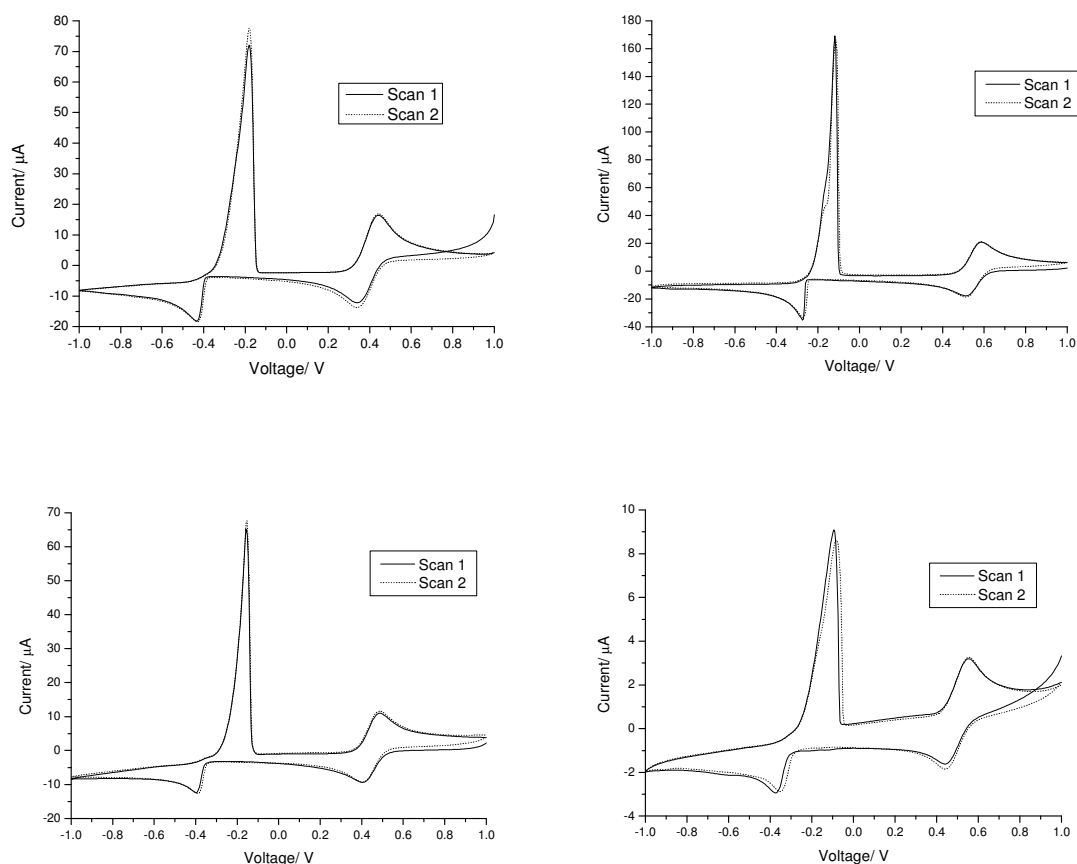


Figure 5.12 Cyclic voltammograms of anhydrous CuCl_2 100 mM in (clockwise from top left) Ethaline, $\text{LiCl}:2\text{H}_2\text{O}$, $\text{LiCl}:2\text{EG}$ and $\text{ChCl}:2\text{H}_2\text{O}$, on 1 mm Pt disc vs. Ag wire reference, at a scan rate of 10 mV s^{-1} .

As would be expected from the colours of the analogue solutions, UV-vis spectroscopy shows similar patterns of absorption and therefore similar speciation for the copper ions. Each of the spectra shows three peaks at around 250, 300 and 400 nm. The exact positions vary between the solutions, with the $\text{ChCl}:2\text{H}_2\text{O}$ analogue being the most similar to the Ethaline solution. In **Section 5.2.1** the peak in the 400 nm region was taken as a reference point for calculating percentage chloride complex and by

examining this peak for the analogues, it can be seen that in both Ethaline and the $\text{ChCl}:\text{2H}_2\text{O}$ solution it remains at 405 nm. However, in the $\text{LiCl}:\text{2H}_2\text{O}$ solution it is at the shorter wavelength of 380 nm, meaning that less chloride complex is present. The $\text{LiCl}:\text{2EG}$ analogue was too viscous to be filtered to remove the cloudiness of undissolved LiCl and hence is not displayed here.

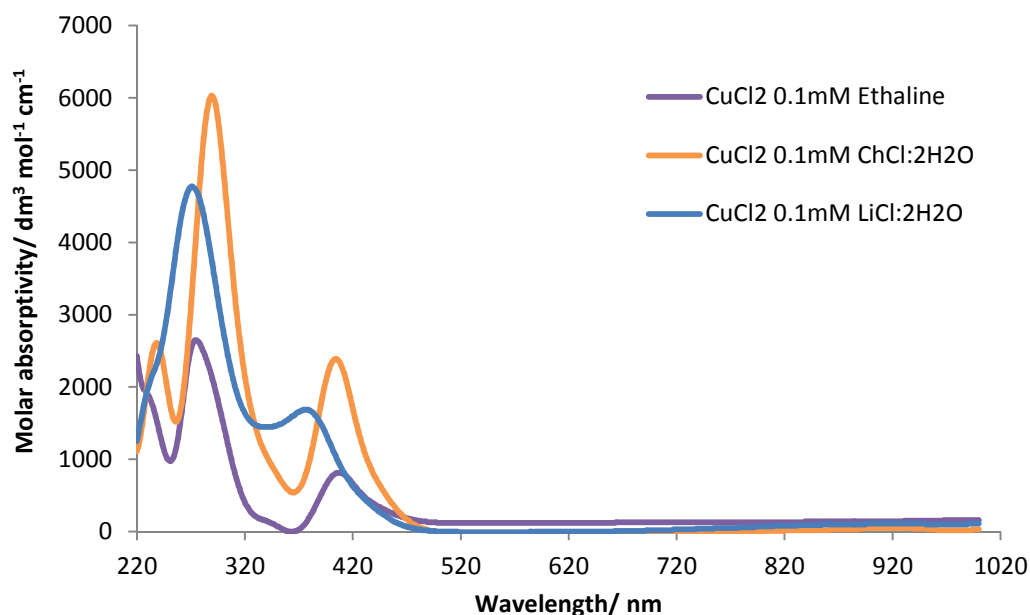


Figure 5.13 UV-vis spectra for solutions of copper chloride in $\text{ChCl}:\text{2H}_2\text{O}$ (yellow), $\text{LiCl}:\text{2H}_2\text{O}$ (blue) and Ethaline (purple).

The ChCl -based aqueous solution produces more of the copper tetrachloride complex than the LiCl -based aqueous solution. Similar UV-vis studies of CuCl_2 in ChCl -water mixtures by De Vreese *et al.*⁷ also saw that the copper remains an almost pure chloride species up to the addition of 49 wt% water (equivalent to a molar ratio of 1:7.5 ChCl to water, assuming 100 g of solution is approximately 100 ml). After addition of 62 wt% water (equivalent to a molar ratio of 1:12 ChCl to water) the speciation was seen to change dramatically. Therefore ChCl is a very good source of chloride for the formation of chloride complexes in the presence of water. The same

general shape for these spectra was also observed by Abbott *et al.* for UV-vis spectra of both anhydrous and hydrated CuCl_2 in Ethaline.⁸ This effect may be due to Li^+ binding to the chloride and lowering the chloride activity of the solution. It is unlikely that the choline would have this effect, as the charge density on the choline is less than that on the Li^+ .

5.4.2 Iron chloride

The iron systems are, however, very different from the other metal chloride solutions. FeCl_3 in the new DES analogue solutions (**Figure 5.14**) has a surprisingly different set of redox responses to Ethaline. When these solutions are compared to Ethaline, it can be seen that the main difference between them is in the shape of $\text{Fe}^{2+/0}$ redox couple, as the $\text{Fe}^{3+/2+}$ redox couple is roughly similar in peak current.

In Ethaline ($\text{ChCl}:2\text{EG}$), an unusual redox event is observed for the $\text{Fe}^{2+/0}$ redox couple, where there is some metal deposition but no clear reoxidation peak. In the corresponding choline-containing analogue ($\text{ChCl}:2\text{H}_2\text{O}$) a small oxidation peak is observed. The anodic section of this redox event displays a small sharp peak, followed by a dip in current. This sudden dip back below zero current could suggest the sudden flaking off of the Fe deposit or formation of a very thin salt passivating layer. When the solution of 0.1 M LiCl in EG is considered, it continues to show irreversible redox behaviour.

However, the voltammetric response of the $\text{LiCl}:2\text{H}_2\text{O}$ solution stands out from the others. Clear deposition and stripping of the $\text{Fe}^{2+/0}$ couple can be seen in this solution, starting at a potential of -0.75 V vs. an Ag wire reference. If examined closely, the beginnings of a nucleation loop can be seen on the first scan and is more distinct on the second scan.

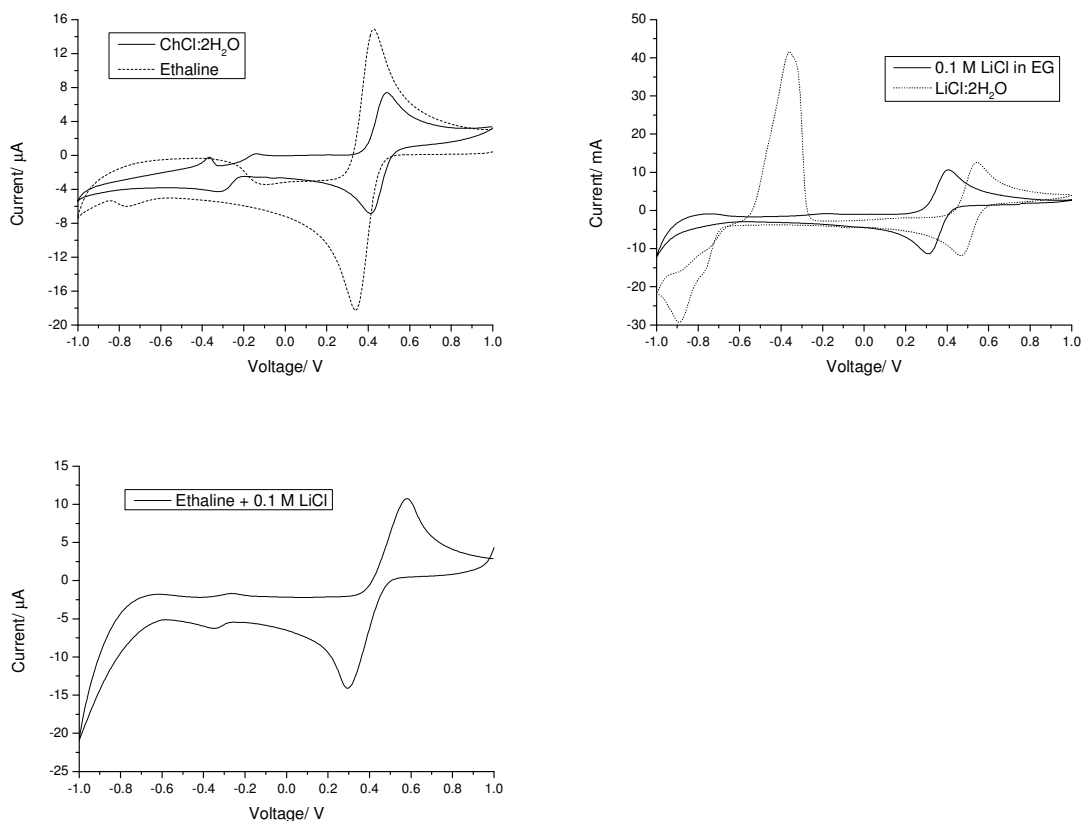


Figure 5.14 Cyclic voltammograms of FeCl_3 (100 mM) in DES analogues. Left – $\text{ChCl}:2\text{H}_2\text{O}$ (solid line) and Ethaline (dashed line). Right – 0.1 M LiCl in EG (solid line) and $\text{LiCl}:2\text{H}_2\text{O}$ (dashed line). Bottom – Ethaline with 0.1 M LiCl. All scans were made on a 1 mm Pt disc vs. Ag wire reference, at a scan rate of 10 mV s^{-1} .

5.4.3 Short summary

DES analogues containing a 1:2 mixture of ChCl or LiCl with EG or water can therefore be used to obtain a tetrachloride speciation of copper and have been seen to have distinctly different voltammetric responses from Ethaline. From this comparison, it could be suggested that there is a cation dependency of metal deposition. The more oxophilic metals, such as the earlier transition metals, *e.g.* iron, are more greatly affected by cation effects. More chlorophilic metals, such as copper, are less affected by cation and are instead affected more by the anion. Choline is a bulkier cation than

lithium and could block the electrode surface, preventing dissolution of the metal. Therefore the presence of Ch^+ in solution may quench electrodeposition. The simplest method of detecting the effect of cation dependency is by taking one of the Ch^+ solutions and adding LiCl. If choline is quenching deposition, then this solution would show irreversible behaviour and the lithium-containing solutions would show reversible or semi-reversible deposition.

Addition of 0.1 M LiCl to Ethaline appears to increase the reduction current and the voltammetry suggests that there may be some underpotential deposition beginning at approximately -0.3 V. There is no obvious reoxidation of the deposited metal and therefore the choline must have a greater effect than the lithium ions on the redox properties of the metals in solution. Since the presence of EG also appears to be blocking the electrode surface, the adsorbed water layer may also be important in the reduction mechanism.

5.5 Conclusions

From the above results, it has been shown that the redox behaviour of a metal salt cannot be used in isolation to predict the speciation of that salt in solution and, conversely, that the speciation of a metal salt in DES media is not a sole indicator of its redox behaviour. Surface effects on the working electrode have been seen to dominate over the speciation of the metal ion in DES media, as seen for metals such as nickel, cobalt and iron, amongst others. It was found that even with a native metal working electrode, the surface needed to be anodically cleaned before deposition would take place.

With the addition of a substantial amount of lithium chloride (8 mol kg^{-1} or 16 mol kg^{-1}), chlorometallate species can be formed in aqueous media, as has been

demonstrated by the CuCl_2 experiments in **Section 5.2.1**. As the speciation changes from aquo to chloro complexes, the change in chemical behaviour can be observed *via* cyclic voltammetry. The addition of LiCl to aqueous solutions has the advantage of stabilising the Cu^+ species, as has been shown by cyclic voltammetry in **Figure 5.12**. The same effects can be obtained by using choline chloride in aqueous solution as the chloride donor, except that it seems to have a more chloride complex inducing effect than the same concentration of LiCl, as seen *via* UV-vis spectroscopy.

When the standard redox potentials of various metal salts in Ethaline are compared to the corresponding potentials in a $\text{LiCl}:2\text{H}_2\text{O}$ solution, a straight line parallel to the line of equivalence is obtained (**Figure 5.11**).

As seen in **Chapter 3**, a solution of FeCl_3 in Ethaline shows rather unusual redox behaviour for the $\text{Fe}^{2+/0}$ couple on a Pt working electrode, and in **Section 5.1** it has been shown that anodic cleaning of the native metal working electrode surface must take place before any deposition can occur. However, in the LiCl-water DES analogue solution, a visible deposition event, followed by a clear stripping peak is observed, along with the $\text{Fe}^{3+/2+}$ reversible couple. The ChCl-water analogue also shows a clear deposition (although of lower current) but a large chunk is cut out of the stripping, possibly due to formation of a salt film. It is possible that the choline is causing some form of blocking effect on the electrode surface, preventing iron deposition. This suggests that the quaternary ammonium cation inhibits the reduction of some metals. The addition of LiCl to Ethaline permits the reduction of Fe^{2+} proving the effect of the double layer in controlling the reduction of metal ions. In addition, the presence of Li^+ may be having reducing the chloride activity of the solution by binding to the chloride.

5.6 References

1. T. Rayment, A. J. Davenport, A. J. Dent, J. P. Tinnes, R. J. K. Wiltshire, C. Martin, G. Clark, P. Quinn and J. F. W. Mosselmans, *Electrochemistry Communications*, 2008, **10**, 855-858.
2. C. M. Ip, MChem thesis, University of Leicester, 2012.
3. C. E. Housecroft and A. G. Sharpe, *Inorganic Chemistry*, Pearson Prentice Hall, 2008.
4. G. Li, D. M. Camaioni, J. E. Amonette, Z. C. Zhang, T. J. Johnson and J. L. Fulton, *The Journal of Physical Chemistry. B*, 2010, **114**, 12614-12622.
5. L. P. Battaglia, A. Bonamartini Corradi, G. Marcotrigiano, L. Menabue and G. C. Pellacani, *Inorganic Chemistry*, 1979, **18**, 148-152.
6. M. Triest, G. Bussière, H. Bélisle and C. Reber, *Journal of Chemical Education*, 2000, **77**, 670.
7. P. De Vreese, N. R. Brooks, K. Van Hecke, L. Van Meervelt, E. Matthijs, K. Binnemans and R. Van Deun, *Inorganic Chemistry*, 2012, **51**, 4972-4981.
8. A. P. Abbott, K. El Ttaib, G. Frisch, K. J. McKenzie and K. S. Ryder, *Physical Chemistry Chemical Physics*, 2009, **11**, 4269-4277.

Chapter 6 Metal processing and recovery

This chapter has been removed for confidentiality reasons.

Chapter 7 Overall conclusions and future research

Chapter 7 Overall conclusions and future research.....212

7.1 Conclusions.....213

7.2 Future research.....216

Chapter 7 Overall conclusions and future research

7.1 Conclusions

Deep eutectic solvents (DESs) are a relatively recent field of research and fundamental properties, such as redox behaviour and speciation, have not previously been studied. In order to use these DESs in the field of metal processing, the behaviour of metals and their salts in solution must first be understood.

To be able to determine redox behaviour in DES media, a stable silver/silver chloride reference electrode has been created and used to determine the activity coefficients of three different systems in Ethaline. These three systems, AgCl, CuCl₂ and triflic acid, were found to have constant activity coefficients, even at high concentrations and including up to the solubility limit for AgCl and CuCl₂ (0.2 M and 1 M, respectively). Therefore the metal ions can be considered as behaving independently and must be somehow shielded from each other. If this is the case for all DES systems, then the activity of the solute can always be considered equal to the concentration.

As triflic acid is likely to be fully dissociated in the DESs the proton activity can be considered equal the concentration and so an Ethaline-based 'standard hydrogen electrode' could be constructed. This gives a potential against which all other potentials in Ethaline can be referenced and potentially allows the construction of pH scales. The corresponding experiments of silver salts in some other ionic liquids do not show this ideal behaviour (*i.e.* activity coefficients change with increasing solute concentration). This is possibly due to bridging action by the anionic component of the IL or from the formation of multinuclear complexes.

The speciation of a range of metal salts in DES media has been determined using extended X-ray absorption fine structure spectroscopy (EXAFS). It was observed that M⁺ salts generally have [MCl₂]⁻ speciation and M²⁺ salts generally have [MCl₄]²⁻

speciation. Deviations from this trend have been seen for nickel chloride, which chelates with ethylene glycol in Ethaline, and the more oxophilic metals, such as manganese or iron, which form a pure oxide coordination in Reline. The addition of metals salt hydrates does not cause any significant deviations from this chloride speciation *i.e.* the water molecules are removed from the complexation shell of the metal ion.

Metal salts in imidazolium ionic liquids tend to form species where the anionic component of the liquid controls the speciation, except in the case of particularly uncoordinating anions, such as FAP and NTf₂. The presence of water has a much greater effect on the speciation of metal ions in these systems, especially when less coordinating anions are present. Identification of specific species was difficult due to the large error of the fits which probably originates from the variety of species which form simultaneously in solution.

With the new reference electrode, a redox series has been constructed for a selection of different metal chloride salts in Ethaline. Certain metal species, such as nickel, cobalt and iron, amongst others, were seen to show unusual redox behaviour during cyclic voltammetry on a platinum working electrode. By examining the speciation of their chloride salts in DES media, it has been deduced that this behaviour is not necessarily due to the speciation and that surface and passivation effects may actually be dominant. Of the three metals mentioned, nickel showed a speciation that suggested chelation with ethylene glycol component of the Ethaline, whilst cobalt and iron showed a tetrachloride species. When cyclic voltammetry was recorded of these solutions on a native metal working electrode, it was seen that the working electrode had to be anodically cleaned before any metal deposition could take place.

To determine what effect the choice of cation or hydrogen bond donor has on the formation of the chloro complex, the redox behaviour of metal chloride salts in DES analogues of 1:2 mixtures of chloride salt to hydrogen bond donor were studied. Similar redox behaviour to the corresponding Ethaline solutions was observed for all solutions. In particular, choline chloride appeared to assist chloro-complex formation more than LiCl. Interestingly, when the voltammetry of FeCl₃ was studied in these DES analogues, it was shown that Ch⁺ inhibited the reduction of Fe²⁺ to the metal irrespective of the HBD whereas when Li⁺ was used metal reduction was observed in both cases. This suggested that the quaternary ammonium cation inhibits the reduction of some metals. The addition of LiCl to Ethaline permits the reduction of Fe²⁺ proving the effect of the double layer in controlling the reduction of metal ions.

The above information about redox potentials and speciation was applied to the dissolution, separation and recovery of copper and gallium from scrap semiconductor alloys, *via* electrodisolution of the CG alloy. Copper could be electrowon and gallium was precipitated out of solution with aqueous ammonia solution as a gelatinous white compound. Almost quantitative separation and recovery of the individual components was obtained, as confirmed by EDAX analysis of the end products.

In the DES environment, the higher oxidation states of chlorophilic late transition elements have been stabilised, making them easier to oxidise. Iodine can be used as a chemical oxidising agent, for the oxidation of CG alloy shavings and the removal of thin gold coatings from paleontological SEM samples, without causing any damage to the substrate.

7.2 Further work

Other metal salts in may also show constant activity coefficients in Ethaline and it would be interesting to see whether this is connected with the speciation or general redox behaviour of the metal salts. For instance, PdCl₂ and CoCl₂ have a simple tetrachloride speciation but unusual voltammetry, whilst NiCl₂ has both unusual speciation and redox behaviour, and it is currently unknown if either of these factors will have a significant effect on the activity coefficients.

Another topic to investigate would be whether the linear trends in activity coefficient observed for AgCl, CuCl₂ and triflic acid in Ethaline also carries through to other DESs, such as Reline, Propaline or Oxaline. Of these three other solvents, Propaline would be expected to have similar properties to Ethaline, as it is the closest in composition but differences may arise in Reline (ammonia evolution) or Oxaline (greater chance of oxalate coordination). Some speciation differences have been observed for metal ions in these DESs; however whether or not these will affect the activity coefficients is not known.

In the imidazolium-based ILs studied, non-ideal behaviour was observed. It would be interesting to determine whether the choice of anion is the cause of this behaviour. For instance, SCN and acetate have the potential to act as bridging ligands between metal ions, whilst an anion such as chloride does not. It is possible that certain of the imidazolium liquids may also act as ideal solutions but that the composition must be carefully selected first.

Whilst copper-gallium dissolution could be assisted by addition of iodine, the individual components could not be recovered in reasonable purities. The proximity of the two electrodes and ability for the iodine to mix throughout the solution may be causing any electrowon metals to be reoxidised and reducing current efficiency.

Separation of the iodine regeneration from metal recovery by either distance or a physical barrier may increase yield and purity from this method.

The current electrolytic dissolution process works successfully for a binary alloy system on a small scale. The next steps would be to scale this process up and to potentially create a flow process, such that disassembly of the reaction set-up to remove the inner beaker for copper electrowinning is unnecessary. It was also be interesting to examine the separation and recovery of tertiary alloy systems on a small scale in greater detail.

Chapter 8: Appendix for EXAFS data

Table 8.1: EXAFS fits of 100 mM solutions of silver chloride in a range of DES.

DES	M–X, where X=?	Number of atoms, n	Distance from centre, r (Å)	Debye-Waller factor, a (Å ²)	Fermi energy, EF (eV)	Fit index, R(min)
Ethaline	Cl	2.5(2)	2.484(7)	0.017(2)	-6.3(6)	4.3 %
Old Ethaline	Cl	2.5(2)	2.483(6)	0.016(2)	-6.3(6)	4.2 %
Reline	Cl	2.9(3)	2.525(8)	0.023(3)	-3.6(7)	7.0 %
Propaline (1,2)	Cl	2.4(2)	2.486(6)	0.016(2)	-5.6(6)	4.2 %

Table 8.2: EXAFS fits of 100 mM solutions of a range of silver salts in Ethaline (top) and 1,2-Propaline (bottom).

Metal salt	M–X, where X=?	Number of atoms, n	Distance from centre, r (Å)	Debye-Waller factor, a (Å ²)	Fermi energy, EF (eV)	Fit index, R(min)
AgCl	Cl	2.5(2)	2.484(7)	0.017(2)	-6.3(6)	4.3 %
Ag ₂ O	Cl	2.1(2)	2.490(7)	0.015(2)	-6.9(7)	6.4 %
	Cl or Ag	1.9(2) 1.8(9)	2.478(7) 2.87(3)	0.014(2) 0.05(2)	-5.0(9)	4.8 %
AgNO ₃	Cl	2.6(2)	2.482(6)	0.017(2)	-4.9(6)	4.6 %
AgAc	Cl	2.4(2)	2.485(7)	0.016(2)	-6.9(7)	6.6 %
AgCl	Cl	2.4(2)	2.486(6)	0.016(2)	-5.6(6)	4.2 %
AgNO ₃	Cl	2.4(2)	2.484(5)	0.014(2)	-5.6(5)	3.7 %
AgAc	Cl	2.0(1)	2.479(5)	0.015(2)	-5.5(7)	2.7 %
	Ag	2.1(3)	2.822(8)	0.026(3)		

Table 8.3: EXAFS fits of 100 mM solutions of gold (I) chloride in a range of DES.

Metal salt	M–X, where X=?	Number of atoms, n	Distance from centre, r (Å)	Debye-Waller factor, a (Å ²)	Fermi energy, EF (eV)	Fit index, R(min)
Ethaline	Cl	1.9(2)	2.262(6)	0.006(2)	-7(1)	5.5 %
Propaline (1,2)	Cl	1.8(1)	2.265(6)	0.007(1)	-7(1)	6.8 %

Table 8.4: EXAFS fits of 100 mM solutions of copper salts in Ethaline (top) and Reline (bottom).

Metal salt	M–X, where X=?	Number of atoms, n	Distance from centre, r (Å)	Debye-Waller factor, a (Å ²)	Fermi energy, EF (eV)	Fit index, R(min)
CuCl ₂	Cl	3.7(2)	2.252(5)	0.008(1)	-7.4(5)	4.5 %
CuCl ₂ ·2H ₂ O	Cl	3.6(3)	2.250(5)	0.007(1)	-7.2(6)	6.2 %
CuCl	Cl	2.4(3)	2.19(1)	0.016(3)	-6.0(9)	10.9 %
CuSCN	Cl or S	2.6(3)	2.21(1)	0.017(3)	-6.5(8)	11.2%
		2.6(3)	2.24(1)	0.015(3)	-6.3(9)	11.9%
CuSO ₄ ·5H ₂ O	Cl	3.8(3)	2.252(7)	0.008(2)	-7.1(8)	8.3 %
Cu(ClO ₄) ₂ ·6H ₂ O	Cl	4.0(3)	2.252(6)	0.008(2)	-2.6(7)	7.5 %
CuCl ₂	Cl	3.9(3)	2.239(7)	0.013(2)	0.2(7)	6.3 %
CuCl ₂ ·2H ₂ O	Cl	3.8(3)	2.233(6)	0.013(2)	0.7(6)	4.9 %
CuCl	Cl	2.5(2)	2.224(7)	0.012(2)	-6.6(7)	7.6 %

Table 8.5: EXAFS fits of solutions of $\text{SnCl}_2 \cdot 2\text{H}_2\text{O}$ in Ethaline.

Conc (mM)	M–X, where X=?	Number of atoms, n	Distance from centre, r (Å)	Debye-Waller factor, a (Å ²)	Fermi energy, EF (eV)	Fit index, R(min)
50	Cl	4.2(3)	2.482(7)	0.017(2)	-9.0(7)	5.6 %

Table 8.6: EXAFS fits of 100 mM solutions of PtCl_2 in a range of DES.

DES	M–X, where X=?	Number of atoms, n	Distance from centre, r (Å)	Debye-Waller factor, a (Å ²)	Fermi energy, EF (eV)	Fit index, R(min)
Ethaline	Cl	3.9(2)	2.309(4)	0.005(1)	-11.4(7)	4.7 %
Reline	Cl	4.7(5)	2.29(1)	0.024(3)	-8(1)	10.0 %
Propaline (1,2)	Cl	4.1(3)	2.307(4)	0.0045(9)	-11.0(7)	4.5 %
Propaline (1,3)	Cl	4.0(3)	2.306(4)	0.005(1)	-11.1(7)	4.5%

Table 8.7: EXAFS fits of 100 mM solutions of PdCl_2 in a range of DES.

DES	M–X, where X=?	Number of atoms, n	Distance from centre, r (Å)	Debye-Waller factor, a (Å ²)	Fermi energy, EF (eV)	Fit index, R(min)
Ethaline	Cl	4.0(2)	2.313(3)	0.0055(6)	-1.1(4)	1.9 %
Reline	Cl	3.9(2)	2.313(4)	0.008(1)	-1.5(6)	3.2 %
Propaline (1,2)	Cl	4.1(2)	2.315(3)	0.0060(7)	-1.2(4)	2.3 %
Propaline (1,3)	Cl	4.1(2)	2.314(3)	0.0056(7)	-2.1(5)	2.3 %

Table 8.8: EXAFS fits of 100 mM solutions of CoCl_2 (top) and $\text{CoCl}_2 \cdot 6\text{H}_2\text{O}$ (bottom) in a range of DES.

DES	M-X, where X=?	Number of atoms, n	Distance from centre, r (Å)	Debye-Waller factor, a (Å ²)	Fermi energy, EF (eV)	Fit index, R(min)
Ethaline	Cl	4.0(2)	2.282(3)	0.0062(7)	-6.6(3)	2.1 %
Reline	Cl	3.4(2)	2.246(4)	0.009(1)	2.4(5)	3.5 %
Propaline (1,2)	Cl	3.9(1)	2.284(2)	0.0056(6)	-6.9(3)	1.6 %
Propaline (1,3)	Cl	3.9(1)	2.281(2)	0.0054(6)	-6.9(3)	1.6 %
Ethaline	Cl	3.9(1)	2.282(2)	0.0053(6)	-7.0(3)	1.5 %
Propaline (1,3)	Cl	3.9(1)	2.282(3)	0.0052(6)	-6.9(3)	1.8 %

Table 8.9: EXAFS fits of 100 mM solutions of MnCl_2 (top) and $\text{MnCl}_2 \cdot 4\text{H}_2\text{O}$ (bottom) in a range of DES.

DES	M-X, where X=?	Number of atoms, n	Distance from centre, r (Å)	Debye-Waller factor, a (Å ²)	Fermi energy, EF (eV)	Fit index, R(min)
Ethaline	Cl	3.8(2)	2.369(3)	0.0048(8)	-6.2(4)	3.0 %
Reline	O	5.9(5)	2.16(1)	0.015(4)	2(1)	11.8 %
Propaline (1,3)	Cl	3.9(4)	2.373(6)	0.006(2)	-6.4(7)	7.4 %
Ethaline	Cl	3.9(2)	2.370(3)	0.0061(9)	-5.9(4)	3.2 %

Table 8.10: EXAFS fits of solutions of zinc chloride in Ethaline.

Conc (mM)	M-X, where X=?	Number of atoms, n	Distance from centre, r (Å)	Debye-Waller factor, a (Å ²)	Fermi energy, EF (eV)	Fit index, R(min)
300	Cl	4.3(2)	2.278(4)	0.0084(9)	-6.2(4)	2.6 %

Table 8.11: EXAFS fits of 100 mM solutions of FeCl₂ (top) and FeCl₂·4H₂O (bottom) in a range of DES.

DES	M-X, where X=?	Number of atoms, n	Distance from centre, r (Å)	Debye-Waller factor, a (Å ²)	Fermi energy, EF (eV)	Fit index, R(min)
Ethaline	Cl	3.8(2)	2.313(3)	0.0065(8)	-7.8(4)	2.9 %
Reline	O	4.8(4)	2.08(1)	0.019(3)	1(1)	6.8 %
Propaline (1,3)	Cl	3.9(2)	2.318(4)	0.0069(9)	-7.7(4)	3.4 %
Ethaline	Cl	3.8(2)	2.312(3)	0.0069(8)	-7.6(4)	2.5 %

Table 8.12: EXAFS fits of 100 mM solutions of nickel chloride hexahydrate in a range of DES.

DES	M-X, where X=?	Number of atoms, n	Distance from centre, r (Å)	Debye-Waller factor, a (Å ²)	Fermi energy, EF (eV)	Fit index, R(min)
Ethaline	O	5.9(2)	2.078(8)	0.011(3)	0.8(8)	6.4 %
	C	4.4(8)	2.86(2)	0.01(?)		
Propaline (1,2)	O	5.2(4)	2.074(7)	0.003(2)	0.3(8)	5.5 %
	C	6(2)	2.90(2)	0.01(1)		
Propaline (1,3)	O	5.6(4)	2.073(7)	0.006(2)	-6.4(7)	6.4 %

Table 8.13: EXAFS fits of 100 mM solutions of metal chloride salts in Ethaline.

Metal salt	M-X, where X=?	Number of atoms, n	Distance from centre, r (Å)	Debye-Waller factor, a (Å ²)	Fermi energy, EF (eV)	Fit index, R(min)
CoCl ₂	Cl	4.0(2)	2.282(3)	0.0062(7)	-6.6(3)	2.2 %
CoCl ₂ ·6H ₂ O	Cl	3.9(1)	2.282(2)	0.0053(6)	-7.0(3)	1.5 %
CuCl ₂	Cl	3.7(2)	2.252(5)	0.008(1)	-7.4(5)	4.5 %
CuCl ₂ ·2H ₂ O	Cl	3.6(3)	2.250(5)	0.007(1)	-7.2(6)	6.2 %
FeCl ₂	Cl	3.8(2)	2.313(3)	0.0065(8)	-7.8(4)	2.9 %
FeCl ₂ ·4H ₂ O	Cl	3.8(2)	2.312(3)	0.0069(8)	-7.6(4)	2.5 %
FeCl ₃	Cl	3.2(2)	2.222(4)	0.009(1)	-6.0(5)	3.4 %
FeCl ₃ ·6H ₂ O	Cl	3.2(2)	2.220(4)	0.008(1)	-6.0(5)	3.4 %
MnCl ₂	Cl	3.8(2)	2.369(3)	0.0048(8)	-6.2(4)	3.0 %
MnCl ₂ ·4H ₂ O	Cl	3.9(2)	2.370(3)	0.0061(9)	-5.9(4)	3.2 %
NiCl ₂ ·6H ₂ O	O	5.9(2)	2.078(8)	0.011(3)	0.8(8)	6.4 %
	C	4.4(8)	2.86(2)	0.01(?)		
PdCl ₂	Cl	4.0(2)	2.313(3)	0.0055(6)	-1.1(4)	1.5 %
PtCl ₂	Cl	3.9(2)	2.309(4)	0.005(1)	-11.4(7)	4.7 %
SnCl ₂ ·2H ₂ O*	Cl	4.2(3)	2.482(7)	0.017(2)	-9.0(7)	5.6 %
ZnCl ₂ *	Cl	4.3(2)	2.278(4)	0.0084(9)	-6.2(4)	2.5 %

*The concentration of SnCl₂·2H₂O was 50 mM and the concentration of ZnCl₂ was 300 mM

Table 8.14: EXAFS fits of 100 mM solutions of metal chloride salts in Reline.

Metal salt	M-X, where X=?	Number of atoms, n	Distance from centre, r (Å)	Debye-Waller factor, a (Å ²)	Fermi energy, EF (eV)	Fit index, R(min)
CoCl ₂	Cl	3.4(2)	2.246(4)	0.009(1)	2.4(5)	3.5 %
CuCl ₂	Cl	3.9(3)	2.239(7)	0.013(2)	0.2(7)	6.4 %
CuCl ₂ ·2H ₂ O	Cl	3.8(3)	2.233(6)	0.013(2)	0.8(6)	4.9 %
FeCl ₂	O	4.8(4)	2.08(1)	0.019(3)	1(1)	6.8 %
FeCl ₃ ·6H ₂ O	O	4.8(3)	2.066(9)	0.017(3)	1.8(9)	6.1 %
MnCl ₂	O	5.9(5)	2.16(1)	0.015(4)	2(1)	11.8 %
PdCl ₂	Cl	3.9(2)	2.313(4)	0.008(1)	-1.5(6)	3.2 %
PtCl ₂	Cl	4.7(5)	2.29 (1)	0.024(3)	-8(1)	10.0 %

Table 8.15: EXAFS fits of 100 mM solutions of metal chloride salts in 1,2-Propaline.

Metal salt	M-X, where X=?	Number of atoms, n	Distance from centre, r (Å)	Debye-Waller factor, a (Å ²)	Fermi energy, EF (eV)	Fit index, R(min)
CoCl ₂	Cl	3.9(1)	2.284(2)	0.0056(6)	-6.9(3)	1.6 %
NiCl ₂ ·6H ₂ O	O	5.2(4)	2.074(7)	0.003(2)	0.3(8)	5.5 %
	C	6(2)	2.90(2)	0.01(1)		
PdCl ₂	Cl	4.1(2)	2.315(3)	0.0060(7)	1.2(4)	2.3 %
PtCl ₂	Cl	4.1(3)	2.307(4)	0.0045(9)	-11.0(7)	4.5 %

Table 8.16: EXAFS fits of 100 mM solutions of metal chloride salts in 1,3-Propaline.

Metal salt	M–X, where X=?	Number of atoms, n	Distance from centre, r (Å)	Debye- Waller factor, a (Å²)	Fermi energy, EF (eV)	Fit index, R(min)
CoCl ₂	Cl	3.9(1)	2.281(2)	0.0054(6)	-6.9(3)	1.6 %
FeCl ₂	Cl	3.9(2)	2.318(4)	0.0069(9)	-7.7(4)	3.4 %
MnCl ₂	Cl	3.9(4)	2.373(6)	0.006(2)	-6.4(7)	7.4 %
NiCl ₂ ·6H ₂ O	O	5.6(4)	2.073(7)	0.006(2)	-6.4(7)	6.4 %
PdCl ₂	Cl	4.1(2)	2.314(3)	0.0056(7)	-2.1(5)	2.3 %
PtCl ₂	Cl	4.0(3)	2.306(4)	0.005(1)	-11.1(7)	4.5%

Table 8.17: EXAFS fits of 200 mM solutions of iodine in two different DES.

DES	M–X, where X=?	Number of atoms, n	Distance from centre, r (Å)	Debye- Waller factor, a (Å²)	Fermi energy, EF (eV)	Fit index, R(min)
Ethaline	I	2.0(2)	2.81(1)	0.026(3)	-6.6(7)	16.4 %
Oxaline	I	1.9(2)	2.901(7)	0.023(2)	-9.5(6)	8.9 %

Table 8.18: EXAFS data fits for 100 mM solutions of metal salts in [HMIM][Cl].

Metal salt	M-X, where X=?	Number of atoms, n	Distance from centre, r (Å)	Debye-Waller factor, a (Å ²)	Fermi energy, EF (eV)	Fit index, R(min)
CrCl ₃ ·6H ₂ O	Cl	5.5(5)	2.347(7)	0.010(2)	-3.1(8)	5.3 %
CrCl ₃ ·6H ₂ O + H ₂ O	Cl	7.8(8)	2.22(1)	0.026(4)	7(1)	7.5 %
	O	6.4(8)	2.08(2)	0.013(4)	-6(1)	12.4 %
CuAc ₂ ·H ₂ O	Cl	3.2(2)	2.226(5)	0.016(1)	-9.9(4)	3.3 %
CuAc ₂ ·H ₂ O + H ₂ O	Cl	2.9(2)	2.184(5)	0.019(2)	-8.5(5)	3.2 %
CuCl ₂ ·2H ₂ O	Cl	3.1(1)	2.230(4)	0.014(1)	-8.1(4)	2.7 %
CuCl ₂ ·2H ₂ O + H ₂ O	Cl	3.1(1)	2.230(4)	0.014(1)	-8.1(4)	2.7 %
CuSO ₄ ·5H ₂ O	Cl	3.2(2)	2.224(5)	0.017(2)	-7.4(4)	3.9 %
CuSO ₄ ·5H ₂ O + H ₂ O	Cl	2.8(1)	2.190(4)	0.017(2)	-6.8(4)	3.2 %
NiAc ₂ ·4H ₂ O	Cl	3.0(2)	2.259(6)	0.011(2)	0.5(7)	4.3 %
NiAc ₂ ·4H ₂ O + H ₂ O	O	5.0(3)	2.070(7)	0.013(2)	13(1)	4.4 %
NiCl ₂ ·6H ₂ O	Cl	4.1(3)	2.271(6)	0.007(2)	-6.2(7)	4.2 %
NiCl ₂ ·6H ₂ O + H ₂ O	Cl	5.7(4)	2.216(7)	0.018(2)	12.2(7)	4.9 %

Table 8.19: EXAFS data fits for 100 mM solutions of metal salts in [EMIM][OTf].

Metal salt	M–X, where X=?	Number of atoms, n	Distance from centre, r (Å)	Debye-Waller factor, a (Å ²)	Fermi energy, EF (eV)	Fit index, R(min)
CrCl ₃ ·6H ₂ O	Cl	7.5(7)	2.24(1)	0.022(3)	3(1)	6.9 %
CrCl ₃ ·6H ₂ O + H ₂ O	Cl	7.1(7)	2.18(1)	0.021(3)	11(1)	5.7 %
NiCl ₂ ·6H ₂ O	O	6.5(5)	2.06(1)	0.015(3)	3(1)	7.8 %

Table 8.20: EXAFS data fits for 100 mM solutions of metal salts in [BMIM][BF₄].

Metal salt	M–X, where X=?	Number of atoms, n	Distance from centre, r (Å)	Debye-Waller factor, a (Å ²)	Fermi energy, EF (eV)	Fit index, R(min)
CrCl ₃ ·6H ₂ O	Cl	7.0(5)	2.244(7)	0.019(2)	2.0(8)	5.3 %
CuCl ₂ ·2H ₂ O	Cl	3.4(2)	2.121(7)	0.021(2)	-0.5(7)	4.6 %
NiCl ₂ ·6H ₂ O	O	5.4(6)	2.10(1)	0.015(4)	-4(1)	15.0 %

Table 8.21: EXAFS data fits for 100 mM solutions of metal salts in [EMIM][FAP].

Metal salt	M–X, where X=?	Number of atoms, n	Distance from centre, r (Å)	Debye-Waller factor, a (Å ²)	Fermi energy, EF (eV)	Fit index, R(min)
CuCl ₂ ·2H ₂ O	Cl	3.1(2)	2.195(5)	0.017(2)	-7.3(5)	4.8 %